UCID-19406-1

MASTER

UCID--19406-1

DE82 017295

Fusion Breeder Program Interim Report

December 1981-February 1982

Ralph Moir, J.D. Lee, Wm. Neef, Tom Ogdon,
Lawrence Livermore National Laboratory;
Dave Berwald, Bob Campbell, S.C. Mortenson,
J.R. Ogren, Y. Saito, TRW;
Ron Rose, J.S. Karbowski, Westinghouse;
Ken Schultz, C.P.C. Wong, R. Creedon, I. Maya,
General Atomic; Jack DeVan, ORNL; Dan Jassby,
Princeton Plasma Physics Lab; Nate Hoffman,
Energy Technology Engineering Center

June 11, 1982

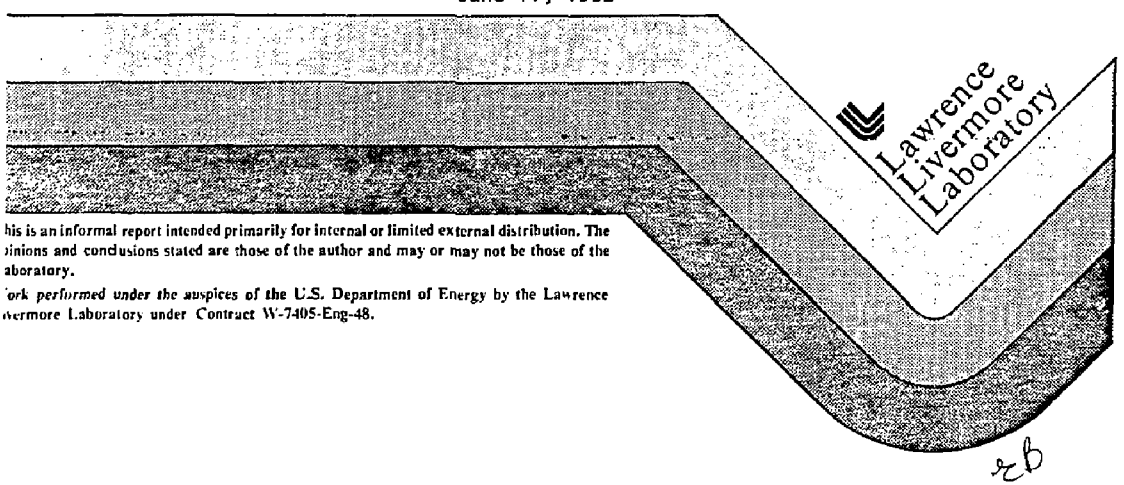

rb

FUSION BREEDER PROGRAM INTERIM REPORT

DECEMBER 1981 — FEBRUARY 1982

R. W. Moir, J. D. Lee, W. Neef, T. Ogden
Lawrence Livermore National Laboratory

D. H. Berwald, R. B. Campbell, S. C. Mortenson, J. R. Ogren, Y. Saito
Energy Development Group, TRW Inc.

R. P. Rose, J. S. Karbowski
Westinghouse Electric Corporation

K. R. Schultz, C. P. C. Wong, R. L. Creedon, I. Maya
General Atomic Company

J. DeVan
Oak Ridge National Laboratory

D. L. Jassby
Princeton Plasma Physics Laboratory

N. J. Hoffman
Energy Technology Engineering Center

ISSUED

MAY, 1982

TABLE OF CONTENTS

CHAPTER I. INTRODUCTION AND OVERVIEW

I.A PROJECT GOALS AND ORGANIZATION

This interim report for the FY82 Fusion Breeder Program covers work performed during the scoping phase of the study, December, 1981 - February 1982. The goals for the FY82 study are the identification and development of a reference blanket concept using the fission suppression concept and the definition of a development plan to further the fusion breeder application. The context of the study is the tandem mirror reactor, but emphasis is placed upon blanket engineering. A tokamak driver and blanket concept will be selected and studied in more detail during FY83.

The design of a fusion-fission hybrid reactors has progressed to a level of conceptual design detail which requires a multi-disciplinary and inter-organizational team approach. The present study includes the participation of the following organizations (see also Figure I.A-1):

Organization	Principal Roles
Lawrence Livermore National Laboratory	Program Manager, Tandem Mirror Physics and Technology, Nuclear Design
TRW, Inc.	Technical Integration, Tandem Mirror Plasma Engineering, Reactor Systems Modeling, Design Support
General Atomic Company	Fluid Mechanics and Heat Transfer, Fuel Management Systems, Reactor Safety Systems, Fuel Reprocessing
Westinghouse Electric Company	Mechanical Design, Operation and Maintenance, Reactor System layout
Oak Ridge National Laboratory	Chemical Engineering and Materials
Princeton Plasma Physics Laboratory	Tokamak Plasma Engineering and Technology

In addition, investigators from the University of California, Los Angeles (radiation damage), the Energy Technology Engineering Center (liquid metals and materials), and EG&G, Idaho (fission reactor test program) are participating in the study.

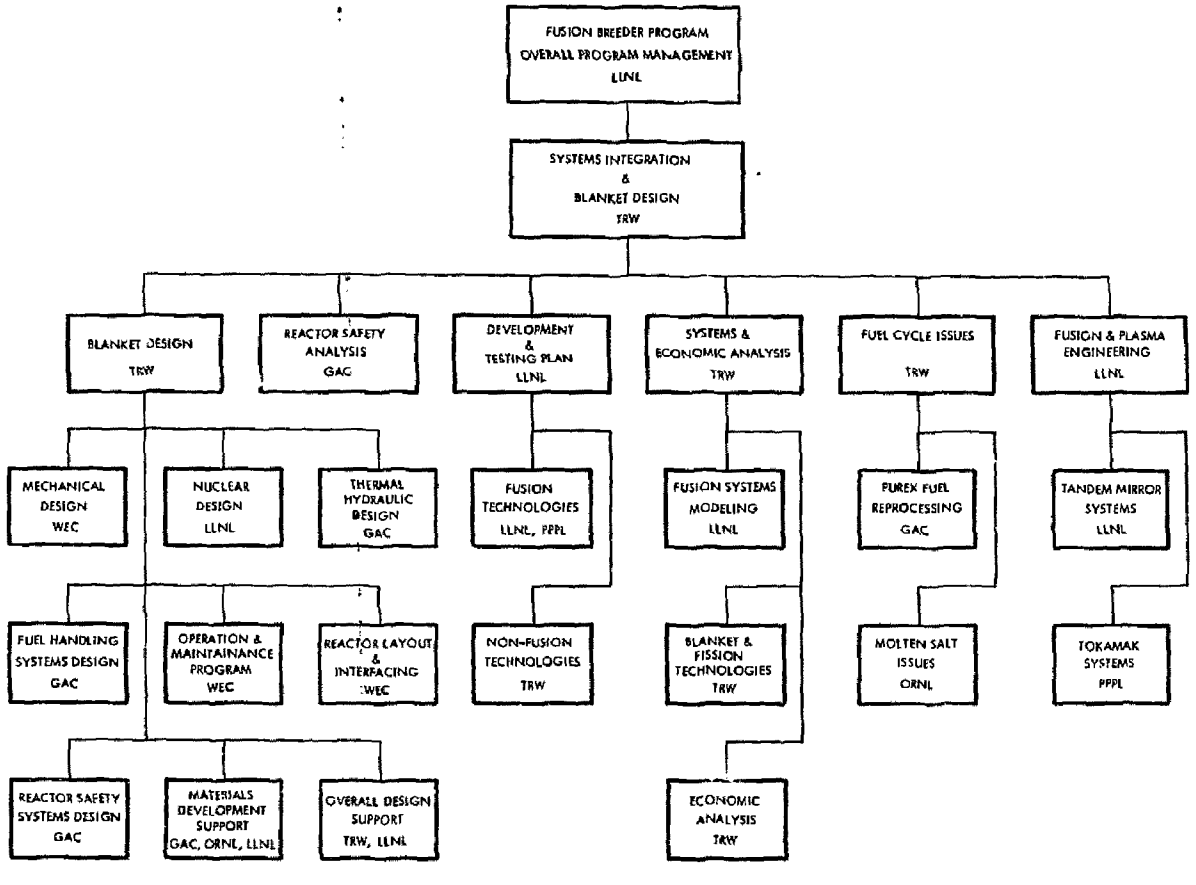

FIGURE I.A.1 Fusion Breeder Program Organization

I.B BACKGROUND

During the past four years the suppressed fission blanket has emerged as a possibly superior path towards achieving a hybrid which maximizes the number of client fission reactors (eg., LWR) which can be supported by a single hybrid.[1] The fission suppressed blanket option (also known as the fusion breeder reactor) is a challenging technological goal, but in comparison with fast fission hybrids the fusion breeder has superior reactor safety and institutional characteristics.[2] Reactor safety advantages result due to its low fission rate (< 0.05 per fusion) and institutional advantages result because a high support ratio fusion breeder would fuel up to 20 1 GWe client LWRs while producing only about 1 GWe locally. In this sense, fuel cycle centers consisting of fusion breeders and the fuel cycle activities associted with the fusion breeders and their LWR clients could replace present day uranium mining and uranium enrichment plants.

Economics and deployment studies have shown that the fusion breeder/LWR option can provide electricity inexpensively (less than 20% above current LWR electricity costs) and could rapidly expand during the next century to satisfy a substantial fraction of our electrical demand.[1] Despite a projected commercial introduction date of ∿ 2015, the fusion breeder can impact electricity generation requirements more quickly than other advanced technologies (eg., LMFBR, fusion electric). As natural uranium resources become depleted, the current plan (without an external source of fissile fuel) would wind down the rate of commitment to new LWR construction. Once the feasibility of fusion breeder technology is demonstrated (perhaps ∿ 2005) LWR operators will have an assured future fissile fuel supply and LWR electricity generation capacity can expand without interruption.

I.B.1 Beryllium/Molten Salt Blanket Developed During FY79 Study

The design of a fission suppressed blanket was first addressed in a 1979 study performed by Lawrence Livermore National Laboratory (LLNL) with the General Atomic Company (GAC), the General Electric Company (GE), and Bechtel National, Inc.[3] As a result of this study a fission suppressed blanket concept based upon beryllium neutron multiplication and a lithium/thorium bearing molten salt coolant was developed. Although the Be/MS blanket performance was excellent, materials problems associated with the use of beryllium and a high temperature salt (> 550°C) in the fusion environment led to the pursuit of other blanket concepts. Nevertheless, due to the superior operational characteristics of Be/MS blankets, modified versions of the original blanket are being considered at a low level of effort in the present study.

I.B.2 Suppressed Fission Blankets Developed During FY81 Study

Two suppressed fission blanket designs were studied in detail as part of a 1981 study performed by LLNL with TRW, GAC, Westinghouse Electric Corp (WEC), and Oak Ridge National Laboratory (ORNL).[4]

I.B.2.a Gas Cooled Beryllium/Thorium Oxide Suspension Blanket. The first of these blankets, shown in Figure I.B-1, featured a one zone design with beryllium as a neutron multiplier, helium as a coolant, and a liquid suspension of thorium oxide particles in lead-lithium (ie., $Li_{17}Pb_{83}$) as a fertile fuel, tritium breeding material and heat transfer medium. In this design, as in other suppressed fission blanket designs, a mobile fuel with on-line reprocessing is necessary to keep fissile content low and suppress fission of the ^{233}U. To obtain maximum irradiation life from the structural material, ferritic steel (HT-9) with a low-pressure corrugated box sub-module design was specified. Thorium oxide was chosen as the fertile material form to be circulated through the blanket because its density is a close match to that of $Li_{17}Pb_{83}$. Cooling is accomplished by helium flowing in reentrant thimble tubes. Neutron multiplication occurs in triangular shaped prismatic blocks of hot pressed beryllium shown in Figure I.B-2. The beryllium blocks are essentially unconstrained to accommodate radiation swelling. Thermal contact between the beryllium blocks and the cooling tubes is maintained by liquid Pb-Li.

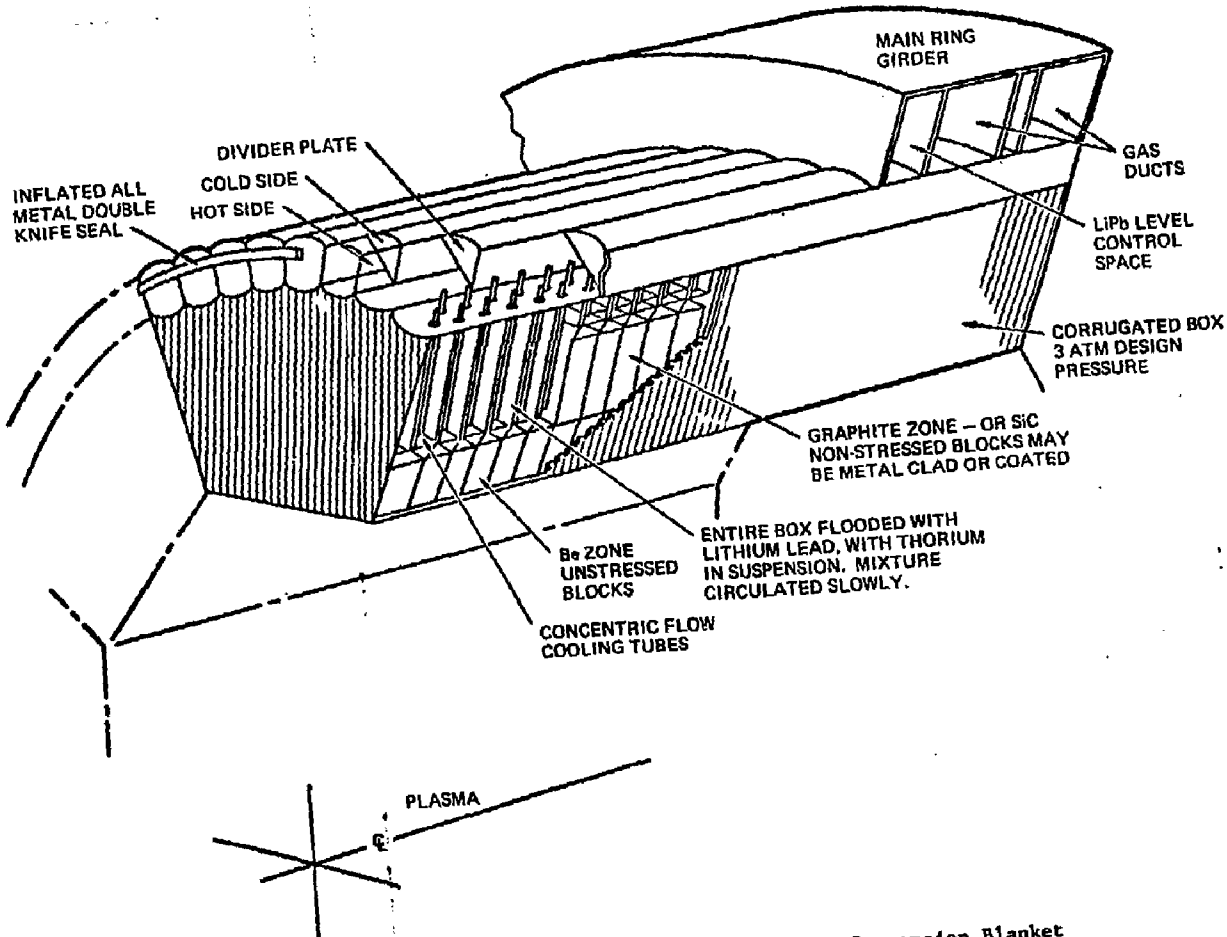

FIGURE I.B-1. Reference Beryllium/Thorium Oxide Suspension Blanket

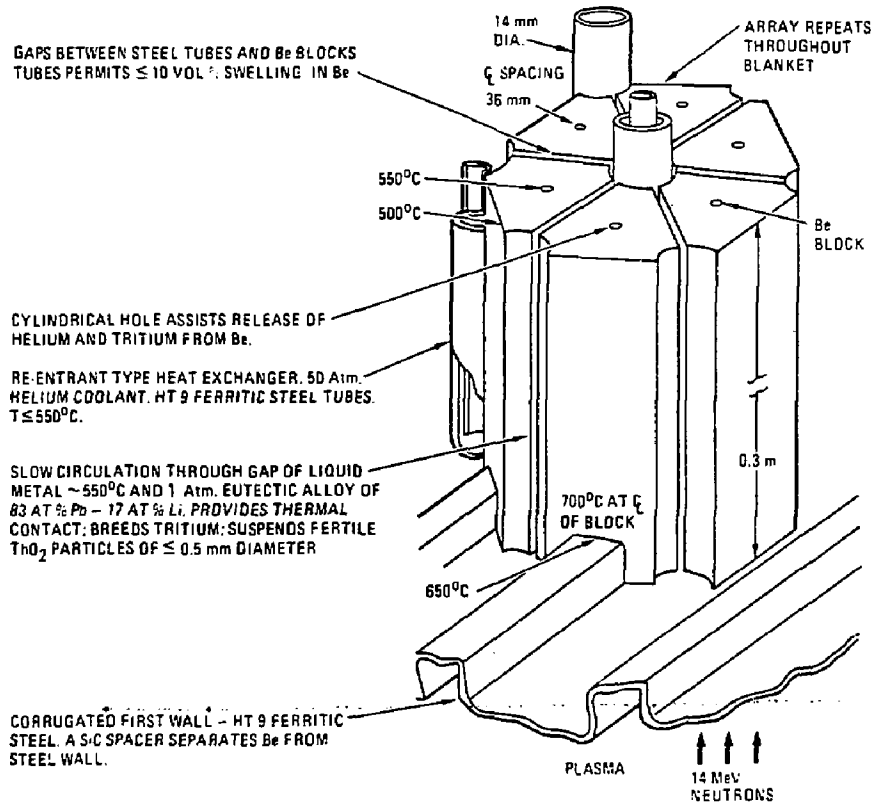

FIGURE I-B.2 Materials and component design for neutron multiplier in TMHR blanket.

The suspension of ThO_2 microspheres in the mixture of Pb-Li is slowly circulated to allow reprocessing to remove bred fuel. Because of the small concentration of Th, a 0.6% concentration of ^{233}Pa plus ^{233}U in thorium is reached in less than 2 months of exposure. The fissile discharge concentration results from a trade-off between fission suppression at low concentration and economical reprocessing at high concentration. The ^{233}U content is only about 0.25% at discharge (ie., $\sim$ .35% ^{233}Pa). The concept of using low thorium concentration to achieve rapid breeding rates is called "fertile dilution." Following the beryllium region is a silicon carbide reflector region which substantially reduces the beryllium requirements. The net breeding of ^{233}U per fusion reaction is quite good (F = 0.73).

Although the gas cooled, Be/ThO_2 blanket resulted in excellent breeding performance and afterheat safety characteristics, a number of design issues including concerns relating to design complexity ($\sim$ 800 pressure tubes/m^2), beryllium irradiation damage and recycling, and chemical compatibility are outstanding.

I.B.2.b Two Zone Lithium/Molten Salt Blanket. The second blanket featured ^{6}Li depleted lithium as a coolant and as an effective neutron multiplier (ie., the $^{7}Li(n,n'\alpha)$ reaction produces tritium without the loss of a neutron). In this two zone configuration, shown in Figure I B-3, a 50 cm thick liquid lithium zone is followed by a flowing molten salt zone. The molten salt contains thorium and also serves as a coolant for the outer zone. Stainless steel was used as the structural material and corrosion is greatly retarded by maintaining a frozen layer of the thorium bearing salt on the steel. However, the steel might last many years without this protective layer. Also, Hastelloy (which is used for the outer wall of the balnket as well as the piping and heat exchangers) might be used with several years of services before radiation damage effects cause end of life. The MHD pressure drop was found to be manageable ($\sim$ 100 psi pressure at the first wall) due to the low magnetic field ($\sim$3T).

The Li/MS blanket resulted in lower breeding performance than the Be/ThO_2 blanket (0.49 vs. 0.73 fissile atoms per source neturon) due to less effective neutron multiplication in lithium as compared with beryllium. However, the reprocessing cost was estimated to be exceptionally low for molten salt and expensive for ThO_2 (2-4 vs. $\sim$40 \$/g ^{233}U recovered).

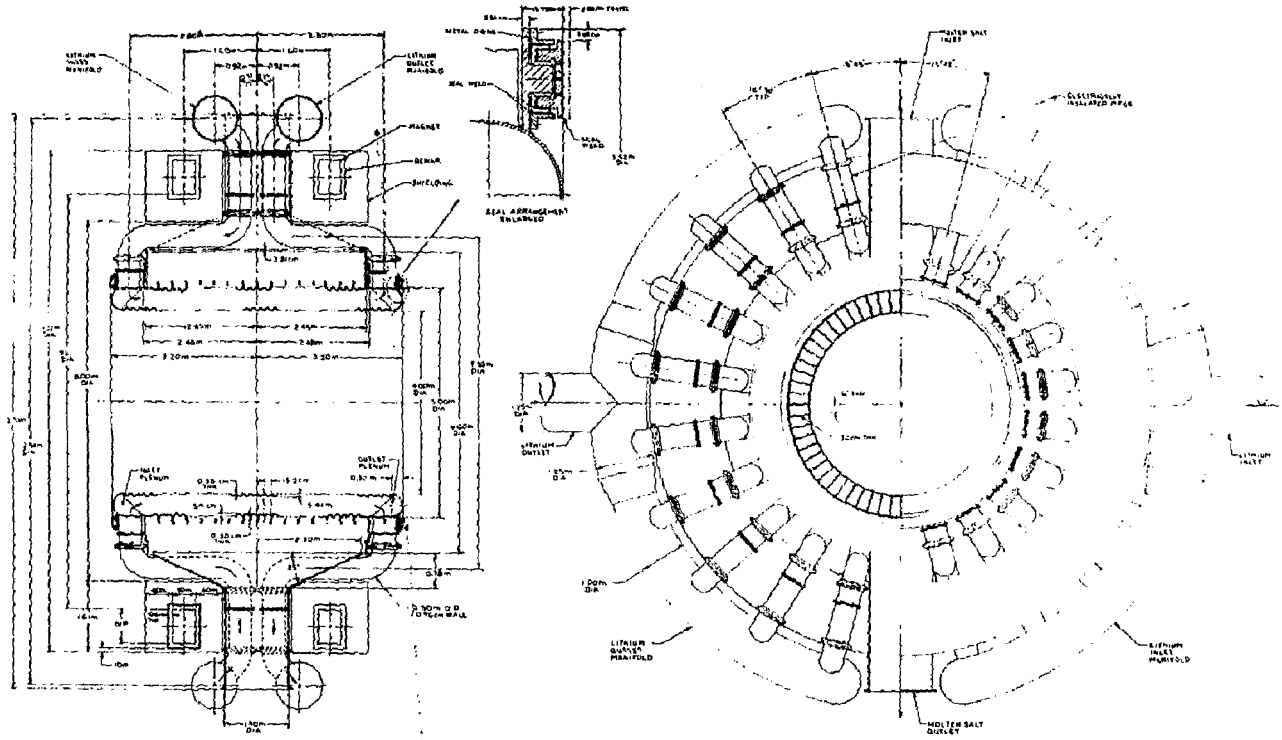

FIGURE I-B.3. Component arrangement and dimensions for the reference TMHR liquid metal cooled blanket module assembly

The following observations results from these two blanket studies:

- beryllium is markedly better as a neutron multiplier than ^{7}Li
- one-region designs performed better than two region designs;
- molten salt reprocessing results in much lower cost than aqueous reprocessing if all other aspects are similar.
- liquid metals have potential to provide less mechanical complexity for suppressed fission blankets.

I.B.3 A New Beryllium/Thorium Metal Blanket Concept.

A third blanket concept, identified during the latter part of FY81 study, was a preliminary attempt to combine the attractive features of beryllium neutron multiplication with the design simplicity associated with the liquid metal coolants. A schematic diagram of an internal pipe cooled beryllium/thorium pebbles blanket option is shown in Figure I.B-4, and the design is more fully discussed in references 1 and 4. This option featured only one neutronic zone and utilized beryllium pebbles as the neutron multiplier. In this design, nonreactive lead-lithium was substituted for liquid lithium as the primary coolant since the neutron multiplication occurs primarily in the beryllium spheres and liquid lithium is not required for neutronic reasons alone. The blanket coolant enters the module on one side, flows through axially oriented pipes (ie., parallel to the central cell B-field) which are embedded within the pebble bed. Heat is conducted from the bed to the coolant. An addition, the first wall would be cooled by axial lithium flow along the wall. The fertile fuel form in the design is metallic thorium pebbles randomly packed between larger beryllium pebbles. The remaining voids in the bed would be filled with the liquid metal (eg., sodium) to improve heat transfer.

This design option offered several potentially attractive features:

1. excellent fissile breeding performance;
2. conventional liquid-metal technologies;
3. possibility for nonreactive primary coolant;
4. continuous recycling of both beryllium and thorium;
5. excellent heat transfer capabilities;
6. fuel cycle flexibility (ie., fertile pebbles can be thorium metal, thorium oxide, or uranium oxide);
7. separation of fissile and tritium breeding
8. structural temperatures below 400°C insure long life.

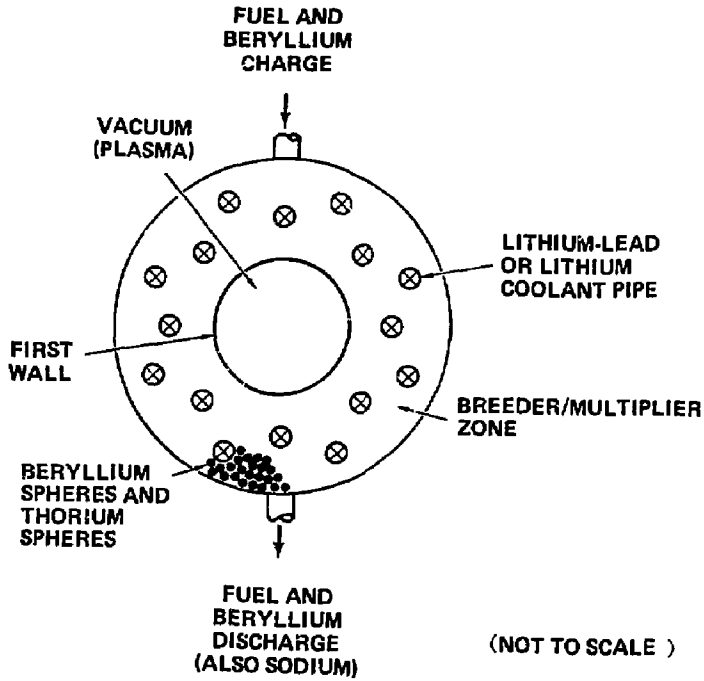

FIGURE I.B-4. Beryllium/thorium pebble blanket option, module end view

Concerning the fissile breeding performance, excellent neutron multiplication can be achieved for two reasons. First, the design featured a high volume fraction of high efficiency neutron multipliers. For instance, the colume fractions in Figure I.B-4 could includes 45% beryllium, 15% $Li_{17}Pb_{83}$, and 3% thorium. The remainder of the blanket region could be 5% stainless steel and 32% sodium. Second, this one-zone option would effectively suppress fission due to fertile dilution and fissile discharge at low concentration. Thermal and epithermal fissioning of the bred ^{233}U material would be largely eliminated in this design (due to fuel discharge at ~0.6% ^{233}U assay in the thorium).

Another advantage that should be highlighted concerns the use of beryllium in the above design. This design would be insensitive to concerns about beryllium swelling since the beryllium pebbles would be circulated frequently within their loose lattice. They could also be easily removed and reworked during fuel management operations. Since beryllium pebble tolerances would be unimportant, the toxic nature of recycled pebbles would be minimized in a rather simple cleanup and refabrication process requiring no precision machining.

The principal design issues identified for the beryllium/thorium pebbles blanket with internal pipe cooling are as follows:

1. thermal constraints which can result in inadequate pipe clearances
2. possibly large MHD pressure drops;
3. achieving satisfactory pebble mixing and packing fractions.

Concerning the issue of pebble mixing and packing fractions, these would be accomplished by charging and discharging the system at several points at the top and bottom of the blanket with a mix of larger beryllium pebbles and smaller thorium pebbles. The size of the beryllium pebbles would be determined by flow requirements (eg., ball diameter less than approximately one-fifth to one-eighth of the minimum pitch between pipes), and the size of the thorium pebbles would be such that the thorium pebbles pack efficiently between the beryllium pebbles. However, non-optimal packing was anticipated to produce minimal impact for the following reasons:

1. long neutron mean-free-paths;
2. only 3% thorium by volume is required to gather the available neutrons;
3. excellent heat transfer is obtained regardless of packing because liquid metal-filled voids;
4. overall power generation rates in the fuel are low.

An artist's drawing of this blanket module is shown in Figure I.B-5.

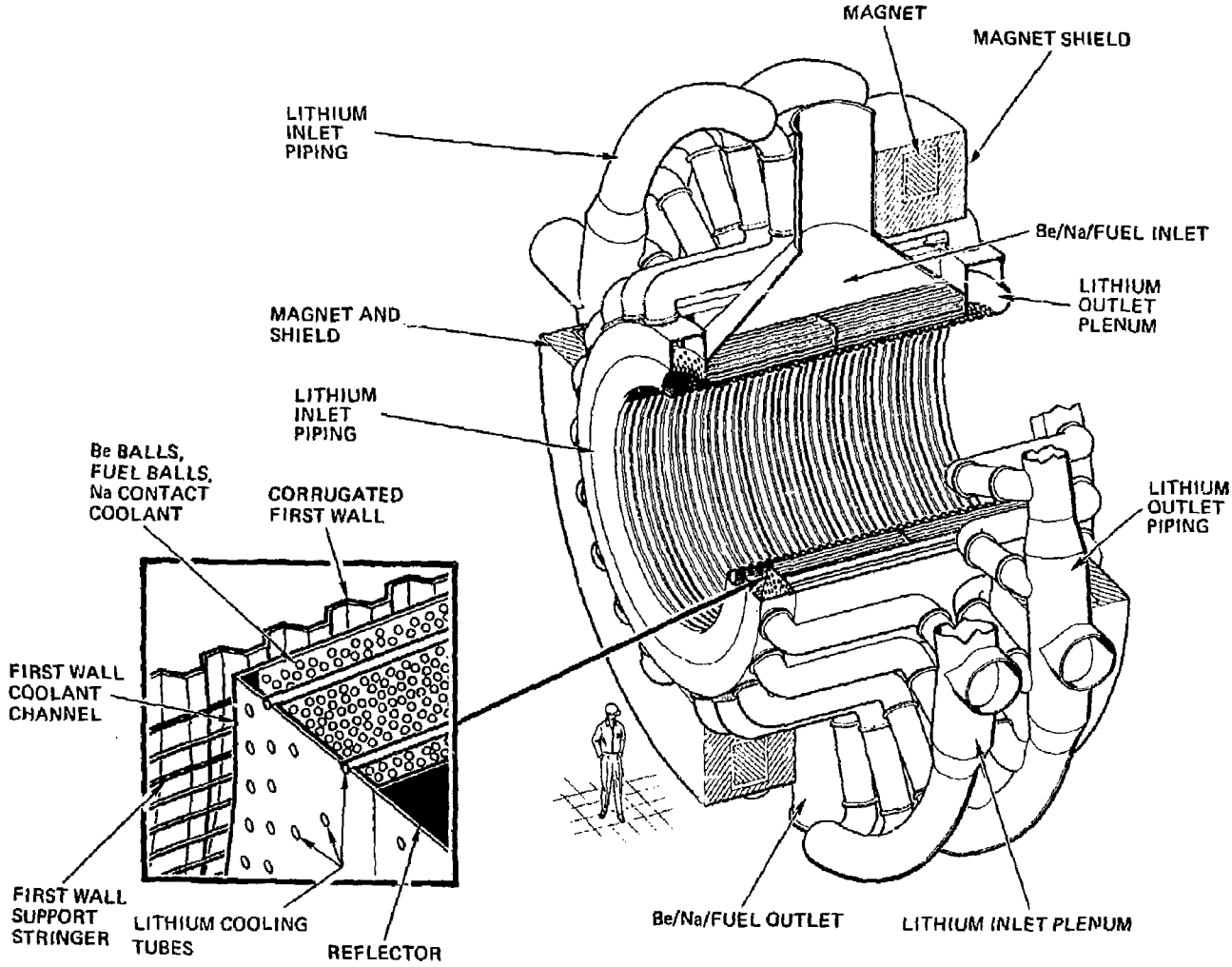
MAGNET
MAGNET SHIELD
LITHIUM INLET PIPING
Be/Na/FUEL INLET
LITHIUM OUTLET PLENUM
MAGNET AND SHIELD
LITHIUM INLET PIPING
Be BALLS, FUEL BALLS, Na CONTACT COOLANT
CORRUGATED FIRST WALL
LITHIUM OUTLET PIPING
FIRST WALL COOLANT CHANNEL
FIRST WALL SUPPORT STRINGER
LITHIUM COOLING TUBES
REFLECTOR
Be/Na/FUEL OUTLET
LITHIUM INLET PLENUM

REFERENCES

1. J.A. Maniscalco, et.al., "Recent Progress in Fusion Fission Hybryd Reactor Design Studies," Nucl. Tech. Fusion, 1, 4 (1981)

2. I. Maya, et. al., "Safety Evaluation of Hybrid Blanket Concepts," GA-A160101, General Atomic Company (1980).

3. R. W. Moir, et.al., "Tandem Mirror Hybrid Reactor Design Study Final Report," UCID-18808, Lawrence Livermore National Laboratory (1980).

4. R. W. Moir, et.al., "Feasibility Study of the Fission Suppressed Tandem Mirror Hybrid Reactor," UCID-19327, Lawrence Livermore National Laboratory (1982).

I.C OVERVIEW OF SCOPING PHASE DESIGN CONCEPTS

Although the internal pipe cooled beryllium/thorium metal design discussed in Section I.B.3 has several attractive features and was chosen as a starting point for the present study, this second generation concept was not subjected to the same level of design detail during FY81 as its precursors. Consequently, several alternative versions of this design were selected for consideration at a project kickoff meeting held on December 2, 1981. The meeting resulted in the identification of the four scoping options shown in Table I.C-1.

This section provides background relating to the initial development of these options. Chapters II, III and IV present more detailed studies performed during the scoping phase of the program which begin to address the design issues associated with the four scoping phase concepts.

TABLE I.C-1. Scoping Phase Options

	1	2	3	4
Fertile fuel form	Th	UO_2	Th	UC (U-Nb)
Primary coolant	Li (Pb-Li)	Li (Pb-Li)	Li (Pb-Li)	Li (Pb-Li)
Coolant configuration	pipes	pipes	direct	direct
Heat transfer fluid	Na	Na	Li	Li
Structural material	SS(FS)	SS(FS)	FS(SS)	FS(SS)
Max. structural temperature	360	360	<500	<500
Max. bed temperature	500	500	<500	<500
Surfaces requiring coatings	(SS)	(SS)	(FS)	(FS)
	(BeO)	(BeO)		
	(ThO_2)			

(NOTE: parenthesis indicate options not necessarily required)

I.C.1 Internal Pipe Cooled Options

In comparison with the original design, Options 1 and 2 provide the closest resemblance. These differ from one another only with respect to the fertile fuel form, but differ from the FY81 design in the following areas:

- lithium is the primary coolant instead of the lead-lithium eutectic
- the maximum bed temperature is lowered from 700°C to 500°C
- the beryllium pebble diameter is decreased from 1.25 cm diameter to <6 mm diameter.

A preliminary choice of lithium over Li-Pb was based upon several factors: a general consensus that liquid lithium safety can be engineered into the design of suppressed fission blanket fusion breeders (especially considering siting in remote fuel cycle centers), better known liquid metal compatibility characteristics, a more established technology base (eg., impurity control), better tritium retention, lower static loading and better heat transfer characteristics. The advantages of Pb-Li over Li include the following: less chemical reactivity in accident situations, better compatibility with some materials (eg., SiC, C, ThO_2) and a lower characteristic MHD pump power (due to lower electrical conductivity). GAC was requested to investigate the safety implications of this choice (see Sections IV.F and IV.G of this report).

The lowering of the maximum temperature from 750°C to 500°C resulted from ORNL's experience with similar systems which, at 600°C, have been found to transport very low (~ ppb) concentrations of beryllium in sodium to attack structural materials.[1] Although the smaller beryllium pebble size allows a closer pipe spacing, the lower temperature limit represents a major design change. This issue was addressed during the scoping phase and is discussed in Chapter II.

Other issues relating to Options 1 and 2 were also discussed at the kickoff meeting. These included the choice of an austenitic stainless or ferritic steel, pebble packing and flow characteristics for beryllium and thorium spheres, and various materials compatibility issues. It was the consensus of the group that all of these issues can be amenable to engineering solutions, but further study was recommended.

The choice of a steel type will be made on the basis of several comparisons. In particular, ferritic steels are expected to have superior radiation damage characteristics in most respects (eg., void swelling, helium embrittlement), but the ductile-to-brittle transition temperature (DBTT) could rise to the blanket operating temperature for operation below 350°C.[2] Depending upon the time to reach this point and our assessment of operation of a blanket below the DBTT (eg., low cycle fatigue, shocks due to magnet quench, plasma dump), a low DBTT could prove unacceptable. Ti-modified 316 stainless steel (PCA) will be acceptable, but has lower strength and thermal conductivity than HT9 or 2-1/4 Cr-1Mo ferritic steels and, most importantly, there is reason to believe that improved 316 stainless steels will swell at a faster rate than low nickel ferritic steels. Tritium diffusion will be less for stainless steels than for ferritic steels. Chromium requirements for some alloys (eg., HT9) may become an issue.

Concerns related to pebble packing primarily involve three issues: packing fraction, beryllium/thorium distribution, and pebble flow. It was anticipated that the pebbles will be batch processed and loaded by layering. If maintaining the required beryllium/thorium distribution proves excessively difficult, a directed thorium flow in wire mesh pipes was suggested, but the reactor safety implications of such a concept require study. LLNL and GAC pursued the pebble packing and flow related issues during the scoping phase (Sections IV.A and IV.H).

The key materials compatibility issues for all four options are given in Table I.C-2. Although materials experts involved in the study predict reasonable confidence of compatibility without coatings at the suggested operating temperatures, beryllium/steel and beryllium self welding issues are sufficiently important that experimental verification of their extent is being pursued (results expected ∿ May, 1982). If compatibility issues are judged to be sufficiently important, coating one or more of the steel structure, beryllium pebbles, or thorium pebbles would be considered. Proposed coatings include aluminides, oxides, carbides, nitrides, and metals such as molybdenum, niobium, and zirconium. Coating techniques could include plasma spraying, ion implantation, magnetron sputtering, and the use of sacrifical layers.

TABLE I.C-2. Key materials compatibility issues investigated during the scoping phase

ISSUE	APPLICABLE BLANKET OPTIONS	SPECIFICATIONS*
1. Extent of steel/beryllium reactions (both solid-solid and beryllium transport in sodium and lithium)	1,2,3,4	With and without oxide coatings. Ferritic and stainless steels
2. Self welding of beryllium pebbles in lithium and sodium	1,2,3,4	With and without oxide coatings
3. Extent of beryllium/thorium reactions ($Th+Be \rightarrow Th_xBe_y$)	1,3	Consider oxides
4. Same as 3 for beryllium/UO_2 ($UO_2+15Be \rightarrow UBe_{13}+2BeO$)	2	
5. Same as 3 for beryllium/UC	4	
6. Ability of oxides to exist in liquid lithium	3,4	Consider BeO, ThO_2, UO_2
7. Tritium/thorium reactions and diffusion	3,4	Consider ThO_2 depending upon results of 6
8. Beryllium recoil into steel		Same as 1 above

*Temperature range is 360-530°C in all cases

I.C.2 Direct Cooled Options.

Comparing Options 3 and 4 with Options 1 and 2, the principal difference relates to the coolant flow. Instead of cooling via internal pipes, Options 3 and 4, the "direct cooling" options, feature a possibly simpler scheme in which coolant flows directly through the bed. For example, one configuration which was studied routes the coolant from the inlet duct to a first wall cooling plenum, through an inner radial flow baffle into the bed, out of the bed and into an exit plenum through an outer radial flow baffle, and out the exit pipes. This type of design, which in some respects resembles an automotive oil filter, could allow larger pebbles than the internal pipe design since piping within the bed is eliminated. Considering the direct cooled options, the following issues arise

- MHD induced effects on heat transfer and pressure drop through a packed bed of larger beryllium and thorium pebbles.
- Lithium replacement of sodium as the heat transfer fluid with consequent impacts on compatibility and coupling to the heat exchanger.
- Tritium is introduced into the fertile breeding region.
- Coolant temperature can rise if advantageous due to less constrained thermal limits.

Despite the new concerns, these concepts have potential to provide a less complex design and improved breeding performance due to reduced structure (provided that the MHD pressure drop through the bed is not prohibitive). Several issues for these designs are similar to those for Options 1 and 2. These include: lithium vs. lead-lithium, ~500°C temperature limit, stainless vs. ferritic steel (baseline choice was switched), pebble packing and flow, and materials compatibility issues (see Table I.C-2). During the scoping phase MHD and compatibility were emphasized as key feasibility issues. To address the MHD effects, a conservative analytical model is required. Information regarding the two key compatibility issues which are unique to Options 3 and 4 (ie., tritium/thorium interactions and the ability of BeO and ThO_2 to survive in lithium) was sought. Scoping phase results relating to the direct cooled blanket designs are discussed in Chapter III.

I.C.3 Reference Concept Selection Process.

The reference blanket concept to be described in Chapter V was selected using the procedure indicated in Figure I.C-1. According to this process, two key decisions were made independently.

The first concerns the choice of a uranium or thorium fuel form. This choice primarily results from systems and economics trade studies which consider breeding performance, the LWR client performance and fuel cycle cost, technology development requirements, and institutional issues. Such as analysis is presented in Section IV.J. Other secondary issues which could factor into this decision are compatibility issues and issues relating to afterheat safety. In particular, the 2.3 day decay half-life associated with ^{239}Np decay to ^{239}Pu is a possible advantage relative to the 27 day half life associated with ^{233}Pa decay to ^{233}U. The second key decision involves the coolant configuration: internal pipes or direct cooling? To address this decision at the February 16-17, 1982 Design Review Meeting several simultaneous analyses and design studies were conducted and are reported in the following chapters.

FIGURE I.C-1. Selection process

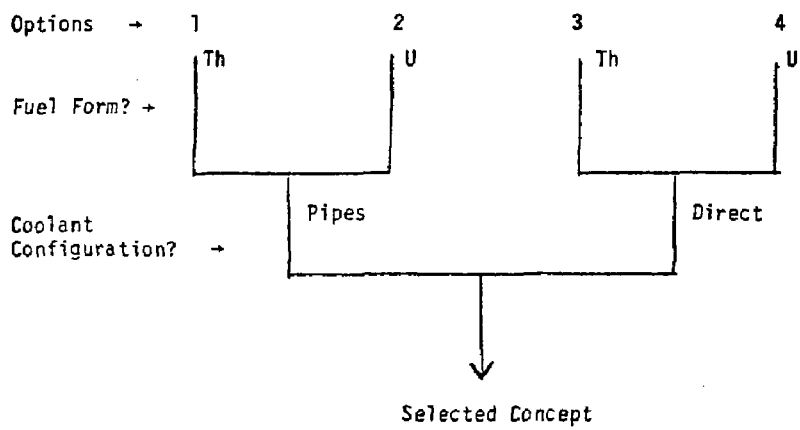

REFERENCES

1. J. DeVan (ORNL), personnel communication (1981).

2. N. Ghoniem and R. Conn, "Assessment of Ferritic Steels for Steady State Fusion Reactors", Proc. of the IAEA Tech. Committee meeting on Fusion Technology, Tokyo, Japan (1981), also published as UCLA report PPG-587 (1981).

CHAPTER I

INTERNAL PIPE COOLING BLANKET CONCEPTS

INTRODUCTION

Chapters II and III discuss the mechanical design, fluid dynamics and heat transport, nuclear performance, and chemical compatibility issues relative to the tandem mirror reactor blanket concepts investigated during the scoping phase of the Fusion Breeder Program (FBP). These topics are addressed in sections A through D, respectively of the two chapters. The intent of the scoping phase of the study was to select a reference design to be developed in greater depth as the study progresses. The four liquid metal cooled blanket design options discussed in Chapter I were identified as possible candidates for the scoping phase at the outset of the FY82 program and the options will be discussed in the following sections.

II.A MECHANICAL DESIGN

II.A.1 Pipe Cooled Concept Considerations

Some of the key considerations for designing the internal pipe cooled blanket are the first wall and other supporting structure within the blanket, the fuel form (which in this case is spheres), the piping/cooling arrangement and the magnet/shielding interfaces. The structure, particularly the first wall, must be thin enough to provide attractive neutronic performance but adequate to sustain the coolant pressure loads and the dead weight of the fuel/heat transfer fluid mixture. Since the heat transfer fluid (sodium or lithium) is low density and the ratio of beryllium to fuel in the blanket is 15:1, the weight of the mixture is not high. The use of higher density $Li_{17}Pb_{83}$ in the blanket would require more structure and its use would not be favored in this respect. The inlet/outlet piping, which must be large as possible to maintain low coolant velocities and minimize MHD pumping power competes for space available with the magnets and their shielding. These considerations have an important effect on determing the size of the module and the size of the fissile breeding region of the blanket.

II.A.2 Pipe Cooled Concept Description

The pipe cooled blanket concept evolved based on guidelines developed in Table II.A-1 and the magnet geometry of Figure II.A-1. The pipe cooled concept is very similar to one investigated during the FY81 study[1] and described in Chapter I.

TABLE II.A-1 Blanket module configuration guidelines.

Total length of module	5 m
First wall radius	1.5 m
First wall loading	1.6-2 MW/M^2
First wall lithium coolant annulus radial gap	0.5-5 cm
Coolant pressure at first wall	∿100 psi
Fertile fueled region thickness	∿60 cm
Graphite reflector region thickness	∿60 cm
Magnet pitch	2.5 m
Fuel and beryllium form	Spheres
Sphere size (dia.)	>1 mm

As shown in Figure II.A-2 the coolant enters the module through a set of radially oriented pipes and the flow enters a common manifold which supplies coolant to the first wall annulus at the main part of the blanket and also supplies coolant through a series of axially aligned pipes to cool the outer blanket region. The fuel spheres are loaded at the top center of the module and are extracted at the bottom (details not shown). The first wall lithium annulus is bounded by the first wall at the inside region of the blanket and the intermediate wall which separates the lithium annulus from the outer fertile fueled region of the blanket. The walls are connected by a series of radial supports for additional structural strength and rigidity. The blanket details have been enlarged for clarity in Figures II.A-3 and 4, and the configuration is essentially that used for the parallel supporting thermal/hydraulics and neutronic analysis performed during the study.

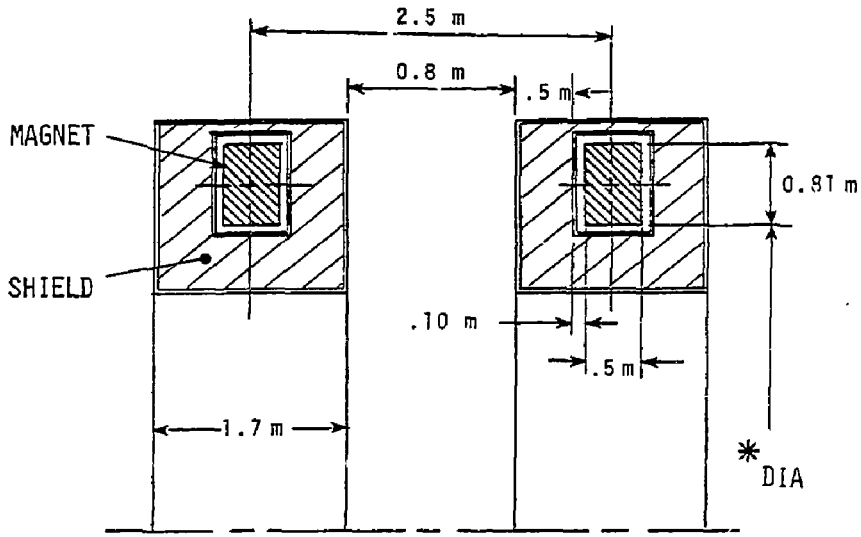

MAGNET BUILD	
- WIDTH	0.5 m
- RADIAL DEPTH	0.81 m
DEWAR ALLOWANCE	0.10 m
SHIELD THICKNESS (SIDES)	0.50 m
SHIELD THICKNESS (INNER BORE)	1.0 m
MAGNET PITCH	2.5 m
CLEARANCE BETWEEN MAGNETS (INCL. SHIELD)	0.8 m
*Magnet Inner Bore Diameter (For Coolant Pipes Outside of Magnets)	~8.0 m

FIG. II.A-1. Magnet geometry for the liquid metal cooled blanket.

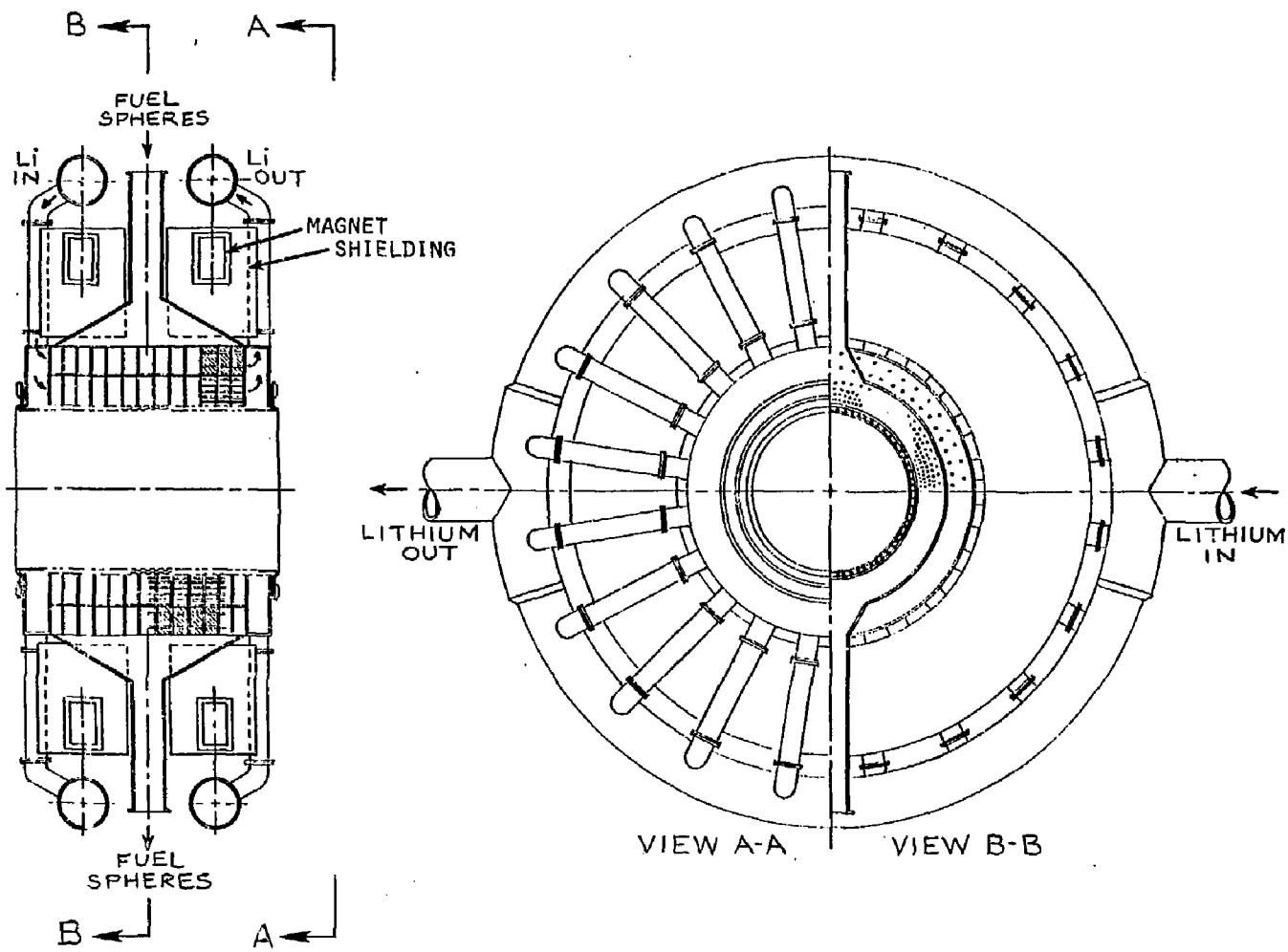
B
A
FUEL SPHERES
Li IN
Li OUT
MAGNET
SHIELDING
FUEL SPHERES
B
A
LITHIUM OUT
LITHIUM IN
VIEW A-A
VIEW B-B

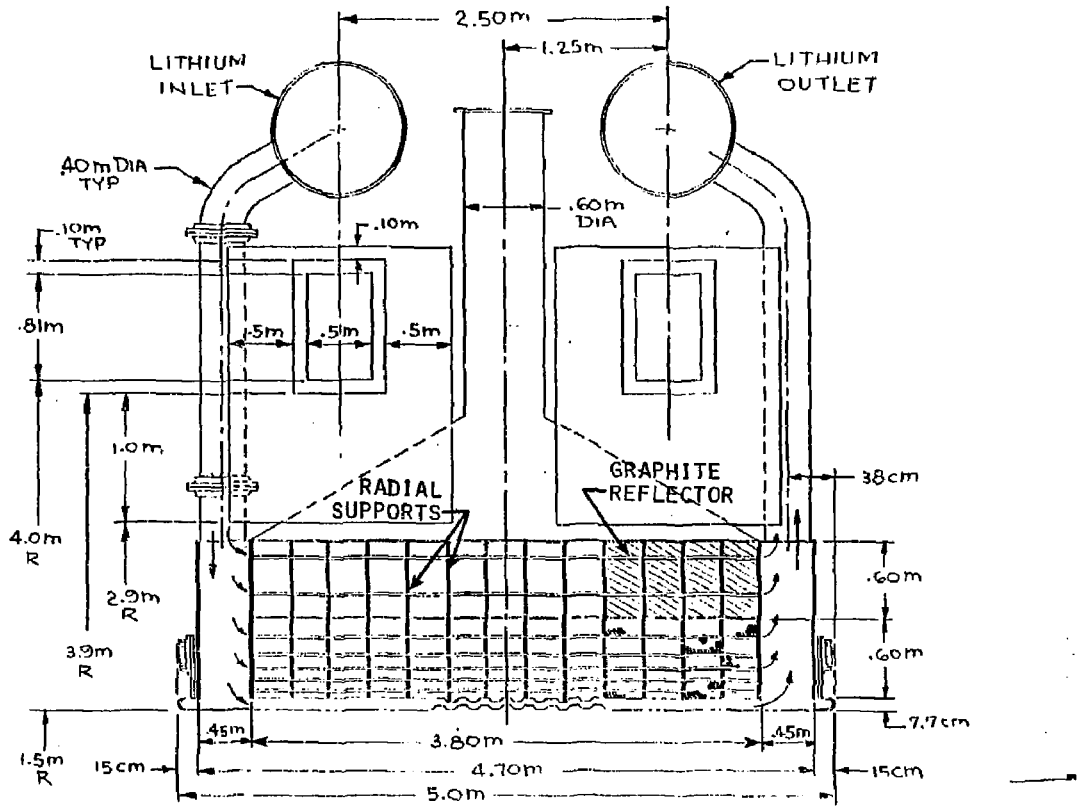

FIG. II.A-3. Fusion Breeder Reactor pipe cooled blanket concept cross section - details enlarged.

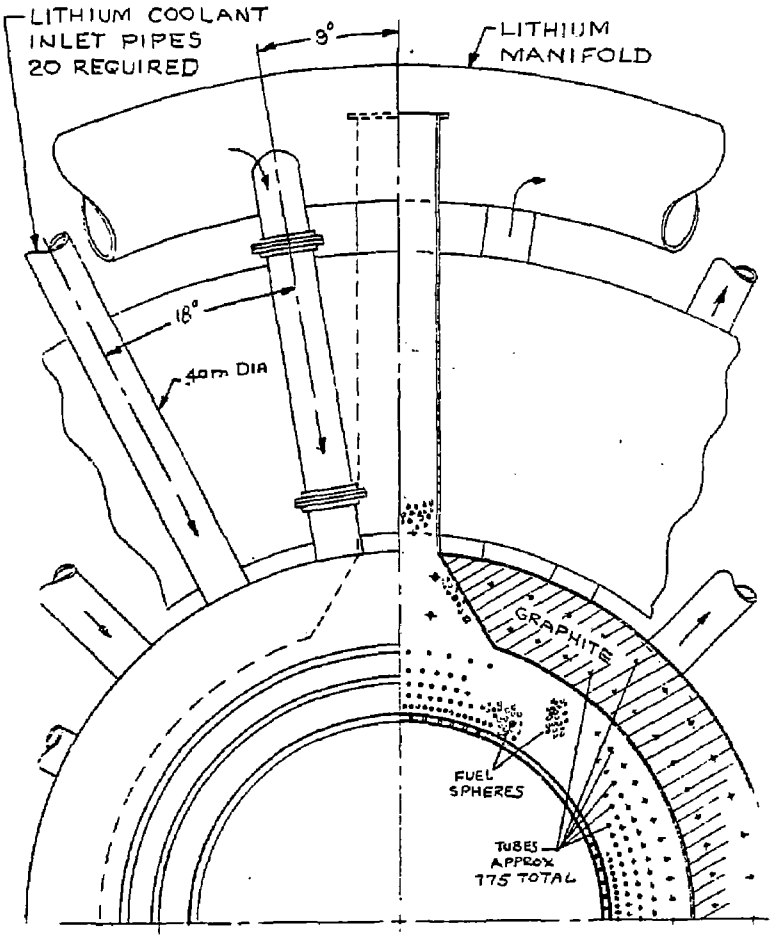

FIG. II.A-4. Fusion Breeder Reactor pipe cooled blanket concept enlarged - end view.

As shown in these figures, lithium coolant from twenty 0.4 m diameter inlet pipes enters the common manifold at the end of the module where the flow divides between the first wall coolant annulus and the ∿800 coolant pipes (2.5 cm in diameter) required to cool the fertile fueled region containing the spheres of fuel and beryllium and a graphite reflector near the outer region. The two flows combine at the common manifold at the opposite end of the blanket module and flow out through another similar set of 20 radial pipes 0.4 m in diameter. Because a structurally thin first wall is a prerequisite to attain satisfactory neutronic performance, the first wall is corrugated to provide stiffness and is connected to the intermediate wall (which is also corrugated) by radial supports on ribs. The ribs are spaced to withstand the ∿100 psi coolant pressure without exceeding permissible bending stresses in the sections of the shell which span the ribs. In addition, this combined double shell is tied to the outermost shell of the module by circumferential stiffeners to help support this shell assembly against buckling due to the pressure in the fertile fuel region. In the event of a coolant leak, this pressure could increase to the 100 psi first wall annulus pressure and the module would not fail due to overpressurization.

The preliminary corrugation sizing and geometry shown in Figure II.A-5 is an enlarged view of a section of both the first and intermediate walls. Although it would be more desirable to have a deeper corrugation for structural stiffness, concerns relating to the MHD effect of undulating lithium coolant flow through the annulus and minimizing the lithium thickness to maximize breeding led to a compromise which limits the depth of the corrugation to the 2.85 cm dimension shown. Although the corrugation is basically the same shape, the thickness and spacing (annulus) between the corrugations (noted by the asterisked dimensions) is increased for the direct cooling case to be discussed in Chapter III. The corrugations were sized based on considering the use of modified 316 SS prime candidate alloy (PCA) identified for use in the STARFIRE DESIGN.[2] Ferritic steels (e.g., HT-9 and 2-1/4 Cr-1 Mo) were identified as alternative structural candidates (see Section IV.D).

Since many (∿800) small coolant tubes are required to cool the outer blanket region, structural loads due to the sphere weight acting on the tubes (when the spheres are being loaded or discharged) limit the span of the tube section if tube bending is to be avoided. The radial stiffeners which support the first wall/intermediate wall assembly, also function as tube sheets which

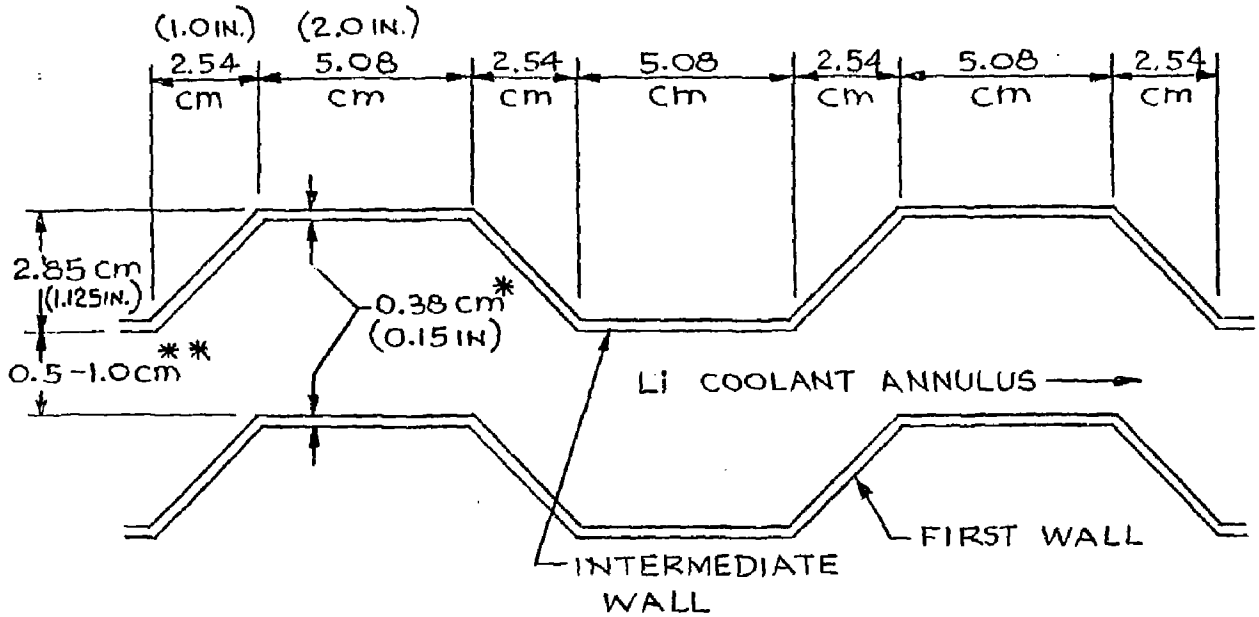

*0.54 (0.21 in), Direct Cooling Case

**5 - 10 cm, Direct Cooling Case

PLASMA

FIG. II.A-5. Fusion Breeder Reactor preliminary corrugation sizing for the pipe cooled

support the tubes at frequent intervals along their length. A spacing between the supports of approximately 30 cm (1 foot) might require about 12 axial fueling stations per module. In addition, the close spacing between tubes requires that the small fuel and beryllium spheres be limited to about 1 mm diameter to assure that the spheres will not jam between the tube-to-tube and tube-to-wall spacing when the spheres are to be released from, or charged to, the blanket. Finally, Figure II.A-6 shows a tentative coolant tube arrangement necessary to cool the outer blanket and graphite reflector.

The design features for the pipe cooled blanked concept are summarized in Table II.A-2. Further discussion of the internal pipe cooled design will be deferred until Chapter III where it is compared with the other scoping phase coolant concepts.

TABLE II.A-2 FBR Internal pipe cooled blanket concept design features

Total Length	5 m
Length of Fertile Region	3.8 m
Fraction of Blanket Length	76%
Lithium Coolant Annulus Thickness	∿3.0 - 3.5 cm*
Fertile Fueled Region Thickness	∿0.6 m
Fuel Sphere Diameter	>1 mm
Graphite Reflector Thickness	∿0.6 m
Corrugated First Wall Thickness	0.36 cm
Pressure Across First Wall	∿100 psi
Corrugated Intermediate Wall Thickness	0.36 cm
Lithium Coolant Tubes - Quantity (est)	700 - 1000
Size	2.54 cm (1.0 in) ID
Thickness	0.05 cm (0.020 in)
Inlet/Outlet Coolant Pipes Required	20 each
Coolant Pipe Diameter	∿0.4 M
Structural Material	316 SS**

*Effective Coolant Channel Thickness is 0.5-1 cm

**Prime Candidate Alloy (PCA - STARFIRE)

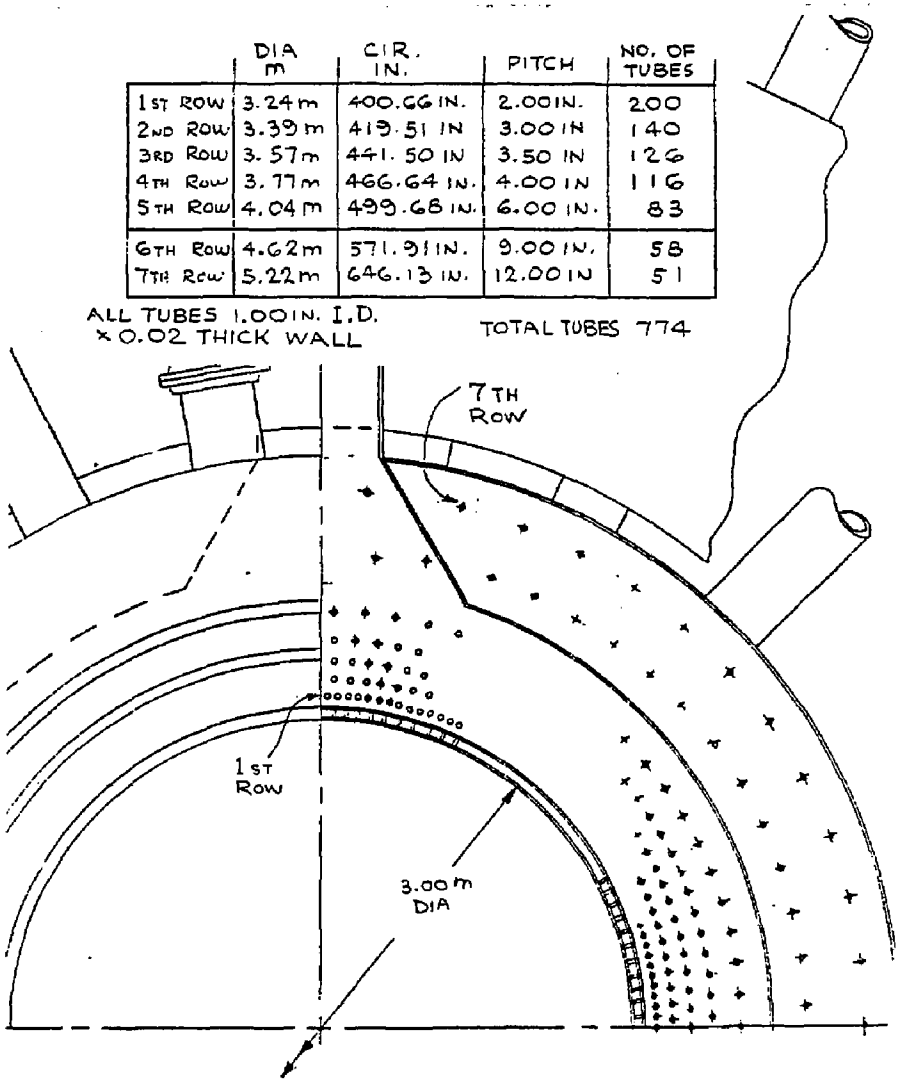

FIG. II.A-6. Fusion Breeder Reactor pipe cooled blanket concept - axial coolant pipe arrangement.

REFERENCES

1. TMHR Study Final Report (to be issued).

2. "STARFIRE: A Commercial Tokamak Fusion Power Plant Study," Argonne National Laboratory Report ANL/FPP/80-1, (Vol. I) September 1980.

II.B FLUID DYNAMICS AND HEAT TRANSPORT

During the scoping phase of this study, thermal-hydraulic calculations were made to compare the internal pipe cooled and direct cooled designs. These calculations include liquid metal circuit pressure drops in the blanket, corresponding pumping power requirements, and maximum temperatures for critical materials in the blanket, i.e., structural material, beryllium, fertile material, and the liquid metal.

The reference reactor parameters for these calculations are the following:

First wall radius	1.5 m
Neutron wall loading	2 MW/m^2
Module length	5 m
Blanket thickness	0.6 m
Graphite reflector thickness	0.6 m
Blanket energy multiplication	1.5
Module thermal power	141 MW

The maximum volumetric power generation was taken to be 20 MW/m^3 and 10 MW/m^3 for the structural material and the homogenized mixture of beryllium and thorium balls in liquid metal, respectively.

The pipe cooled blanket option has lithium circulating in axially oriented pipes and a separate lithium-cooled first wall. The fertile material, beryllium balls, and sodium heat transfer medium fill the space between the pipes. The pressure drops were evaluated for two parallel circuits, the axial pipe flow, and the first wall flow between the inlet-outlet coolant plena. Results for the pipe cooled blanket are presented in this section. The comparison of the pipe cooled blanket with the direct cooled blanket is presented in Section III.B of this report.

Figure II.B-1 illustrates the first wall configuration under consideration. The wall has to be corrugated for configurational stability.

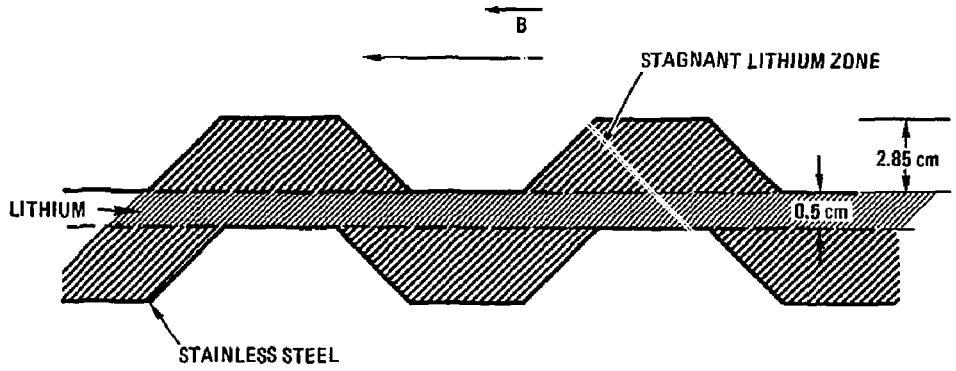

FIG. II.B-1. Corrugated first-wall configurations.

irradiation. Development of a detailed multidimensional MHD-flow model of this flow configuration was not possible within the limits of the scoping phase of this study. The following simplified flow model was assumed.

Because of the presence of the strong magnetic field at 3T, the fluid flowing against the field lines will be strongly retarded. Therefore, the coolant lithium was assumed to flow in the 0.5 cm width annulus along the direction of the magnetic field, where the lithium in the "troughs" to each side of the annulus was assumed to be stagnant. The power generated in the metallic structure, in the lithium coolant, and 5 cm into the blanket was conservatively assumed to be carried by the circulating first wall lithium coolant.

Figure II.B-2 illustrates the unit cell configuration of the first row of cooling tubes closest to the first wall. The power generated in the unit cell is assumed to be conducted to and removed by the circulating lithium coolant. The coolant circuit under consideration is given in Figure II.B-3. The notation used in the pressure drop calculations as illustrated in this figure are given in the following:

A = inlet pipe, fluid flow through a B-field gradient, $\Delta B = B$, (pipe diameter = 0.4 m)
AB = inlet plenum
B = corner
BE = first row of cooling tubes
E = corner
BC = first wall inlet plenum
C = corner
CD = first wall
D = corner
DE = first wall outlet plenum
E = corner
EF = outlet plenum
F = outlet pipe, fluid flow through a B-field gradient, $\Delta B = B$, (pipe diameter 0.4 m)

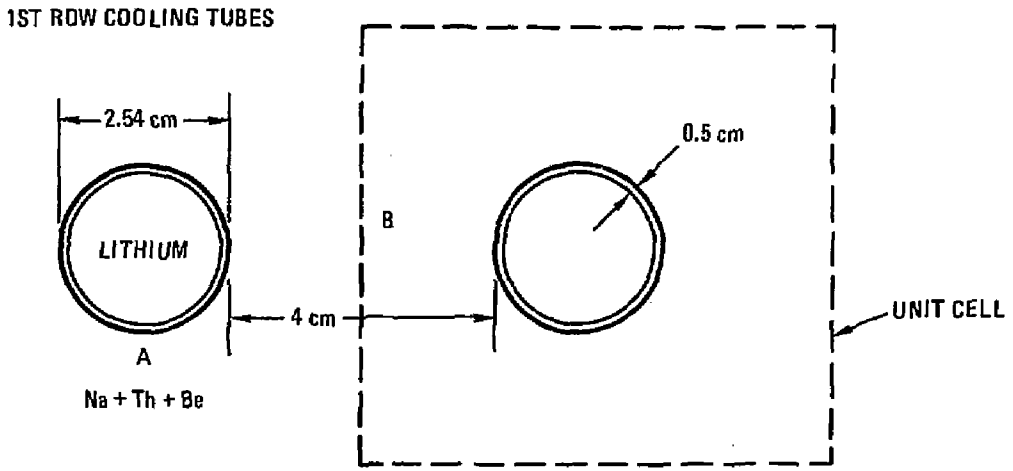

FIG. II.B-2. Tube flow unit cell configuration.

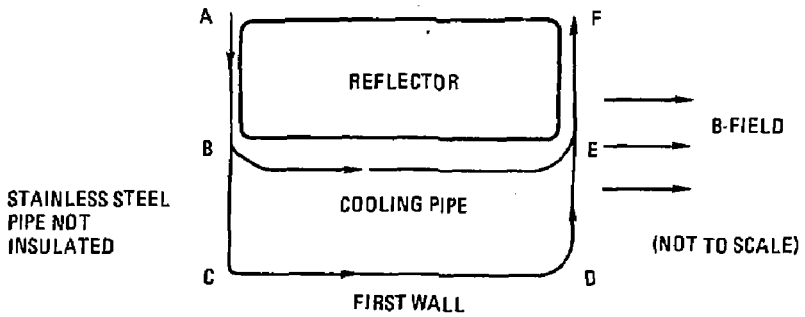

FIG. II.B-3. Tube flow lithium coolant circuit.

The key equations used in the MHD-fluid calculations are described below.

For the pressure drop due to fluid flowing in and out of a B-field increment equal to $\Delta B = B$ and the pressure drop due to a 90 degree corner, the following equation was used,[1]

$$\Delta P = 0.062\ VB^2 a\sigma \qquad (1)$$

where

V = bulk fluid velocity,

B = magnetic field strength,

a = flow channel width,

σ = fluid electrical conductivity.

This equation is applicable for insulated pipes covering a range of Reynolds numbers from 5×10^5 to 2×10^6 and Hartmann numbers (H) from 320 to 1400. It is used here to compare the designs. For conducting pipes, the turning pressure losses can increase by a factor of two. More detailed considerations will be needed for the reference design.

For the pressure drop due to MHD effects of flow across lines of contant B-field, the following equation was used,[1]

$$\Delta P_{\perp} = \frac{2VB^2 \sigma_w T_w L}{a\,(1 + C)} \quad \text{for } H \gg 1 + \frac{1}{C} \qquad (2)$$

where σ_w = wall electrical conductivity,

T_w = wall thickness,

L = channel length,

$C = 2\sigma_w T_w / \sigma a$

H = Hartmann number

$$= \frac{a}{2} B \sqrt{\frac{\sigma}{\mu}} \quad \text{(e.g., } H \approx 6.5 \times 10^{4} \text{ for 0.4 m pipe)}$$

where μ = fluid viscosity.

The ranges of C and H are $10^{-1} \rightarrow 10^{-3}$ and $10^{3} \rightarrow 10^{4}$, respectively, in these calculations.

Equation (2) is applicable for a conducting rectangular channel of width equal to a. A factor of 1.3 increase was recommended for pressure drop in circular pipes. Again, this equation is used for the scoping phase of this study only. More explicit presentation of suitable equations will be needed in the reference design.

With reference to Figure II.B-3, results of the calculations for the tube cooling design are given in Table II.B-1. These results indicate that the first wall will need to be designed to withstand a pressure of at least 0.39×10^{5} Pa (56 psi) which is reasonable from mechanical design and pumping power considerations. The 501°C maximum temperature of the first wall was calculated by taking the maximum coolant outlet temperature of 420°C and adding the temperature differentials of the stagnant lithium in the "trough" to each side of the annulus (77.7°C) and of the stainless steel structure (3.8°C). The stainless steel piping maximum temperature of 447°C was calculated by adding the coolant outlet temperature of 420°C to the lithium film drop temperature and the piping solid temperature differentials of 27° and 0.05°C, respectively. In the stagnant Na + Th + Be mixture, the maximum temperature is 475°C, from the addition of the conduction temperature differential to the maximum pipe temperature, which is less than the maximum allowable temperature of 500°C.

From these thermal-hydraulic evaluations, it may be concluded that the pipe cooling design has acceptable pressure drops and pumping power requirements. The maximum material temperatures are also acceptable. Comparison of this design with the direct cooling design is presented in Section III.B.

TABLE II.B-1. Pressure drops and pumping power of pipe cooled design with lithium coolant. [For B = 3T and $\sigma_{Li} = 3.3 \times 10^6$ $(\Omega m)^{-1}$]

Pressure Drops Pa (psi)	First Row Tube Circuit	First Wall Circuit
ΔB-field at A	1.7×10^5	1.7×10^5
Inlet tube, AB	0.5×10^5	0.5×10^5
Corner at B	1.1×10^5	--
First row of tubes, BE	170	--
Inlet pipe, BC	--	0.25×10^5
Corner at C	--	0.6×10^5
First wall flow, CD	--	0.12×10^5
Corner at D	--	0.6×10^5
Outlet pipe, DE	--	0.25×10^5
Corner at E	1.1×10^5	--
Outlet pipe, EF	0.5×10^5	0.5×10^5
ΔB-field at F	1.7×10^5	1.7×10^5
Total	6.6×10^5 (96)	6.2×10^5 (90)
Pumping power (MW)	0.35	0.33
Pumping power fraction	0.25%	0.23%

Reference

[1]M. A. Hoffman and G. A. Carlson, "Calculation Techniques for Estimating the Pressure Losses for Conducting Fluid Flows in Magnetic Fields," UCRL-51010, TID-4500, UC-20, 1971.

II.C Nuclear Design, Analysis and Performance

Objectives - Tritium and U233 breeding, energy multiplication, power density, fissile buildup and other isotopics, are nuclear parameters important in the design and evaluation of blankets for fusion breeders. The basic nuclear objective of a fission-suppressed blanket is to maximize fissile breeding while breaking even in tritium ($T \sim 1.0$) and suppressing fission of both the fertile and bred fissile materials. In addition to the nuclear objectives, blanket structure, heat transfer and fuel handling requirements must be met. Thus an interactive and iterative design processes is required.

If nuclear performance was the only requirement, the blanket would consist of beryllium (Be) plus a few atom percent Li-6 and Th 232 and its breeding ratio (T + F) would be about 2.7.[1] Thus the potential nuclear performance of the Be blanket is high. The question now is how much of this potential performance can be achieved when structure, heat transfer and other blanket requirements are met. To answer this question the blanket(s) must be modeled and analyzed by one or more neutron and gamma transport methods. For this work the 3D Monte Carlo code TARTNP with the 175 group ENDL data library is used.[2,3]

Modeling - The basic model used to analyze the "Pipe-Cooled Blanket" is a nested set of concentric cylindrical shells surrounding a cylindrical source of 14 MeV neutrons. End effects were not included but will be later in the study. The geometry and composition of the blanket shells for the base case is shown in Figure II-C-1. Starting at the left the blanket consists of a first wall consisting of 2, 0.25-cm walls (Fe) separated by a 3-cm coolant plenum containing Li + 2.5 v/o Fe. The 2.5 v/o Fe accounts for the stiffening ribs. Following the first wall is a 60-cm Be zone composed of homogenized unit cells. Each unit cell is 6.6 cm square and consists of a Li coolant pipe surrounded by Be and thorium spheres (62 v/o) in a 14-to-1 ratio. The space between the spheres (38 v/o) contains sodium (Na). In addition to the pipe wall (0.92 v/o) the Be zone contains 3 v/o Fe to account for internal structure. The Be is at 90% of theoretical density to account for swelling. The Be zone is followed by 2 cm of Fe and a 60-cm graphite reflector.

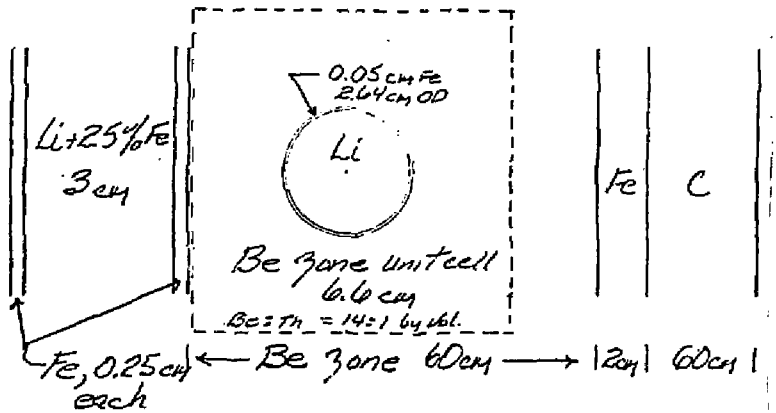

Be Unit Cell Volume Fractions

Material	VF
Be (0.9 Th)	0.490
Li	0.115 (5% ^{6}Li)
Fe	0.0392
Th	0.0350
U233	0.25% of Th
Na	0.321

FIGURE II.C-1. Base case blanket description

Performance - The nuclear performance parameters for this base case are listed in Table II.C.1. The "bottom line" is that this blanket model gives a net breeding ratio (T + F) of 1.83 and an energy multiplication (M) of 1.63. Reactions of interest in the various blanket zones are listed in the table. Breeding reactions account for 95% of total captures in this blanket, thus parasitic capture is low. When compared with the theoretical value of 2.7 this blanket design achieves 70% of theoretical breeding. The difference is the result of moderation by materials other than Be, thus reducing Be (n,2n) reactions.

TABLE II.C.1 - BASE CASE BLANKET RESULTS:
(Pipe Case)

Zone	T^6	T^7	Th (n,γ)	Fe (n,γ)	Cap. TOT.
Fe(1)	-	-	-	.004	.01
Li	.198	.082	-	.001	.208
Fe(2)	-	-	-	.005	.009
Be	.672	.039	0.855	.034	1.73
Σ	.870	.121	.855	.044	1.96

ADDITION Be ZONE DATA

Na (n, gamma)	.019
Be (n, gamma)	.002
U233 (n, fission)	.012
U233 (n, gamma)	.002
Th (n, fission)	.011

BOTTOM LINE:

T = 0.991 F = .855 T + F = 1.85
(94.5% of Cap. TOT.)

M = 1.63 F_{net} = .841 T + F_{net} = 1.83

Captures in outer Fe zone = .005
Captures in outer C zone = .006

First wall thickness and composition have an important effect on breeding. To quantify this effect first wall Fe, Li, and Fe + Li thickness was decreased by 90% and increased by 100%. As shown in Figure II.C.2, Fe thickness has the most significant effect (ΔF = + 12%, - 8%) while Li the least (ΔF = + 3%, - 3%). It is interesting to note that increasing (or decreasing) both Fe and Li together has less effect (ΔF = + 11%, - 6%) than Fe alone.

Structure in the Be zone may also have a significant effect. When the Fe volume fraction is doubled (to 7.8 v/o) fissile breeding (F) drops by 5%. When the Fe is reduced to 0, F increases by 12%. Because the Fe is homogenized in the Be zone its effect is probably overpredicted.

The Li-6 isotopic concentration is 5 atom % for the base case. When it is increased to 50 atom % T increased and F decreased, but total breeding (T + F) did not change.

Spatial heating by neutrons and gammas is an important aspect of blanket nucleonics for it specifies heat transfer requirements which in turn affects structural requirements which then in turn affects breeding. Neutron and gamma heating vs radius calculated for the base case blanket is shown in Figure II.C.3 for a 2 MW/m^2 first wall loading (energy current of 14 MeV OT neutron). Maximum heating (14 w/cc) occurs in the first Fe zone. Average heating in the 3-cm Li zone is 11 w/cc, and is 13 w/cc in the 2nd, 0.25-cm Fe zone. Average heating in the first 7 cm of the Be zone is 10 w/cc dropping to 0.8 w/cc in the outer 14 cm of this 60-cm zone.

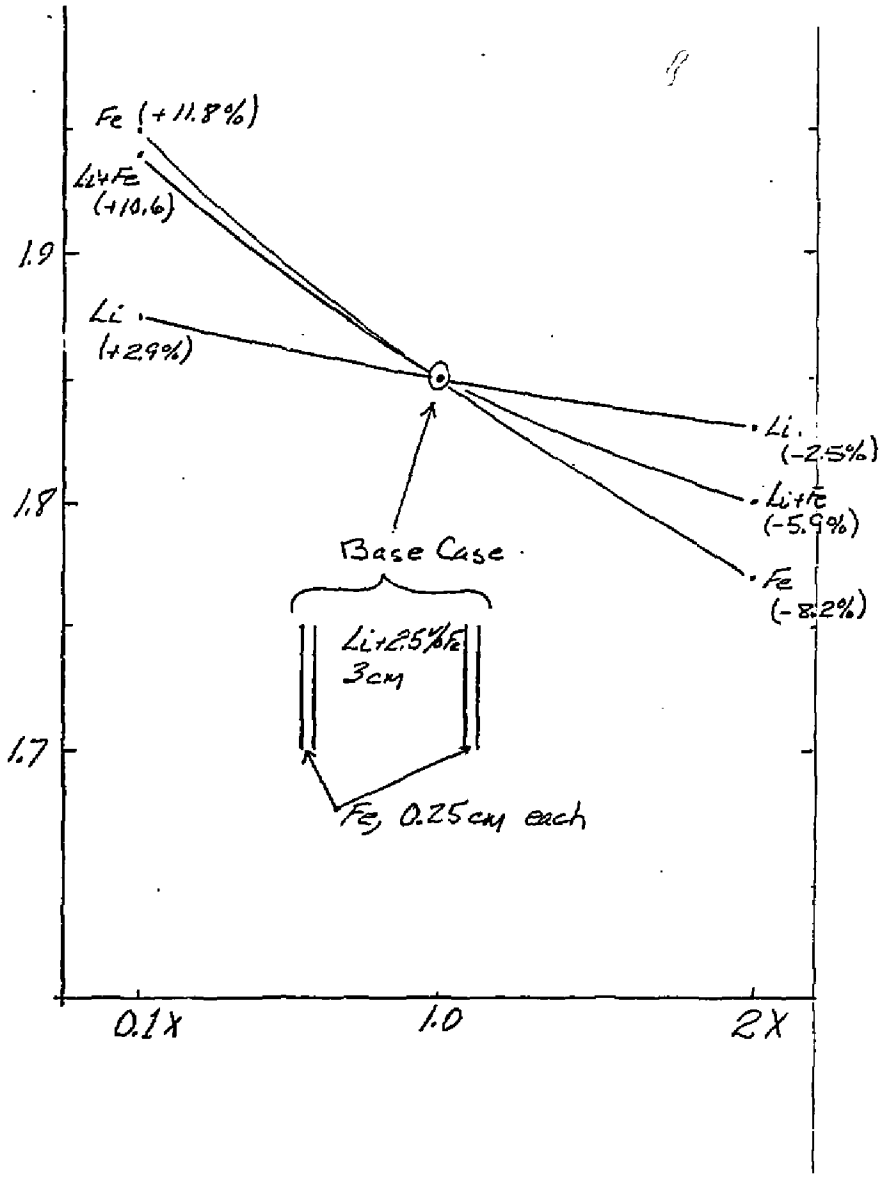

FIGURE II.C-2. T+F vs. first wall variations (ΔF%, F = T+F - 1.0)

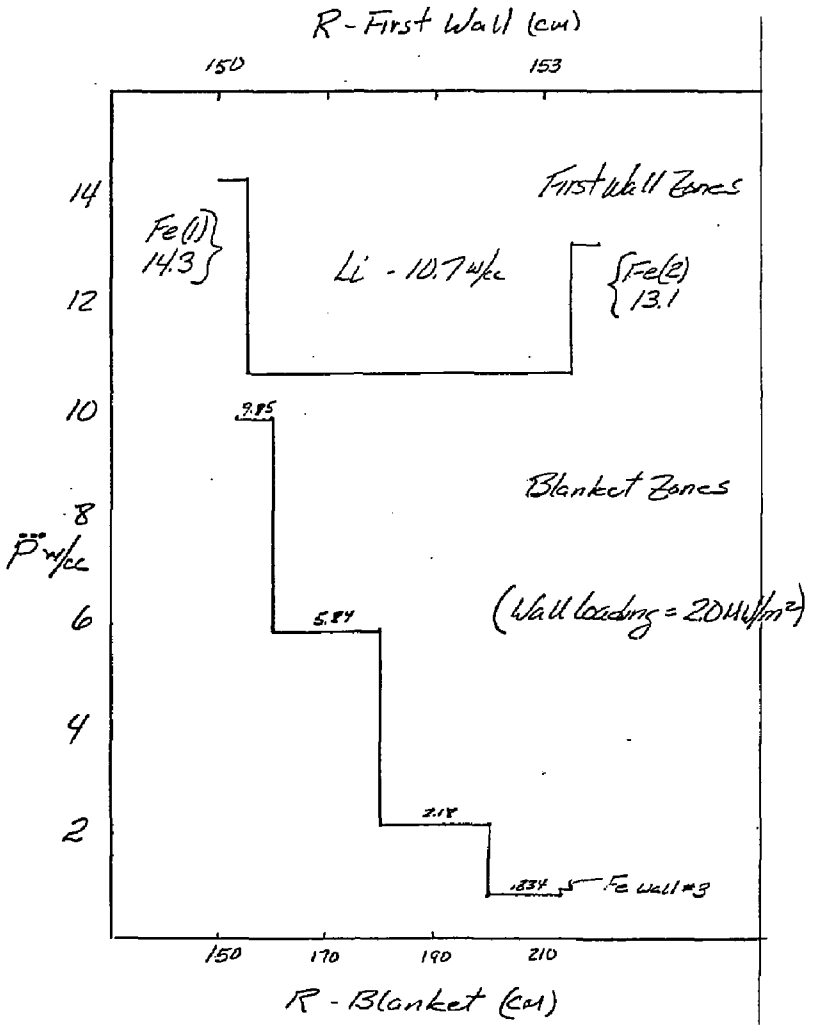

FIGURE II.C-3. Power density (n+γ) vs. R for base case

Spatial buildup of U233 and its precurser Pa 233 in the thorium is another important nucleonics parameter for it influences what the fuel management scheme should be. As shown in Table II.C.2 the buildup rate (Th (n, gamma)) in the first 7 cm of the Be zone is 0.54 atom % per month dropping to 0.07% in the outer 13 cm. Because the peak to average buildup rate is 2 to 1 and the ratio of maximum to minimum is almost 10, this blanket should probably be broken into one inner (27 cm) and one outer (33 cm) fuel management zone. If a discharge enrichment of ∿ 0.5 atom % is required the inner zone must be changed every month, the outer zone every 5 months.

TABLE II.C.2 - SPATIAL BUILDUP

Be Zone	R Inner (cm)	Th(n, gamma) (per DT-neut.)	Buildup* (% Th/month)	Buildup (relative)
1	153.5	0.168	0.542	2.1
2	160	0.448	0.426	1.7
3	180	0.201	0.173	0.7
4	200	0.054	0.066	0.3
	213			

*For a first wall loading of 2.0 $MW.m^2$

There is some interest in using LiPb in place of Li. From a nucleonics view point there appears to be little difference between the two; T + F is the same when LiPb replaces Li in the base case. Table II.C.3 compares the two.

TABLE II.C.3 - Li vs LiPb COOLANT (17v/o ^{6} Li + 83v/o Pb)

	Li	LiPb
T^6	.870	1.23
T^7	.121	-
T TOT	.991	1.23
Th (n, gamma)	.855	.612
T TOT + F	1.85	1.84

Heterogeneous Effects - The analysis discussed in the previous sections treated the Be zone as a homogeneous mixture. This section discusses an initial attempt to determine heterogeneous effects on breeding and heating.

Model - The model used to estimate these effects is shown in Figure II.C.4. It is a unit cell consisting of a thorium sphere, a Fe pipe containing Li and a proper mixture of Be and Na in the remaining volume. All six sides of the unit cell have reflecting boundaries so it appears to a 14 MeV source neutron like an infinite assembly of these unit cells.

Results - When the unit cell is homogenized and compared to the heterogeneous case; the homogeneous case overpredicts breeding by 5% and M by 3% for the Th only case and overpredicts breeding by 2% and underpredicts M by 16% for the Th + .25 a/o U233 case.

The fraction of total heating in the Th sphere was 24% and 49% for the Th only and Th + .25 a/o U233 case, 28% and 18% in the Li and 47% and 37% in the Be + Na mixture. More complete results are listed in Table II.C.4.

At this point the bottom line is that homogeneous modeling of the Be zone does an acceptable job of predicting breeding and that between 24% and 49% of total heating is in the thorium + U233 spheres. A finite heterogeneous model of the blanket is being developed so the spatial effects of energy partitioning can be determined.

References:

1. J. D. Lee, "The Beryllium/Molten Salt Blanket," Lawrence Livermore National Laboratory, Livermore, CA, UCRL-82663 (1979); also published in Proceedings of the 3rd US/USSR Symposium on Fusion-Fission, Princeton, NJ (1979).

2. TARTNP: A Coupled Neutron-Photon Monte Carlo Transport Code, Lawrence Livermore National Laboratory, Livermore, CA, UCRL-50400, Vol. 14 (July 1976).

3. The LLL Evaluated Nuclear Data Library (ENDL): Evaluation Techniques, Graphical Displays and Descriptions of Individual Evaluations, Lawrence Livermore National Laboratory, Livermore, CA, UCRL-50400, Vol. 15 (September 1975).

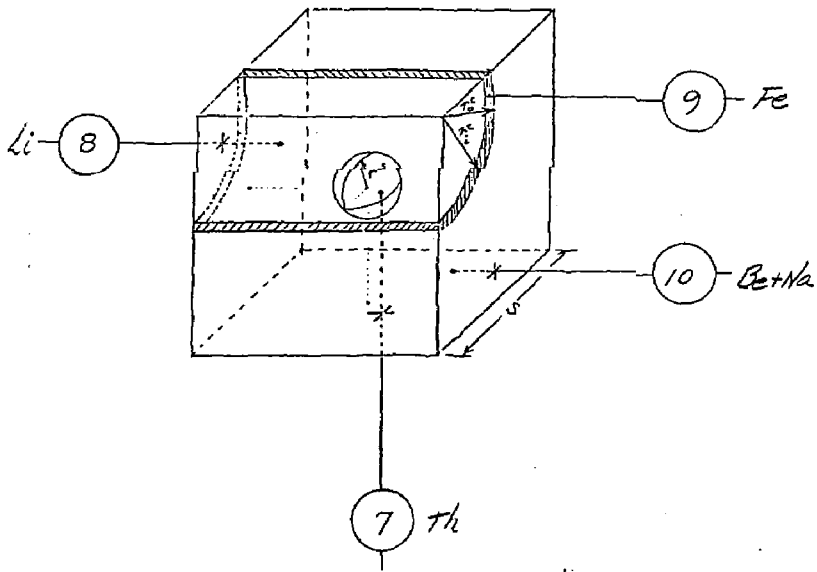

	DIMENSIONS (cm)
S	3.32
r^s	0.68132
r_i^c	1.27
r_o^c	1.32

FIGURE II.C-4. Unit cell heterogenious model

TABLE II.C.4 - HETEROGENEOUS EFFECTS IN PIPE BLANKET

RESULTS	CASE	
	Th	Th + 0.25a/o U233
T + F (He)	1.99	2.09
T + F (Ho)	2.09	2.13
Relative T + F		
He/Ho	0.95	0.98
M(He)	1.55	2.43
M(Ho)	1.59	2.09
Relative M		
He/Ho	0.97	1.16
E* - thorium (%)	24	49
E - Fe pipe (%)	1	1
E - Li (%)	28	18
E - Be + Na (%)	47	32

*Energy deposition

II.D Chemical Compatibility Issues

II.D.1 Introduction

This report considers the chemical compatibility issues that are associated with the internal pipe cooled breeder blanket design. In this concept, the structural materials and pipe materials are constrained to be the same: One question was whether they should be an austenitic steel (AISI 316) or a ferritic steel (AISI 410 or ASME 387 Grade 22). The other questions concerned the compatibility of the various solid materials with each other and the two molten metals. General considerations relating to liquid metal compatibility and the choice between ferritic and austenitic steels are discussed further in Section IV.B.

The pipe cooling blanket concept is illustrated schematically in Figure II.D.-1. Beryllium and thorium spheres (1 - 5 mm diameter) are packed in liquid sodium, while the coolant, liquid lithium, flows in the steel pipes. A maximum temperature in the packed bed is expected to be $\sim 500^{\circ}C$ and the maximum temperature of the cooling pipes is to be $400^{\circ}C$. Major chemical compatibility issues in this packed bed are solid-solid interactions, corrosion of berryllium and thorium in molten sodium and corrosion of steel in molten lithium.

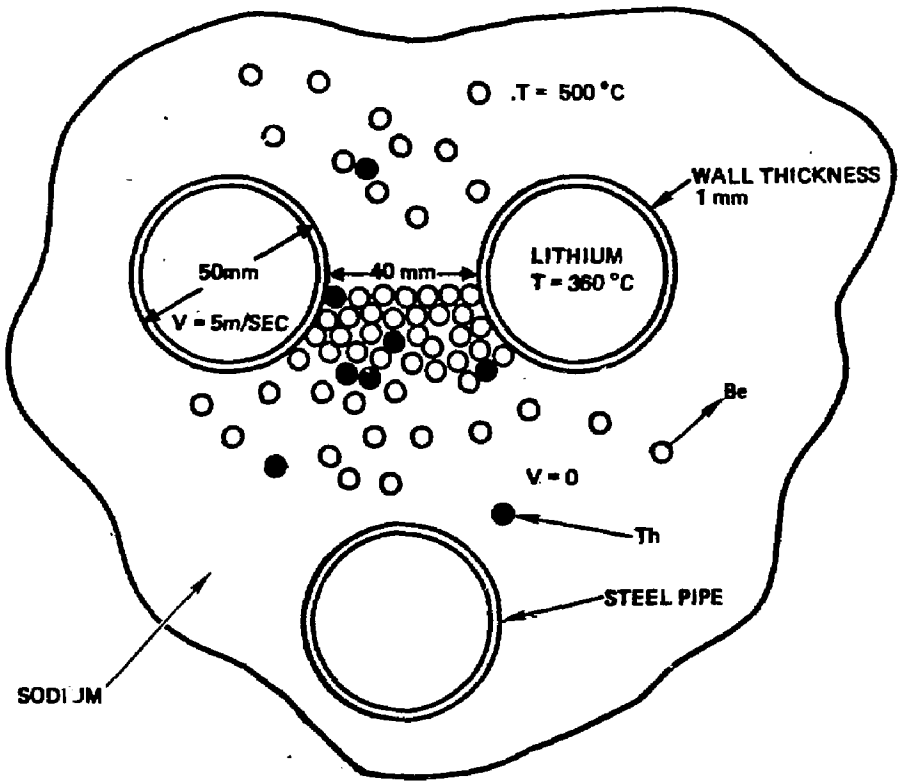

Figure II.D.-1. Pipe Cooling Blanket

II.D.2. Solid-Solid Interactions

II.D.2.a. Beryllium-Beryllium Interactions

Sintering of beryllium spheres may cause a serious problem in the pipe cooling concept. In the case of solid-solid contact in liquid, the sintering may take placed by dissolution-precipitation, volume diffusion or surface diffusion. In addition, a hot pressing may occur because of the small contact area and close packing of beryllium spheres.

Mass transfer of beryllium in liquid sodium is described in Figure II.D.2

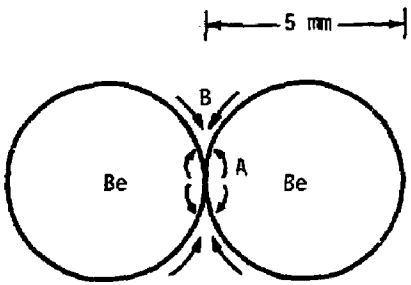

Figure II.D.-2.

Because surface diffusion data for beryllium on an oxide-free beryllium surface are not available, it is difficult to make a firm quantitative prediction. However, a rough estimate can be made based on a value for the bulk self diffusion of Be in Be at 500°C,

$$D(\text{self}) = 4.5 \times 10^{-12}\ \text{cm}^2/\text{sec}$$

Considering a diffusion zone thickness similar in concept to that when chemical interdiffusion occurs, the thickness is the distance over which the chemical composition has changed from its original value to half of the final value. The expression is

$$\underline{X} = \sqrt{Dt}$$

so for the case of Be in Be,

$$\underline{X} = 120\ \mu\text{m/yr}$$

$$= 0.12\ \text{mm/yr}$$

Since the radius is 0.5 - 2.5 mm, this zone is an appreciable fraction of the total sphere. This calculation, despite its simplifying assumptions,

may indicate that self-sintering (or self-welding as it is sometimes called) may be an important phenomenon in the bed.

It should be noted that the kinetics of self-sintering may be much faster than that calculated above because mass motion due to surface diffusion is generally more rapid than that computed from bulk diffusion values. Also, mass transfer by dissolution and precipitation is probably more rapid than bulk diffusion.

The effects of self-sintering are detrimental to the operation of the breeder blanket:

1. Sintering complicates removal of the beryllium spheres from the blanket during fuel recycling.
2. Beryllium sintering complicates the removal of thorium spheres because thorium spheres are distributed among the beryllium spheres*.

Up to this point, no consideration was given to the fact that under ordinary conditions of handling, beryllium is covered with an oxide film of approximately 10 nm. This oxide is fairly adherent and, if left intact, can prevent self-sintering. Using the same quantitative approach as above, we find that the "zone thickness" for Be diffusion in BeO is

$$X = \sqrt{Dt}$$

$$= 2 \times 10^{-3} \text{ μm/year at } 500°C$$

This assumes a diffusion coefficient value for Be in BeO of

$$D(Be) = 1.4 \times 10^{-21} \text{ cm}^2/\text{s}$$

at 500°C.[2]

The zone thickness is only a few atomic diameters per year and suggests that BeO is a good diffusion barrier.

However, it is not known if a BeO coating (or film) will remain stable in the presence of molten sodium at temperatures as high as 500°C.

II.D.2.b. Beryllium-Steel Interactions

A degree of beryllium-steel interaction is uncertain because of limited available data. ^{7}Be tracer studies show that beryllium penetrates

* The ratio of beryllium to thorium spheres is about 14:1.

into type 304 SS in liquid lithium; a depth penetration is found to be 5.5 μm at 4000 hr and 270°C.[3] This corresponds to ~8.1 μm/y with an assumption of parabolic reaction kinetics. At higher temperature, ~400°C, the penetration could be larger and a need for experimental studies are indicated.

II.D.2.c. Thorium-Beryllium Interaction

The formation of intermetallic compound $Be_{13}Th$ is known[4], but data for the diffusion rate of beryllium in thorium is unavailable in open literature. Therefore, a degree of interaction cannot be estimated. However, because the number of thorium spheres is small, the beryllium-thorium contact area per volume of bed is small compared to beryllium-beryllium case.

II.D.2.d. Thorium-Thorium Interaction

A self-diffusion of thorium was investigated by Schmitz and Fock.[5] The diffusion coefficient was reported as 1.9×10^{-32} cm^2/s at 500°C. Since this value predicts the diffusion zone thickness of 7.8×10^{-4} μm/y self-welding of thorium will not occur. Besides, thorium-thorium interaction will be nil because it is highly improbable that one thorium sphere will stay in contact with another thorium sphere for a significant length of time. If this improbable event does occur, it will not upset fuel removal in the way that Be-Be self-welding would.

II.D.2.e. Thorium-Steel

It is known that thorium forms intermetallic compounds with iron and nickel, but diffusion of thorium in iron is insignificant at 500°C. We estimated the diffusion zone thickness of 0.5 μm/y at 500°C, based on the diffusion coefficient determined by the extrapolation of 720 or 763°C data.[6]

II.D.3. Liquid Metal Corrosion

II. D.3.a. Corrosion of Steel Pipes in Liquid Lithium

Corrosion studies of steel in liquid lithium are not as extensive as in liquid sodium. However, in recent years, corrosion of steel in liquid lithium has become important because liquid lithium is one of the prime candidate breeding and cooling materials for fusion reactors.

In fusion breeder reactor design, type 316 stainless steel and 2 1/4Cr-1Mo steel are two major candidates for the structural and piping materials at present stage.

Whitlow et al[7] showed a comparison of corrosion rates between ferritic steels and stainless steels in the flowing lithium at 538°C. They reported that the corrosion rates of stainless steels are considerably higher than ferritic steels (shown in Figure II.D-3). The reason for the higher corrosion rate of the 300-series stainless steels is that the dissolution of nickel and chromium is faster than iron. The corrosion rates of the stainless steels decrease and eventually become equal to ferritic steels (not shown in Figure II.D-3) but reported verbally by J. DeVan of (ORNL).

The preferential dissolution of nickel and chromium is illustrated in Figure II.D-4.[8] The major concern in the dissolution of nickel and chromium is that these species may deposit in the colder region of the lithium loop, which can plug the heat exchanger pipes. Therefore, stainless steel in liquid lithium will cause more problems than ferritic steel.

A change of mechanical properties of one particular austenitic stainless steel, AISI 316, was investigated by Penici et al.[9] Their research concluded that a change of mechanical properties was mainly due to thermal aging (see Tables II.D-1 and 2) and not due to exposure to liquid lithium.

II.D.3.b. Corrosion of Beryllium and Thorium in Liquid Sodium

Solubilities of beryllium and thorium in molten sodium are unavailable in open literature. Hansen[10] noted that thorium was not attacked by sodium at 650 to 800°C. According to liquid metal handbooks, beryllium in liquid sodium maintains its stability up to 600°C.[11] We tentatively conclude that both are compatible with sodium at 360-500°C.

II.D.4. Summary

Table II.D-3 summarizes the chemical compatibility of the pipe cooling blanket concept. A major concern is the interactions of beryllium-beryllium and beryllium-steel in liquid sodium. The interactions of other material combinations appear to be nil at temperatures less than 500°C.

Testing of the chemical compatibility of berylliym-beryllium, beryllium-thorium and beryllium-steel in liquid sodium at 350 to 500°C is underway at the TRW Capistrano Test Site.

Testing of the chemical compatibility of beryllium, thorium and steels in lithium is currently conducted by Dr. DeVan at ORNL and the data will be available in the near future.

Reference: Whitlow, G.A., W.L. Wilson, W.E. Ray and M.G. Down J. Nucl Mater 85 & 86, P283, 1979

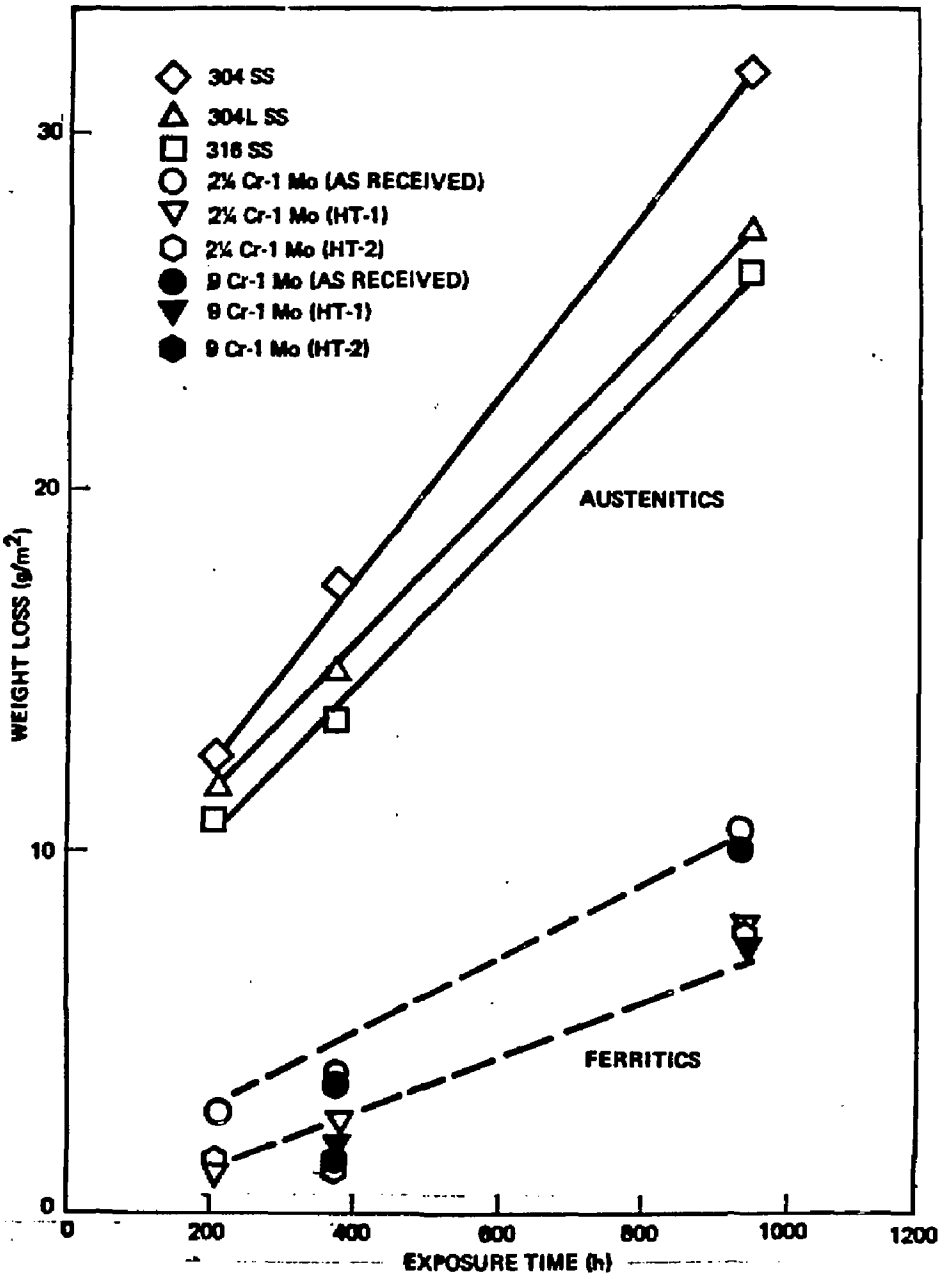

Figure II.D-3. Weight Loss of Austenitic and Ferritic Materials as a Function of Exposure Time in Flowing Lithium at 538°C (1000°F)

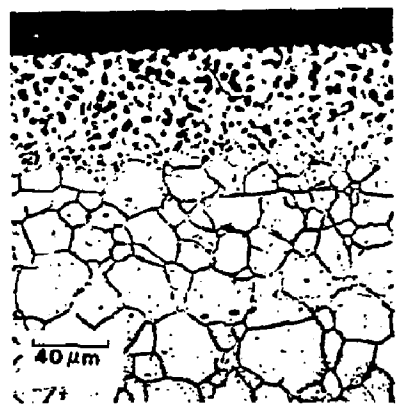

FIGURE II.D-4. COUPON H3 FROM LOOP 1 AFTER 9000 HR (596°C).

REF: TORTORELLI, P. F. AND J. H. DEVAN, J. NUCL. MATER. 85 AND 86, P 289, 1979.

TABLE II.D-1. ROOM TEMPERATURE TENSILE DATA OF VARIOUS TREATMENTS OF 316 SS OBTAINED AT INITIAL STRAIN RATE OF 7.57×10^{-4}/SEC

	0.2% YIELD STRESS		ULTIMATE TENSILE STRENGTH		PLASTIC STRAIN
	MPA	(KSI)	MPA	(KSI)	(%)
SOLUTION ANNEALED	379.5	(54.7)	588.4	(84.8)	58.6
AGED IN VACUUM FOR 1500 HR AT 600°C	315.7	(45.5)	607.5	(87.5)	69.3
EXPOSED TO Li FOR 1500 HR AT 600°C	263.8	(38)	612.2	(88.2)	80.7
EXPOSED TO Li + 40 PPM H FOR 1500 HR AT 600°C	312.3	(45)	585.9	(84.4)	63.4

TABLE II.D-2. 600°C TENSILE DATE OF VARIOUS TREATMENTS OF 316 SS OBTAINED AT INITIAL STRAIN RATE OF 7.57×10^{-4}/SEC

	0.2% YIELD STRESS		ULTIMATE TENSILE STRENGTH		PLASTIC STRAIN
	MPA	(KSI)	MPA	(KSI)	(%)
SOLUTION ANNEALED	203.3	(29.3)	383.6	(55.3)	37.2
AGED IN VACUUM FOR 1500 HR AT 600°C	132	(19)	328.9	(47.4)	58
EXPOSED TO Li FOR 1500 HR AT 600°C	128.1	(18.5)	352.3	(50.7)	43
EXPOSED TO Li + 40 PPM H FOR 1500 HR AT 600°C	166.2	(23.9)	369.4	(53.2)	36.1

REF: PENICI, P. V. COEN, J. ARRIGHI, H. KOLBE, T. SASAKI, E. RUEDL, J. NUCL. MATER. 85 AND 86, P 277, 1979.

TABLE II.D-3.

CHEMICAL COMPATIBILITY SUMMARY

PIPE COOLING BLANKET CONCEPT

COMBINATION OF MATERIALS	SUMMARY
Be-STEEL (AUSTENITIC, FERRITIC)	UNCERTAIN AT 400°C
Th-STEEL (A,F)	NO PROBLEM AT T $\leq$500°C
Li-STEEL (A,F)	~40 μM/YR AT 596°C Ni-DEPLETED ZONE IN AUSTENITIC (316) LOWER RATE WITH FERRITIC STEEL
Na-STEEL (A,F)	NO PROBLEM AT T $\leq$500°C
Be-Na	NO PROBLEM AT T $\leq$600°C
Th-Na	PROBABLY NO PROBLEM AT T $\leq$650°C
Be-Be	MORE ANALYSIS NEEDED
Be-Th	PROBABLY NO PROBLEM AT T $\leq$500°C
Th-Th	NO PROBLEM

SECTION II.D. REFERENCES

1. Pavlinov, L. V., G. V. Grigorev and V. G. Sevastianov, Fiz. Metal. Metalloved. Vol. 25, No 3, pp 565-567, 1968.
2. Cline, C. F., H. W. Newkirk, W. L. Barmore and R. R. Vandervoort, J. Amer. Ceram. Soc., Vol. 50, pp 221-2, 1967.
3. Anantatmula, R. P., W. F. Brehm, D. L. Baldwin and J. L. Bevan. J. Nucl. Mater., 85 & 86, pp 311-315, 1979.
4. Elliott, R. P., Constitution of Binary Alloys, First Supplement, p 172, McGraw-Hill Book Co., 1965.
5. Schmitz and Fock, J. Nucl. Mater,Vol 21, pp 317-322, 1967.
6. Patil, R. V., G. B. Kale and S. K. Khera, J. Nucl. Mater, Vol 97, pp 192-202, 1981.
7. Whitlow, G.A., W. L. Wilson, W. E. Ray, and M. G. Down, J. Nucl. Mater. 85 & 86, pp 283-287, 1979.
8. Tortorelli, P. F. and J. H. Devan, J. Nucl Mater., 85 & 86, pp 289-293, 1979.
9. Fenici, P., V. Coen, J. Arrighi, H. Kolbe, T. Sasaki, E. Ruedl, J. Nucl. Mater., 85 & 86, pp 277-281, 1979.
10. Hansen, P. M., "Constitution of Binary Alloys" McGraw-Hill Book Co., 1958.
11. Lyon, R. N., "Liquid Metals Handbook", 2nd ed., Report NAVEXOS, p 733, 1952.

CHAPTER III
DIRECT COOLING BLANKET CONCEPT

INTRODUCTION

This chapter discusses the mechanical design, fluid dynamics and heat transport, nuclear performance, and chemical compatibility issues relative to the direct cooled blanket concepts investigated during the scoping phase of this study. These topics are addressed in Sections A through D respectively. The concepts are compared with the internal pipe cooled concept presented in Chapter II in order to aid in a reference concept selection (see Chapter V).

III.A MECHANICAL DESIGN

III.A.1 Direct Cooled Concept Consideration

Both the internal pipe cooled and direct cooled concepts utilize a spherical fuel and multiplier form and lithium coolant.* Since the coolant flow rates for both concepts are similar, and it is still necessary to maintain low coolant velocities to minimize the MHD pumping power, the coolant inlet/outlet pipe sizes will be similar. Again the coolant piping will compete for space necessary to accommodate the magnets and their shielding. The first wall and structure design must be as light as possible, to achieve attractive nuclear performance consistent with the higher coolant operating pressures for the direct cooled design.

III.A.2 Direct Cooled Concept Description

The direct cooled concept presented is based on the guidelines developed in Table III.A-1 and the magnet geometry was previously presented in Figure II.A-1.

---

*As discussed in Chapter I, the Pb - Li coolant option was discarded during the scoping phase.

TABLE III.A-1 Blanket, module configuration guidelines for the direct cooled concept.

Total Length of Module	5 m
First Wall Radius	1.5 m
First Wall Loading	1.6-2 MW/m^2
First Wall Coolant Annulus Radial Gap	5-10 cm
Fertile Fueled Region Thickness	~60 cm
Graphite Reflector Region Thickness	~60 cm
Magnet Pitch	2.5 m
Fuel and Beryllium Form	Spheres
Sphere Size (dia.)	<5 cm

In certain respects the direct cooled concept (Figures III.A-1 and 2) is similar to the pipe cooled concept described in Chapter II. By eliminating the axial coolant pipes from that concept the lithium coolant is fed directly to the first wall as shown. The coolant enters the left side of the module through a set of 20 radial inlet pipes 0.4 m in diameter and discharges into the first wall coolant annulus composed of the inner first wall and intermediate wall which separates the outer fertile fueled region of the blanket from the coolant annulus. As the coolant travels toward the right side of the blanket, portions of the flow are uniformly bled off through holes in the intermediate wall. The coolant then travels radially outward to cool the fuel and beryllium spheres and the graphite reflector. The coolant emerges into a plenum at the outer region of the blanket where it flows to the 20 radial pipes (also 0.4 m in diameter) to be discharged from the blanket at the right end.

The fuel spheres are loaded through a pipe at the top of the module (detail not shown) and are extracted at the bottom for refueling as in the case of the pipe cooled concept. Because of the absence of the axial coolant pipes and fewer radial stiffeners in this concept, the sphere flow is less impeded and larger fuel and beryllium spheres can be used. The sphere size will then be limited by heat transfer and fueling pipe size constraints.

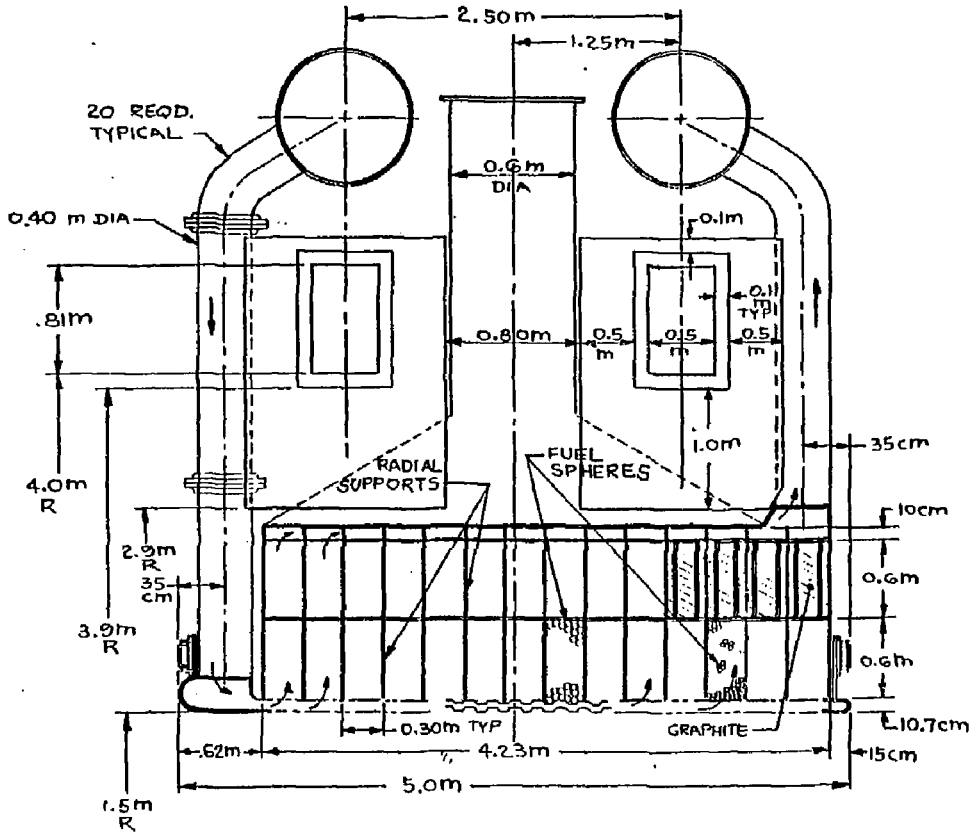

FIG. TTT A-1 Fusion Breeder Reactor direct cooled blanket concept cross

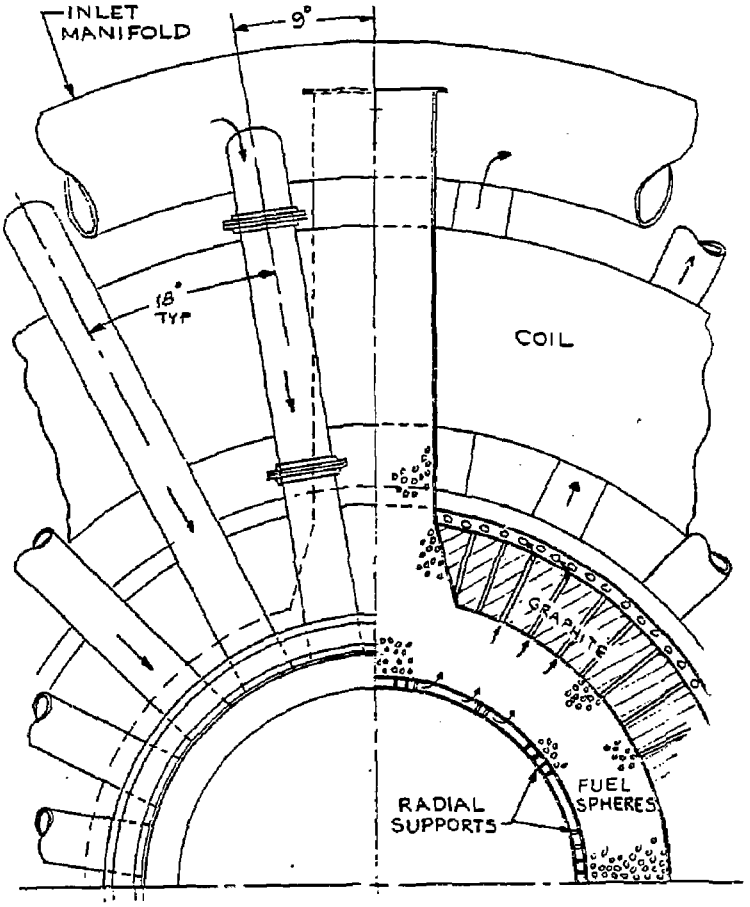

FIG. III.A-2. Fusion Breeder Reactor direct cooled blanket concept - end view.

Both the first wall and intermediate wall are corrugated (as in the pipe cooled concept) to achieve increased stiffness while minimizing the thickness to enhance neutronic performance. Similarily the two walls are connected by radial support ribs in order to withstand the coolant pressure in the first wall annulus without exceeding the allowable bending stresses in the sections of the shells which span the space between ribs. Because of the higher coolant pressure for this concept (200 psi versus 100 psi for the pipe cooled concept) the first wall/intermediate wall thickness is increased. In addition it is still necessary to connect this double shell assembly to the outer shell of the module by supports, possibly spaced at ~30 cm intervals, to provide additional radial support to sustain the coolant pressure buckling load. The sphere diameter will be limited to 3-5 cm if a minimum of 6-8 sphere diameters is required between supports to prevent sphere jamming during refueling. The preliminary corrugation geometry and sizing (shown in Figure III.A-3) are similar to that required by the pipe cooled case except that the wall thickness and coolant annulus thicknesses are increased to 0.54 cm and 5-10 cm respectively as shown by the asterisked dimensions in the figure. The corrugations were sized based on considering the STARFIRE[1] modified 316 SS prime candidate alloy (PCA) as the structural material.

Two plenum arrangements Figures III.A-4 and 5, are shown as possible methods for distributing the flow from the first wall annulus to the blanket fertile region if determined necessary (See Section III.B). The first includes a tapered flow baffle between the intermediate and first wall, with the plenum region between the baffle and the intermediate wall. The second or alternate arrangement has the baffle (if required) located on the outer side of the intermediate wall as shown in Figure III.A-5. The latter arrangement is considered to be more attractive since it appears to be more difficult to accurately locate the flow baffle (with such a small taper) over the 5 meter length of the module. In addition, for the alternate arrangement, the intermediate wall itself could possibly serve the plenum function without need for an additional baffle.

The design features for the direct cooled concept are summarized in Table III.A-2.

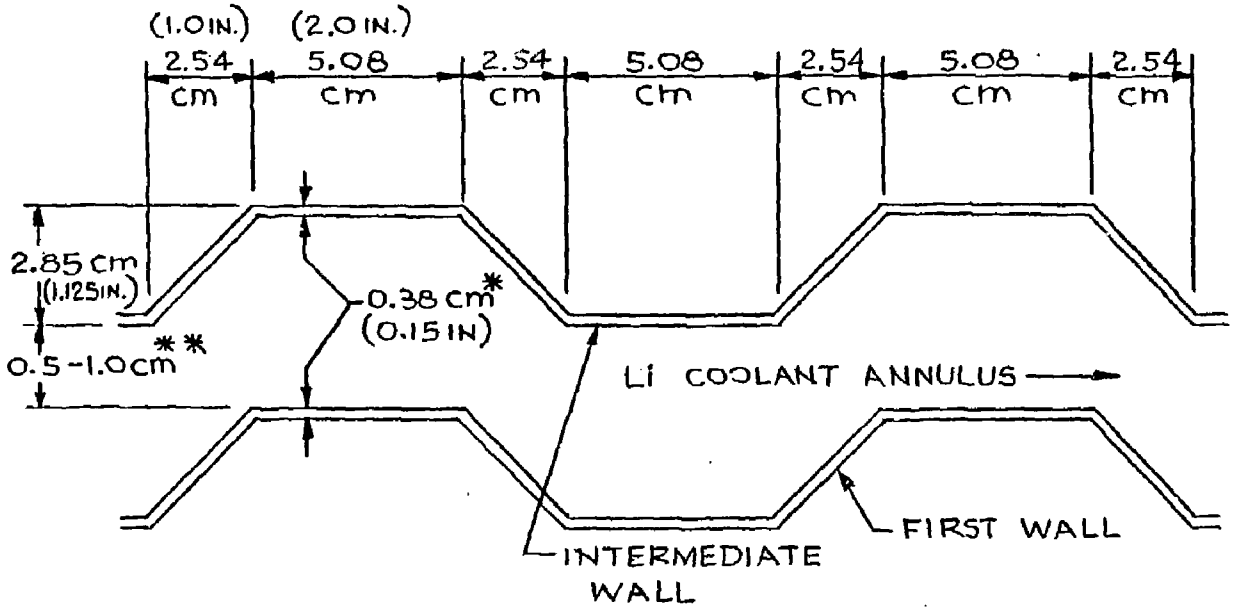

*0.54 (0.21 in), Direct Cooling Case

**5 - 10 cm, Direct Cooling Case

PLASMA

FIG. III.A-3. Fusion Breeder Reactor preliminary corrugation sizing.

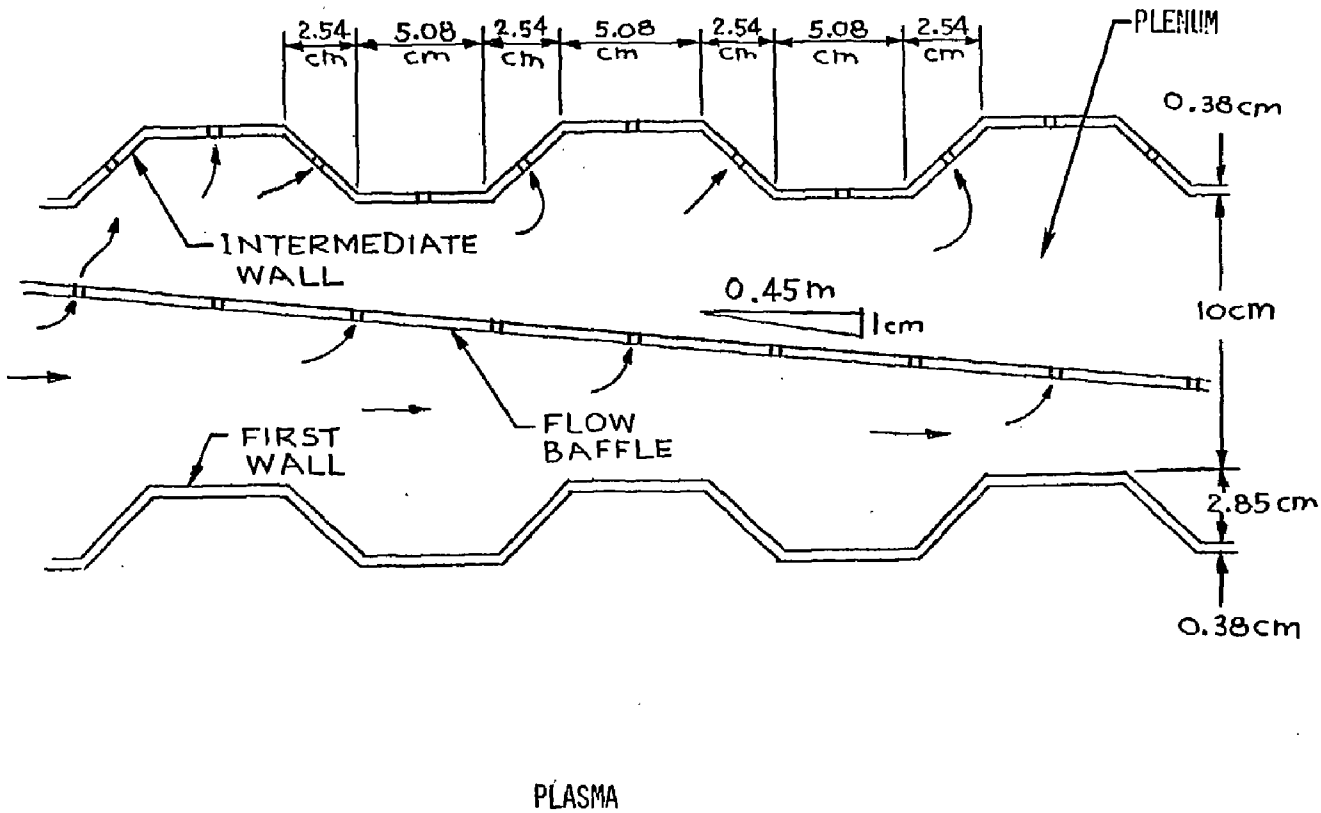

FIG. III.A-4. Fusion Breeder Reactor direct cooling blanket concept plenum arrangement.

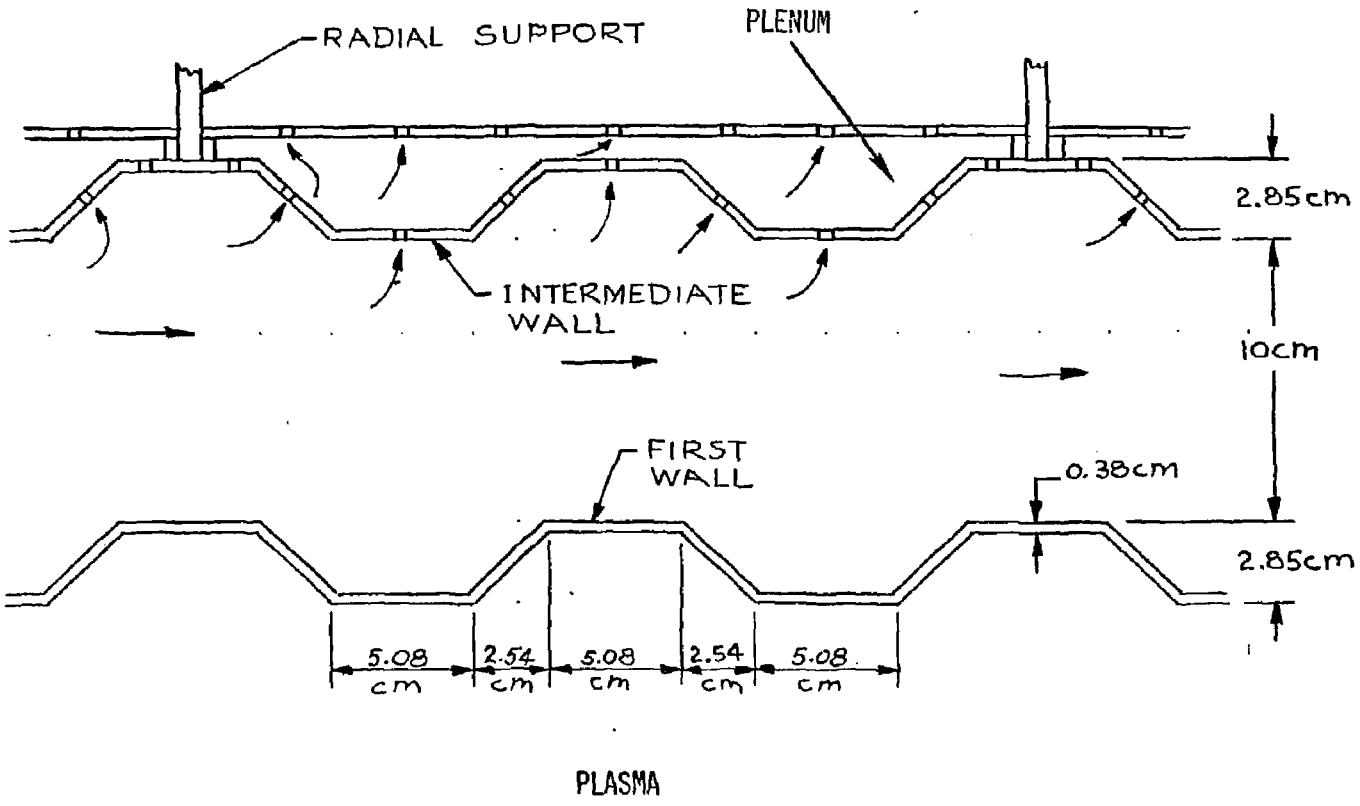

FIG. III.A-5. Fusion Breeder Reactor direct cooling blanket concept alternate plenum arrangement.

TABLE III.A-2 Direct cooled blanket concept design features.

Total Length of Module	5 m
Length of Fertile Region - Fraction of Blanket Length	4.2 m 84%
Fertile Fueled Region Thickness	0.6 m
Fuel Sphere Size (dia.)	<5cm
Lithium Coolant Annulus Thickness	8 - 13* cm
Graphite Reflector Thickness	0.6 m
Corrugated First Wall Thickness	0.54 cm (0.21 in)
- Pressure Across Wall	200 psi
Corrugated Intermediate Wall Thickness	0.54 cm (0.214 in)
Clear Opening Between Shells	5 - 10 cm
Inlet/Outlet Coolant Pipes Required	20 each
- Coolant Pipe Diameter	~0.4 m

*Effective Coolant Channel Thickness is 5-10 cm

Alternate Direct Cooled Concept

An alternate concept for the direct cooled concept investigated is shown in Figures III.A-6 and 7. This concept differs in the method in which the lithium coolant flows through the blanket. The coolant enters the module at the ends through 20 radial pipes (at each end), enters the first wall plenum and flows toward the center of the module. As the coolant flows toward the center it is bled off radially through the intermediate first wall, is collected at the plenum in the back of the module and exits at the center of the outside of the module through 16 larger diameter pipes. Since approximately the same coolant pressures are anticipated, other blanket features are similar. It is possible to route the inlet/outlet pipes between and under the magnets to permit removal of the magnets without removing the

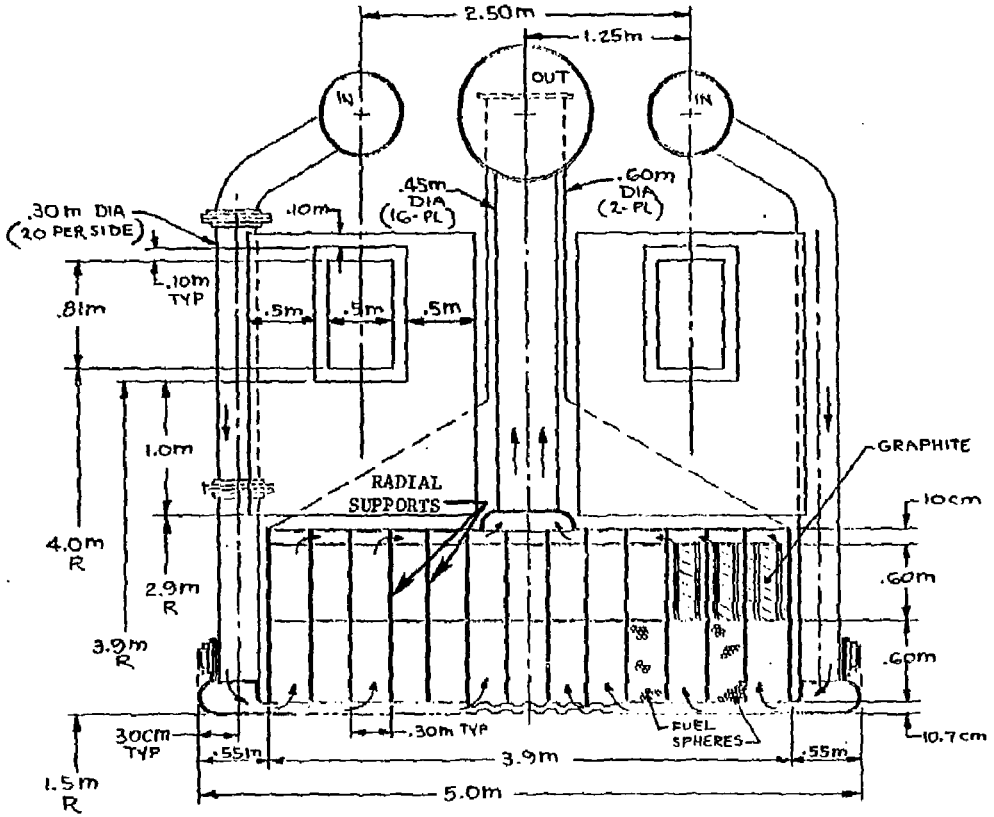

FIG. III.A-6. Fusion Breeder Reactor alternate direct cooled blanket concept cross section.

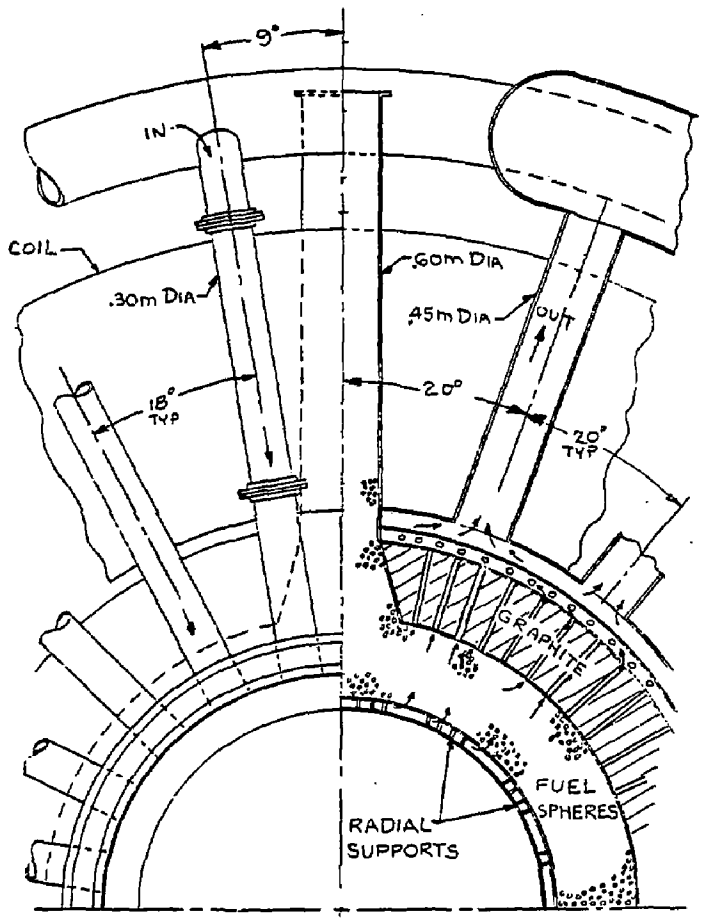

FIG. III.A-7. Fusion Breeder Reactor alternate direct cooled blanket concept - end view.

pipes in the pipe cooled concept and direct cooled concept presented earlier. With this alternate concept it is not possible because of the additional set of outlet pipes required between the magnets. The design features for the alternate cooled concept are listed in Table III.A-3.

TABLE III.A-3 FBR direct cooled blanket design features of alternate cooling concept.

Total Length of Module	5 m
Length of Fertile Region - Fraction of Blanket Length	3.9 m 78%
Lithium Coolant Annulus Thickness	8 - 13* cm
Fertile Fueled Region Thickness	0.6 m
Corrugated First Wall Thickness - Pressure Across Wall	0.54 cm (0.214 in) 200 psi
Corrugated Intermediate Wall Thickness	.54 cm (0.214 in)
Inlet Coolant Pipes Required - Inlet Pipe Diameter	40 0.3 m
Outlet Coolant Pipes Required - Outlet Pipe Diameter	16 0.45 m

*Effective Coolant Channel Thickness is 5-10 cm

III.A.3 Design Concept Overview

A list of design considerations was tabulated to compare the three concepts described here and in Chapter II. These are presented in Table III.A-4. The numerical values assigned, which range from 1 to 3, compare the design considerations or design issues with (1) being the most and (3) being the least desirable. There was no attempt to rank the concepts by totaling these values since the difference between two numbers is subjective only and not meaningful on a strictly quantitative basis. Except for the last entry where it is not possible to incorporate piping under magnets for the alternate direct cooled case, there are not any go/no-go issues. From a mechanical

standpoint there is no clear preference for any of the concepts and a selection could not be made without addressing other issues such as thermal/hydraulic, neutronic, fuel processing and other considerations. The reference concept selection and rationale for selection are discussed in Chapter V of this report.

TABLE III.A-4 Summary of design issues for Fusion Breeder Reactor blanket concepts.

	Internal Pipe Cooled Concept	Direct Cooling	Alternate Direct Cooling
Complication of design concept	3*	1	2
Large number of coolant pipes	3	1	2
Complexity of coolant flow paths	1	2	3
Control of fuel/beryllium distribution	3	1	1
Difficulty in mechanical separation Be/fuel spheres by size variation	2	1	1
Size of fuel spheres	3	1	1
Mechanical support of graphite reflector	2	3	3
Cooling of graphite	1	2	2
Tube sheet connection to outer shell	2	3	3
Uniform cooling of blanket	1	2	2
Possible flow stagnation at center of lithium annulus	1	1	3
High first wall pressure	1	2	2
Difficulty in incorporating piping under magnets	1	2	N

*1 represents most favorable, and 3 represents least favorable;

N - not possible

REFERENCES

1. "STARFIRE - A Commercial Tokamak Fusion Power Plant Study", Argonne National Laboratory Report ANL/FPP/80-1 (Vol I) September 1980.

III.B FLUID DYNAMICS AND HEAT TRANSPORT

The second blanket option that we have investigated in the scoping phase of this study is the direct cooled design. For this design, instead of cooling by lithium in axial tubes, the blanket is cooled by radial or axial flow of lithium or $Li_{17}Pb_{83}$ through a packed bed composed of beryllium and fertile material balls. The radial and axial flow configurations are illustrated in Figure III.B-1.

The reactor parameters used in the calculation are the same as those presented in Section II.B.

The key difficulty in the calculation of the pressure drops of the direct cooled design is the lack of analytical support from the literature for liquid metal flow through a packed bed in the presence of a magnetic field. The lithium coolant can be directed to flow perpendicular or parallel to the magnetic field by routing the coolant radially or axially through the blanket. The coolant paths formed by the close-packed balls are a very tortuous and coolant traveling in and out of magnetic field lines is unavoidable for both flow options. Because of the relatively high electrical conductivities of lithium, beryllium, and thorium metal, induced currents will be formed inside the blanket, which will in turn generate body forces against the direction of fluid flow. Precise analysis of the aggregate or cancelling effects of these body forces as formed by surrounding coolant paths is impossible because of the 3-D geometric complication and the unspecified packing structure of the balls, (which is a function of the method of packing) and the ball channel characteristic dimensions. Physically, one can observe that the coolant will flow through the blanket by taking the paths that have the least resistance, which implies paths that would contribute least pressure drop. This observation will lead to widely different flow paths for the radial and axial flow options. During this phase of the study, simplified assumptions were made in considering the pressure drops through the packed bed. The results can be used as indications of design feasibility. More detailed ananysis is required. Bench scale experiments may be the best approach to obtaining design-relevant

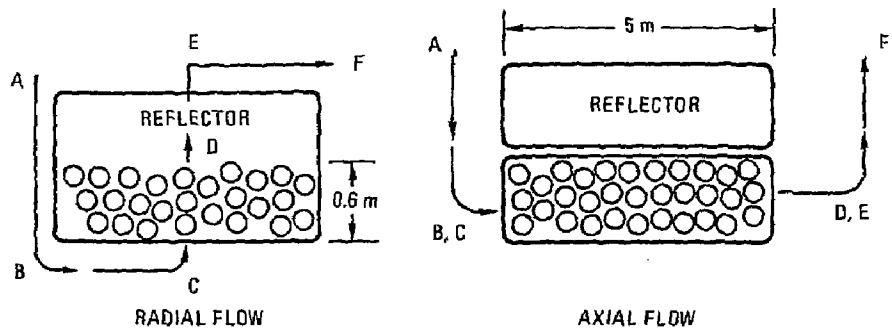

FIG. III.B-1. Direct cooled blanket flow configurations.

parametric equations. During the scoping phase of this study, the following assumptions were made in completing the pressure drop estimates.

- For the general flow direction perpendicular to the magnetic field corresponding to the radial flow option, the pressure drop through a straight channel formed by the cusp between three balls was calculated. The channel wall thickness and electrical conductivity were taken to be those of the ball radius and of beryllium, respectively. The local maximum fluid velocity was used in the calculation. This model is illustrated in Figure III.B-2.

- Pressure drops from turning losses through the packed balls in the presence of a uniform magnetic field were estimated by the entrance and exit loss of liquid metal through a field gradient of $\Delta B = B$, multiplied by the number of turns as defined by the number of balls along the flow path and the resulting pressure drop was added to that associated with cusp flow. Equation (1)* was used to approximate the turning loss around a ball. This model is illustrated in Figure III.B-2. It was selected instead of summing up the total fluid paths traversing the B-field, because the Hartmann flow equation is only valid for well developed pipe flow, whereas, the situation for the flow around packed balls is that the fluid flow has short flow paths, and is not developed at all.

- Pressure drop through a packed bed in the absence of magnetic field was also calculated and added to the other pressure drops.

For the radial flow case, the mean coolant flow orientation is perpendicular to the magnetic field lines. The total pressure drop was approximated by the sum of contributions from fluid flowing through the straight cusp and the in and out coolant turning losses around the balls (the $B = 0$ packed bed pressure drop is negligible). For the axial flow case, the mean coolant flow orientation is parallel to the magnetic field lines. The total pressure drop was approximated by the sum of contributions from the packed bed and the in and out coolant turning losses around the balls. Based on the above models, it was found that the pressure drops due to MHD flow effects are independent of ball sizes. At this preliminary stage of

---

* from Section II.B

PACKED BED PRESSURE DROP ESTIMATES:

FLOW PARALLEL TO B-FIELD

(A) $\Delta P_{\parallel}$ = PRESSURE OF PACKED BED + N ($\Delta P_{IN\text{-}OUT}$)

(B) FLOW PERPENDICULAR TO B-FIELD

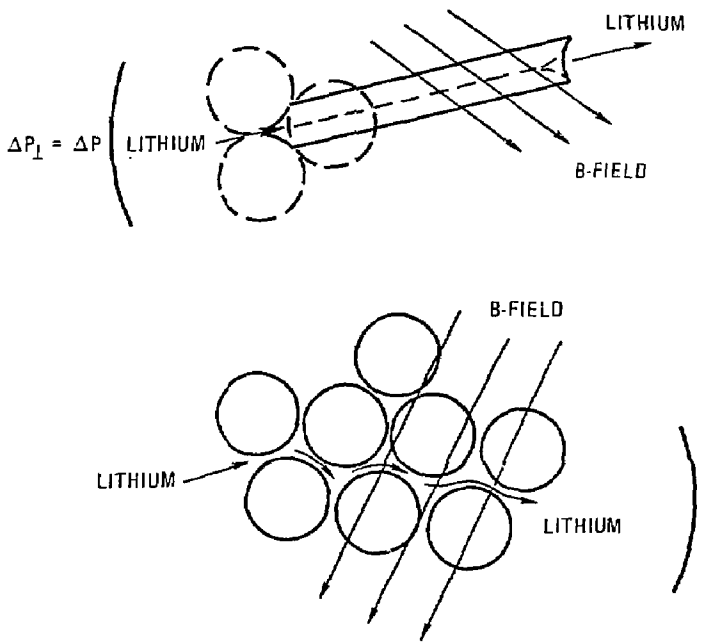

N = BLANKET DEPTH/BALL DIAMETER

$\sigma_W = \sigma_{Be}$

T_W = BALL RADIUS

FIG. III.B-2. Packed bed pressure drop estimates.

analysis, the validity of this observation remains to be proved experimentally and/or by more detailed analysis.

Key input parameters for pressure drop calculations are summarized in Table III.B-1. Similar calculations for a $Li_{17}Pb_{83}$ coolant, instead of liquid lithium, were also performed.

Circuit pressure drops similar to calculations performed for the pipe cooled option were calculated for the direct cooled design option. Table III.B-2 summarizes the results for different design and coolant selection options including the pipe cooled design. These calculations were performed with a coolant inlet to outlet temperature differential of 120°C. As expected, further design optimization can be performed by increasing this temperature differential. Table III.B-2 shows that $Li_{17}Pb_{83}$ has lower pressure drops and pumping power requirements than lithium because of its lower electrical conductivity. Comparing design options using the same fluid, the pipe cooled design has the lowest pressure drop and pumping power required, and the direct cooled radial flow has the highest pressure drop and pumping power required, close to a factor of two higher than axial flow.

By using a larger coolant temperature differential of 490 - 340 = 150°C, the pressure of the first wall for the lithium direct cooled radial flow design can be reduced to ~2.07 MPa (300 psi). Further outlet plenum design and reduction of packed bed blanket thickness can further reduce this pressure to the level of ~1.38 MPa (200 psi), an acceptable first wall design pressure. This direct cooled flow design could be preferred as the reference design, despite its relatively higher pressure drop and pumping power, because of its simpler mechanical design and its advantage of delivering the cooled inlet coolant to the first wall where the volumetric power generation is the highest. Heat transfer calculations indicate that for the lithium coolant design, the maximum structure and large thorium ball (5 cm in diameter) temperature in front of the blanket would be <400° and <500°C, respectively. The maximum temperature for the structure and similar thorium ball at the back would be <510°C. These temperatures are quite acceptable from material compatibility considerations.

TABLE III.B-1. Key input parameters for the direct cooled option calculations.

Blanket Thermal Power: 141 MW

Beryllium Electrical Conductivity: $5.6 \times 10^6\ (\Omega m)^{-1}$

	Lithium	$Li_{17}Pb_{83}$
T_{in}, °C	300	330
T_{out}, °C	420	450
Mass flow rate, kg/sec	281	6994
Volume flow rate, m^3/sec	0.54	0.74
Electrical conductivity $(\Omega m)^{-1}$	3.57×10^6	0.8×10^6

TABLE III.B-2. Pressure drop and pumping power estimates.
(Coolant ΔT = 120°C)

	Pipe Cooled		Direct Cooled[a]			
			Radial Flow		Axial Flow	
	Lithium Pa (psi)	$Li_{17}Pb_{83}$ Pa (psi)	Lithium Pa (psi)	$Li_{17}Pb_{83}$ Pa (psi)	Lithium Pa (psi)	$Li_{17}Pb_{83}$ Pa (psi)
Tube ΔP	170	2280	--	--	--	--
First wall ΔP	0.2×10^5	0.15×10^5	--	--	--	--
Cusp ΔP, $\perp$ to B-field	--	--	2.2×10^6	0.72×10^6	--	--
Packed bed ΔP, $B = 0$	--	--	27.2	968	0.001×10^6	0.34×10^6
Packed bed ΔP, in and out B-field	--	--	0.015×10^6	0.0047×10^6	0.88×10^6	0.245×10^6
Blanket circuit total ΔP[b]	0.7×10^6 (100)	0.33×10^6 (54)	2.98×10^6 (432)	1.55×10^6 (224)	1.6×10^6 (232)	1.03×10^6 (149)
First wall *minimum pressure*	0.37×10^6 (53)	0.193×10^6 (28)	2.6×10^6 (377)	1.32×10^6 (191)	1.24×10^6 (179)	0.81×10^6 (117)
Pumping power (MW)	0.38	0.246	1.6	1.15	0.86	0.77

[a] Ball diameter - 3 cm.
[b] Including inlet-outlet plena, blanket and turns ΔPs.

III.C Nucleonics for Direct Cooling Blanket Concept

The objectives and methods of nuclear design and analysis for the direct-cooled blanket are the same as discussed in Section II.C for the pipe blanket concept. There are three differences in the two concepts that will affect nuclear performance. First, there are no pipes so less structure in the Be zone. Second, lithium replaces sodium. And third, the first wall must be thicker (~ twice) because of higher MHD pressure drop. The first two will improve breeding while the third will reduce breeding.

Initial results indicate that the plus and minus effects on breeding of the three differences are about equal. Breeding (net) for this blanket is 1.84 compared to 1.83 for the blanket with pipes. There is more difference in M, 1.50 vs 1.63. This blanket is also more sensitive to first wall thickness. When the first wall thickness is cut in half fissile breeding increases by 18% (T + F = 1.99). We should endeavor to reduce first wall thickness, especially its structure.

III.D. Chemical Compatibility Issues

III.D.1. Introduction

In the direct cooling blanket concept, liquid lithium comes in contact with the beryllium and thorium spheres as shown in Figure III.D.1. The chemical compatibility tends to be more complicated in this concept than in the pipe cooling blanket concept because of the mass transfer effect on the corrosion of beryllium and thorium. The main concern in the chemical compatibility area is the corrosion of beryllium and thorium in liquid lithium with possible redeposition elsewhere in the loop. Corrosion of steel in the presence of beryllium in the flowing lithium might also be an important point due to the possibility of mass transfer of beryllium in liquid lithium.

III.D.2. Solid-Solid Interactions

Since beryllium and thorium spheres are 20-50 mm in diameter, compared to 1-5 mm in the pipe cooling case, self sintering will not be a major problem. The relative surface area will be reduced by a factor of 25. However, the mass transfer effect on dissolution-precipitation of beryllium and thorium will be of a greater concern in this concept. Although the self-welding by sintering may not occur, the flow path will be plugged up by those deposits which will cause hot spots in the packed bed. In spite of the contact area between beryllium and steel being much smaller in this design concept, the steel temperature will be higher and beryllium penetration into steel may cause a weakening of the steel.

A major area where the two blanket concepts differ is in the fact that native oxide scales on beryllium, thorium and steel, which are believed to be stable in liquid sodium, are unstable in liquid lithium; hence, the scales cannot be relied upon to be interaction barriers in the direct cooling concept. Further investigation of the kinetics of oxide attack by lithium is needed.

III.D.3. Liquid Metal Corrosion

III.D.3.a. Corrosion of Beryllium and Thorium in Liquid Lithium

Corrosion data for thorium in liquid lithium are unavailable in open literature and solubility values for beryllium in lithium are not reliable. As shown in Table III.D-1, reported solubility values differ by large amounts. Solubility values for beryllium and thorium at 400 to 500°C are needed.

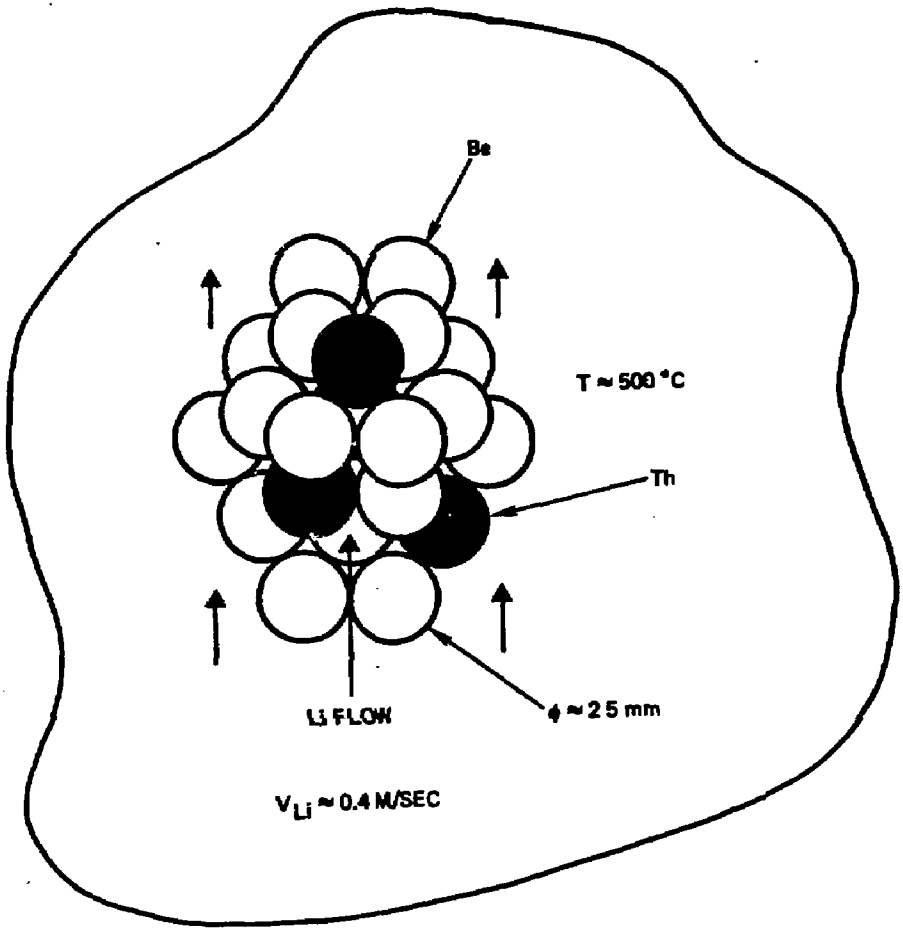

Figure III.D-1. Direct Cooling Blanket

Table III.D-1. Solubility values for Beryllium in Lithium

TEMPERATURE °C	SOLUBILITY %	REFERENCE
700	0.5	1
732	0.23	2
1000	8.5	1
1016	1.08	2

Contrary to the pipe cooling concept, beryllium and thorium spheres will be exposed to flowing lithium, thus their corrosion rate is expected to be higher. The corrosion rate is a function of the liquid flow rate. Roy and Schad [3] showed that the corrosion rate of steel increases with the flow rate of liquid sodium. Although the velocity of the lithium in the packed bed is low, mass transfer by dissolution-precipitation may play a major role in the direct cooling concept.

On the other hand, in the direct cooling concept, the bed temperature can be lower than in the pipe cooling concept. The corrosion rate of these spheres would be lower if the dissolution rate is kinetically controlled. If the corrosion rate of beryllium, thorium and steel is mass transfer controlled, then MHD effect on the corrosion should be taken into consideration.

Impurities (C,N,O) are important parameters in the corrosion of beryllium in liquid lithium [4-6]. Minge[4] investigated the effect of impurities on the corrosion of beryllium in liquid lithium and showed that a trace amount of carbon and nitrogren is much more important for the corrosion of beryllium.

III.D.3.d. Corrosion of Steel in Liquid Lithium

The corrosion of steel pipes in liquid lithium is discussed in Section II.D.3. The contact area between steel and lithium is much smaller in the direct cooling concept than in the pipe cooling concept, thus the corrosion of steel seems to be less important. However, the chemical compatibility becomes more complicated because of direct contact of

beryllium, thorium and steel with flowing lithium. Hoffman[7] performed a chemical compatibility study of Hastelloy B and beryllium in liquid sodium for 1000 hr at 650°C. He found that when the spacing between beryllium and steel is <20 mils, beryllium is transferred to the steel and then forms brittle intermetallic compounds. Kovacevich and Devan[8] also reported the formation of intermetallic compound ($Be_{21}Ni_5$) when beryllium and Inconel were spaced 20 mils in the flowing sodium for 1000 hr at 704°C. We expect similiar mass transfer effect in our packed bed and the temperature dependence of this effect should be studied.

Another issue in the chemical compatibility is carburization and decarburization of steels in liquid lithium.[9-14] It is believed that carburization and decarburization of steel occurs due to the differences in carbon activities in different steels. Thus, the use of dissimilar steel in the flowing liquid should definitely be avoided.

III.D.4. Summary

It appears that mass transfer effects in the flowing lithium and the effect of impurities are major issues in the direct cooling concept. MHD effect on dissolution-precipitation of beryllium, thorium and steel may also be important issues.

SECTION III.D. REFERENCES

1. Lemm, K. and D. Kumze, Int. Symp. The Chem Soc. Special Publ. No. 22 p 3, London, 1967.
2. Jesseman, D. S., G. D. Roben, O. A. Grundwald, W. S. Fleshman, K. Anderson, V. P. Galkin, USAEC, NEPA-1465, 1950.
3. Ray, R. and M. K. Shad, J. Nucl. Mater. 47, p 129, 1973
4. Migge, H. J. Nucl. Mater. 85 & 86, pp 317-321, 1979.
5. Mansteller, J. W., F. Tepper, and S. J. Rodgers., Alkali Metal Handling and Systems Operating Techniques, Gordon and Breach, New York, 1967.
6. Weeks, J. R., Materials and Fuels for High Temperature Nuclear Energy Applications, ed by M. T. Simnad, R. Zumwalt, MIT Press, Cambridge, p 345, 1964.
7. Hoffman, E. E. ORNL-2061, p 128 March 10, 1956.
8. Kovacevich, E. A. and J. H. DeVan, ORNL-2157, p 140 Sept 10, 1956.
9. Klueh, RL. L. and J. M. Leitnaker, Met. Trans., 6A, pp 2089-2093, 1975.
10. Klueh, RL. L. J. Nucl. Mater., 96, pp 187-195, 1981.
11. Krankota, J. L. and J. S. Armijo, Met. Trans., 3, pp 2515-2518, 1972.
12. Baerlecken, E., K. Korenz, E. Kranz and D. Schlegel, proceedings of a Symposium, Vienna, Nov 28 - Dec 2, pp 145-157, 1966.
13. Natesan, K., O. K. Chopra, and T. F. Kassner, Nucl. Tech., 28, pp 441-451, 1976.
14. Shida, Y., K. Yoshikawa and T. Moroishi, Met. Soc. Japan, pp 697-705, 1977.

IV.A SOLIDS HANDLING OUTSIDE THE REACTOR

The fertile-dilute fission-suppressed fusion breeder concept requires a short fuel exposure time in the fusion reactor and thus mobile fuel. In this section, options for handling the fuel and neutron multiplier outside the reactor are discussed.

IV.A.1 Requirements

Two types of solid material present in the blanket require handling outside the reactor. First, the beryllium neutron multiplier, because of its propensity for radiation swelling, requires occasional refabrication and fairly frequent movement to prevent jamming in the blanket. Second, the fertile fuel itself, which will become radioactive after irradiation, must be separated from the beryllium and reprocessed.

The systems considered were as follows:

1. Uranium oxide or thorium pellets with beryllium pellets, around 1 mm diameter. U/Th:Be = 1:14. Liquid sodium immersed. Stainless steel structure.

2. UO_2 or Th balls with beryllium balls, 1 to 5 cm diameter. U/Th: Be = 1:14. Lithium-lead ($Li_{17}Pb_{83}$) immersed. Ferritic structure.

3. UO_2 or Th balls with beryllium balls, 1 to 5 cm diameter. U/Th: Be = 1:14. Lithium immersed. Ferritic structure.

System 1 is for the pipe cooling design and systems 2 and 3 are potential selections for the direct cooling design. Data in Table IV.A-1 gives the assumed throughput requirements of the design under consideration during the scoping phase of this study.

A number of important features appear to be common to any choice made concerning the handling system. The system must be air tight to prevent the escape of tritium and potential fire hazard concerns from the interaction of air and liquid metal. Moreover, tritium may well be expected to occur in non-negligible amounts at any point in the solids handling system, since both beryllium and lithium produce tritium under irradiation. A further

TABLE IV.A-1. Fuel handling system requirements.

Number of modules	20
Module mobile material volume	34 m^3
Fertile material dwell time	60 days
Fertile and beryllium materials volume ratio	1:14
Beryllium residence time	60 days
Bimonthly batch, 34 m^3	37% liquid-metal 63% solid
Daily throughput per module, 0.57 m^3	40 litre fertile/fissile fuel and 526 litre beryllium and liquid
Assumed beryllium life	600 days 2 modules always on refabrication
Beryllium refabrication throughput	1052 litre/day
Fuel reprocessing (total)	800 litre/day (504 litres solid)

feature is that the fuel will require cooling for about six months to a year following discharge. The adiabatic meltdown time for a freshly enriched fertil fuel ball is of the order of one to five minutes indicating that good control of the enrichment and high assurance of cooling is essential.

IV.A.2 Heat Transfer Fluid Density Considerations

The second system of UO_2 or Th and beryllium balls in $Li_{17}Pb_{83}$ has the feature that the density of the heat transfer fluid is between that of the beryllium and fertile pebbles. Therefore, unless special (and probably expensive) steps are taken to lower the fertile ball density, separation of the fuel and multiplier will occur due to floatation of the beryllium in liquid lithium lead. However, if a fuel ball is lifted out of the lithium lead by floatation, it will lose its cooling and may melt, damaging itself and other particles with which it is in contact. Control of the pebble flow, even in the simplest gravity assisted dumpout scenarios, is difficult, and blanket fluidization would seem to be necessary for the blanket motion to be under control with a high density heat transfer fluid.

The obvious advantage of easy separation of the fuel and multiplier is not considered sufficient to make the choice of a "floating" system attractive. From the viewpoint of blanket solids handling, the "sinking" systems 1 and 3, which use sodium or lithium as the immersion fluid, are preferred.

IV.A.3 Ball-Size Considerations

The most important advantage of the smaller particle (~1 mm size) is that it has higher hydraulic effect per unit volume than the larger one. This enables it to be handled with more assurance when slurry-type handling is envisaged, but may give a high and potentially unacceptable viscous pressure drop for direct cooling. Virtually all handling considerations favor the small pellet; the posaibility of jamming is much reduced, blanket zoning is easier, and solid transport as a slurry results in very small, hence, more

economic systems. Arguments in favor of the larger ball (1 to 5 cm in diameter) are its lower surface area/volume ratio, the credibility of individual ball fissile enrichment interrogation (improved fuel management), and a much larger allowable cost for ball fabrication and handling on a per ball basis (e.g., the ability to fabrication low density thorium balls at accepted cost). There may be some question of practicality of handling the large balls in view of the possible blanket zoning necessary and the inevitably large passages required for large ball transport.

IV.A.4 Batch versus Continuous Operation

Figures IV.A-1 and IV.A-2 show solids handling option outlines. Batching is seen as having several disadvantages. First, a continuous system is, in any case, inevitable for processing; a batch system adds two interposed steps between the reactor and the reprocess cycles. Second, batching requires large intermediate facilities and possibly frequent shutdowns for charging. Third, blanket internal radial zoning for selected radial zone batching (in order to achieve uniform enrichment) is likely to be very difficult. The sole advantage of batch operation is the elimination of potential solid stagnation (ball holdup) in a continuous circulation blanket. The feasibility of close local control of the blanket flow and the small equipment associated with continuous processing is attractive as is the closed system with its superior tritium confinement ability. The requirement to extend the emergency dump system to accommodate batch working is a complication which might cause the batch working system to have a negative impact on reactor safety if indeed it is practical.

IV.A.5 Conclusions

The design having the smallest and most economical installation for handling breeder/multiplier solids outside the blanket is the continuously operating 1 mm pellet handling system which requires for each module, only two 2.5 cm diameter lines flowing at speeds of about 2.5 cm/sec.

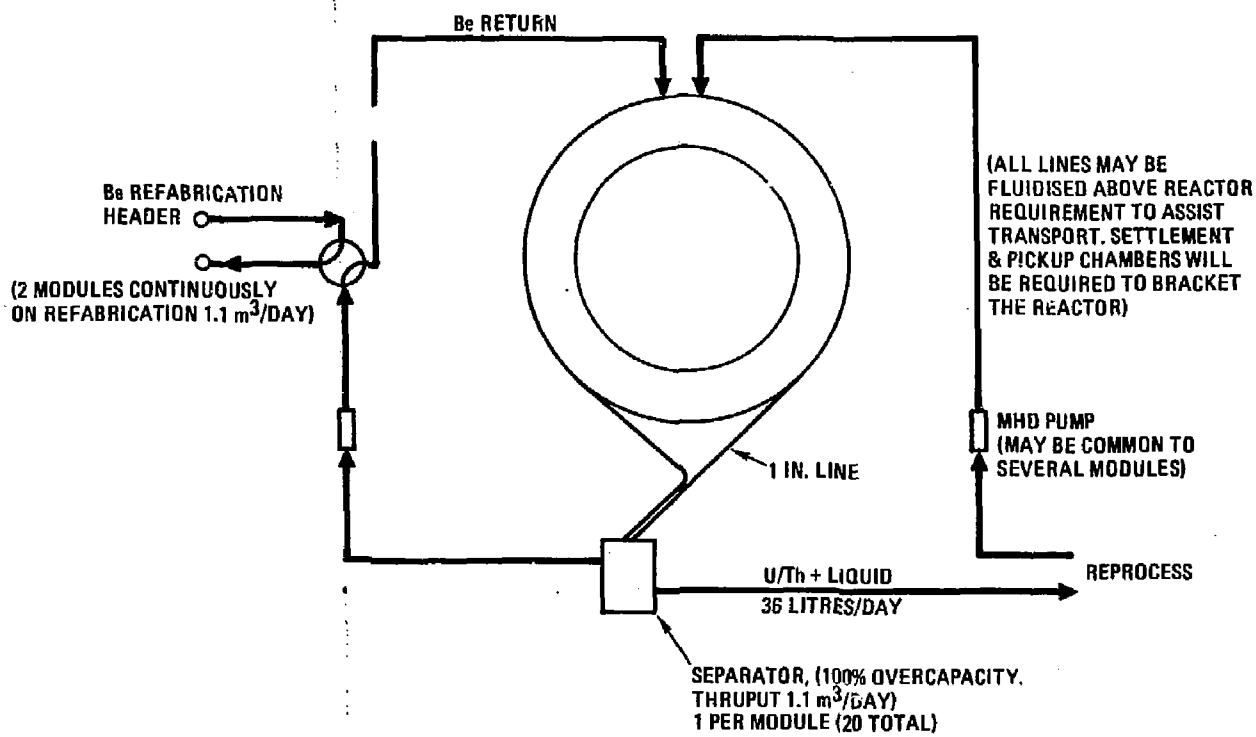

FIG. IV.A-1. Fusion breeder reactor continuous solid processing

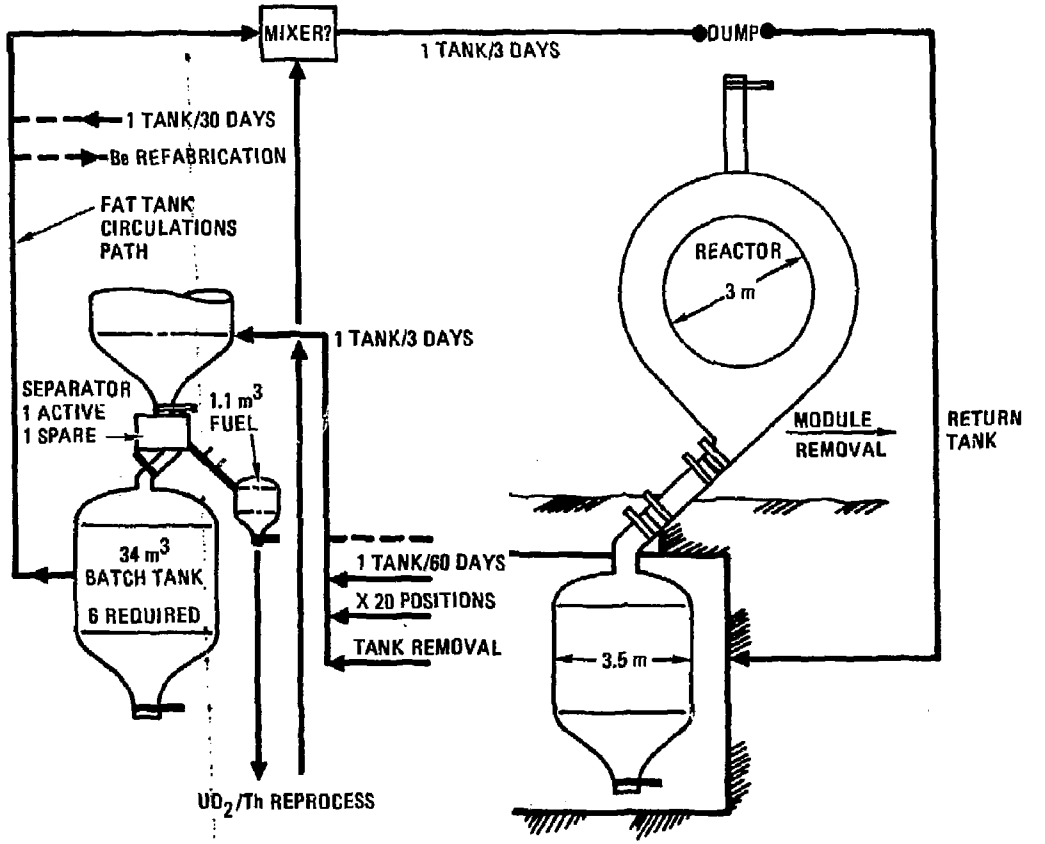

FIG. IV.A-2. Fusion breeder reactor batch solid processing.

The burdens engendered by this system are that the blanket fuel/beryllium flow itself must be well controlled (e.g., mixing, uniform flow, etc.) and that the coolant ΔP must be held to an acceptable level. There is no reason to suppose that the former problem is without acceptable solution, even though initial studies indicate that segregation of the fuel/beryllium mixture could occur due to the large density ratio (6.5:1). The latter requirement can be satisfied by the pipe cooling design option, but the ~800 coolant tubes in this design have an unknown input on fuel segregation and further study is required. With the large density difference between multiplier and breeder, separation should not be difficult. Remixing under fluid, where segregation by energy of fall is inhibited and mixer chamber size is small in relation to blanket volume, should be straightforward.

For the direct cooling design, assurance of adequate ball mixing and flow characteristics should be improved due to a less complex blanket and the possibility of one density fertile and beryllium pebbles. However, large ball design may be required in order to maintain acceptable pressure drop. Nevertheless, the advantages of continuous operation are still applicable. Similar care in blanket and internal design to prevent over-enrichment from solid stagnation remains necessary.

IV.B LIQUID METAL COMPATIBILITY CONSIDERATIONS

IV.B.1 Overview

The chemical compatibility issues associated with the internal pipe and direct cooled blanket designs are specific to the types of materials used, the temperature of operation, and other design factors discussed in Sections II.D and III.D. Nevertheless, several general considerations apply to all blankets employing liquid metal coolants and/or heat transfer fluids. As part of the scoping phase of the FY82 fusion breeder program, materials compatibility issues and, in particular, those associated with the use of liquid metals, have been emphasized. This section presents a general and non-design specific overview of liquid metal compatibility considerations including chemical activity aspects, mass transfer, stress assisted liquid metal corrosion, liquid metal embrittlement, and impurity interactions between the melt and structural alloys.

IV.B.2 Considerations specific to liquid metal engineering.

The pressure of oxygen over cold-trapped alkali liquid metals is usually far below typical values obtainable in inert gases or even in high vacuum environments, as can be seen in Table IV.B-1. Since high temperature fatigue, corrosion fatigue, and certain other modes of failure are ameliorated significantly with low oxygen pressures, liquid alkali metal are considered a less severe environment for steels in the 400°C range than are inert gases. Liquid metal environments at 500°C and above, however, create conditions where materials interfaces bathed by the same liquid pool tend to approach equal chemical activity for each element. The two most important manifestations of this phenomena for steels in an alkali metal liquid are carbon transfer and deposition of dissolved elements in cooler portions of a circulating liquid circuit. Carbon transfer away from a steel, or decarburization, leads to a less wear resistant, weaker and more ductile alloy. Carbon transfer into a steel creates a more wear resistant alloy with, possibly, a more brittle surface with consequent degradation of fatigue life. Use of steels with different carbon activities can create conditions of carbon transfer under isothermal conditions. If the same steel is used throughout a liquid metal circuit, a temperature gradient is required before a significant carbon activity gradient can be created.

TABLE IV.B-1. Typical oxygen and hydrogen pressures in high purity sodium and helium

Species	Coolent Type	Partial Pressure (Torr)
Oxygen	cold trapped sodium	$<10^{-57}$
Oxygen	1 atm He with 1 ppm O_2	$>7 \cdot 10^{-4}$
Hydrogen	cold trapped sodium	$\sim 10^{-4}$
Hydrogen	1 atm He with 1 ppm O_2	$>7 \cdot 10^{-4}$

A very rough rule of thumb for designers is to estimate the activity of any element in a liquid metal or solid structural alloy as the ratio of actual concentration to the concentration at saturation for the particular tempemature involved. Since the saturation concentration in a liquid metal usually lowers rapidly with decreasing temperature, the actual concentration of solute element in a liquid may exceed the solubility limit of the same liquid metal in the cool leg of the heat transfer loop. The consequent supersaturated liquid solution will crystallize out solute, particularly at locations with relatively thin boundary layers. Some hypothetical examples of phases approaching equal chemical activity of element i are shown in Tables IV.B-2 and IV.B-3. In Table IV.B-2, we postulate an isothermal system with two steels, one ferritic and one austentic, immersed in a liquid metal. In Table IV.B-3, we assume a system with one steel, a stainless grade, immersed in a liquid metal with a temperature gradient across it. In each case, the concentration of element i, in parts per million, changes such that the activity of element i in solution, A_i, moves towards one equal chemical activity value (arbitrarily set to $A_i = 0.05$). Note that the chemical gradient, in terms of ppm, can migrate "uphill" as long as the chemical activities of element i in each phase tend towards a common value. The above treatment is not rigorous as standard states for each element i have not been defined, but the overall concept is quite important to the designer of liquid metal systems. Solutes will move in and out of liquid and solid solutions in response to chemical activity considerations. The rate of such solute movement is significant at 500°C or above.

TABLE IV.B-2. Hypothetical chemical activity considerations in an isothermal, bimetallic liquid metal system

	C	C_{SAT}	A_i	ΔC IF $A_i \rightarrow 0.050$	Final Concentration
Stainless	150	10000	0.015	+350	500
Ferrite	100	1000	0.100	- 50	50
Liquid metal	0.1	1	0.100	-0.05	0.05

TABLE IV.B-3. Hypothetical chemical activity considerations in a monometallic liquid metal system with temperature gradient

	C	C_{SAT}	A_i	ΔC IF $A_i \rightarrow 0.050$	Final Concentration
Stainless at T_1*	150	10,000	0.015	+350	500
Stainless at T_2	150	500	0.300	-125	25
Liquid metal at T_1	0.100	1.0	0.100	-0.050	0.05
Liquid metal at T_2	0.100	0.100	1.00	-0.095	0.005

* $T_1 > T_2$

Although the slight amount of structural alloy that dissolves in liquid alkali metal will usually not thin a wall sufficiently to be of concern, the subsequent highly localized precipitation of dissolved solute can often be a problem. The dissolution that occurs can result in either uniform retreat of surfaces or granular, etched surfaces depending on the relative liquid velocity (Figure IV.B-1). If the liquid boundary layer is thick enough, the rate controlling mechanism will be diffusion through the boundary layer. Each point on the surface dissolves back perpendicular to the original surface. This regime is called the "polishing" regime even though machine marks are preserved in a widened form. If higher velocities thin the boundary layer to a degree such that atoms escaping from individual crystal faces is the slowest (hence rate-controlling) process, crystal faces are etched out and individual grains can fall into the liquid. Systems should be designed to operate in the "polishing" regime. For high purity sodium, this regime extends from 0 to 7 meters/seconds. The range for lithium has not as yet been established.

Other aspects uniquely associated with liquid metals include liquid metal embrittlement -- both transgranular and intergranular (Figure IV.B-2). In the transgranular mode, an invading atom interferes with the metallic bonding in the structural alloy. The invading atom cannot bond to a fixed site but must be free to migrate. Improsed strain is accommodated by fracture rather than by plastic deformation.

In the intergranular mode, the surface free energy between solid alloy and liquid metal, γ_{SL}, is balanced against the grain boundary surface energy, γ_{SS}. The equilibrium angle formed between two grains at the liquid/solid interface (Figure IV.B-2) can be found from the equation $\gamma_{SS} = 2\gamma_{SL}\cos\theta$. If γ_{SL} is less than one half of γ_{SS}, the contact angle θ goes to 0° and the bulk liquid metal forces its way between the grains. The structural alloy will then fall apart. Intergranular liquid metal embrittlement is a rare phenomenon, highly specific to certain liquid metal/solid metal combinations.

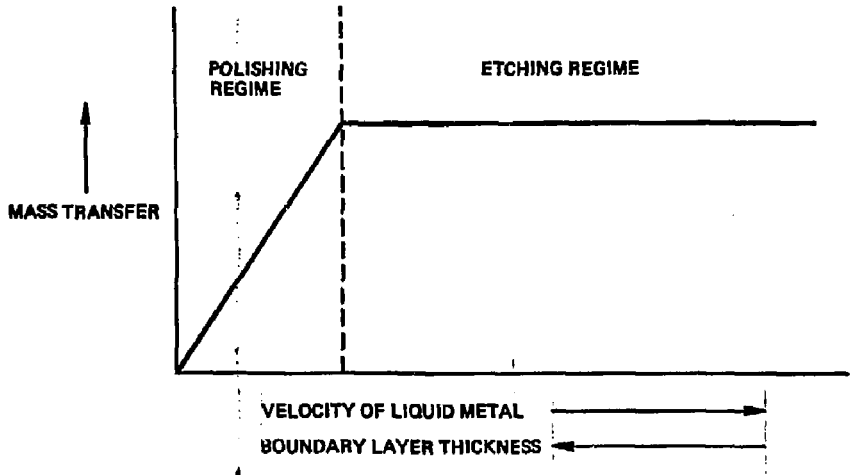

FIGURE IV.B-1. Velocity effects in liquid metal corrosion

Transgranular liquid metal embrittlement

- usually curable by heat treatment
- occurs within 100°C of melting point
- observed with heavy metals and with atoms that do not form compounds

Intergrangular liquid metal embrittlement

(wetting phenomena)

equilibrium angle: $\gamma_{SS} = 2\,\gamma_{SL}\,\cos\theta$

unstable: $\gamma_{SS} > 2\gamma_{SL}$

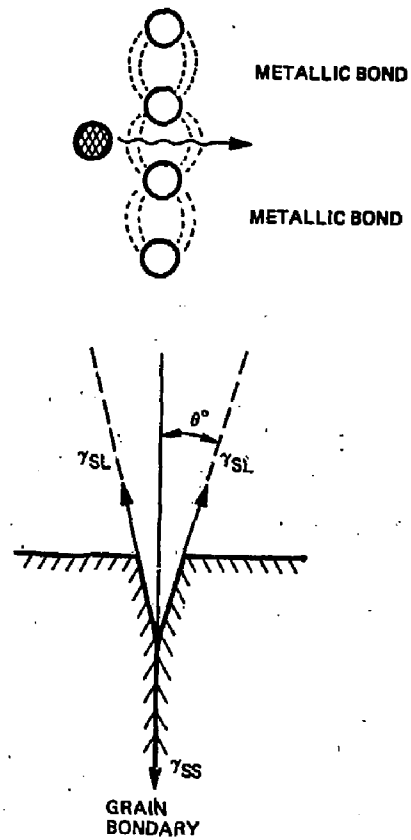

FIGURE IV.B-2 Liquid metal embrittlement

Stress-assisted corrosion is another phenomena associated with liquid metals, particularly lithium (Figure IV.B-3). Low alloy steels with semi-continuous carbides are particularly sensitive to this effect. Proper heat treatment will eliminate this deleterious effect, but the designer must keep in mind that such heat treatments must be applied after field welds. The most sensitive microstructure to stress assisted corrosion is the heat affected zone by a weld prior to a stress-relieving heat treatment.

Perhaps the most serious problems associated with structural alloys operating in liquid metals involve impurities within the structural alloy undergoing stress enhanced diffusion to gain boundaries (Figure IV.B-3). When grain boundaries become laden with As, Sb, S, P or O atoms, liquid metals can become aggressive. Steel melting practice with impurity control during the steel melting can eliminate this problem.

FIGURE IV.B-3. Stress assisted corrosion

- Rupture of metal between particles that are attacked by liquid (curable by heat treatment or chemical stabilizers)
- Enhanced diffusion of impurities to grain boundaries -- temper embrittlement (curable by melting practice)

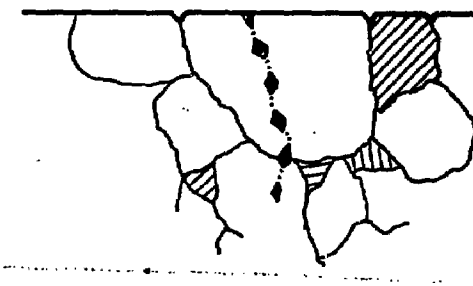

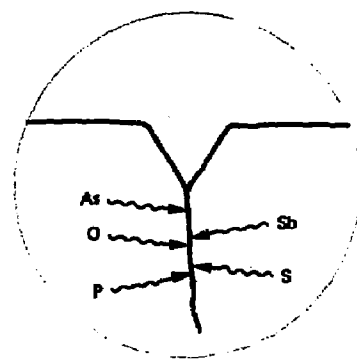

IV.C LITHIUM COMPATIBILITY WORK AT OAK RIDGE NATIONAL LABORATORY (ORNL)

Work has been done at ORNL over the past seven years to study corrosion by molten lithium in support of the U.S. magnetic fusion energy program.[1] More recently, the work has been extended to include Pb-Li alloys.[1] In the former studies, experiments with static and flowing lithium have been conducted using capsules and thermal-convection loops, respectively.[2,3] The fusion work has principally involved corrosion studies of austenitic and ferritic steels and, to a lesser extent, higher nickel alloys. Lithium corrosion studies at ORNL, however, predate the fusion program; work in this area in the 1950's was supported by the Aircraft Nuclear Propulsion Program and, in later years, by space reactor and advanced technology programs. In these earlier programs, much of the effort was concentrated on refractory metals (particularly group VB) although iron-, nickel-, and cobalt-base alloys were also studied.[4–6]

There are several compatibility issues that are involved in a lithium-containing blanket of the fusion-fission hybrid. These will differ depending on the design concept and whether the blanket choice is lithium or a Pb-Li alloy. However, we are generally concerned with four compatibility couples:

1. lithium-structural alloy (austenitic or ferritic steel)
2. lithium-thorium
3. lithium-beryllium
4. beryllium-structural alloy

The latter two reaction couples are of particular interest to the fusion-fission hybrid; we are already generating information about the first couple in on-going studies funded by the magnetic fusion energy program as discussed above. There is limited information for Reaction (3) that suggests that reasonable compatibility exists for beryllium and lithium below 600°C. No Be-Li compounds have been reported and there is only limited solubility of beryllium in lithium. However, the reactions of beryllium with the elements of the structural alloy, particularly nickel, are known to be significant at 600°C. In order to study Reactions (3) and (4) and the synergistic effects associated with Reactions (1), (3), and (4), we have initiated a series of capsule tests using diffusion couples like the one shown in Fig. IV.C-1. The experiment is designed to examine the reactions

occurring between beryllium and stainless steel (1) in direct contact and (2) separated by static lithium. Accordingly, gaps of two different widths are included in the compatibility couple. The couples are submerged in lithium in capsules of like composition to the steel in the couples. Such capsules containing couples of type 316 stainless steel are currently being exposed at 350, 450, and 550°C for 1000, 3000, and 5000 h. Similar experiments with 2 1/4 Cr-1 Mo (wt %) steel are being planned. After exposure, the couples will be carefully sectioned, metallographically examined, and analyzed in order to characterize the type and extent of reactions that occurred.

Experiments are also being planned to evaluate the compatibility of thorium metal with lithium. These experiments, in addition to examining standard corrosion phenomena, are intended to investigate the possibility of self-welding and densification of thorium while it is in contact with molten lithium. The start of such experiments is awaiting input from the design project on the size and shape of the thorium particles.

REFERENCES

1. Alloy Development for Irradiation Performance Progress Reports, U.S. Department of Energy, DOE/ET-0058/1–7 (March 1978–September 1979) and DOE/ER-0045/1–7 (December 1979–September 1981).
2. P. F. Tortorelli, J. H. DeVan, and R. M. Yonco, "Compatibility of Fe-Cr-Mo Alloys with Static Lithium," *J. Mater. Energy Systems* 2 (1981) 5–15.
3. P. F. Tortorelli and J. H. DeVan, "Thermal-Gradient Mass Transfer in Lithium-Stainless Steel Systems," *J. Nucl. Mater.* 85&86 (1979) 289–93.
4. E. E. Hoffman, "Corrosion of Materials by Lithium at Elevated Temperatures," Oak Ridge National Laboratory report, ORNL-2674, March 1959.
5. J. R. DiStefano and E. E. Hoffman, "Corrosion Mechanisms in Refractory Metal-Alkali Metal Systems," Oak Ridge National Laboratory report, ORNL-3424, August 1963.
6. J. H. DeVan and R. L. Klueh, "The Effect of Oxygen on the Corrosion of Vanadium and V-20% Ti by Liquid Lithium," *Nucl. Technology* 24 (1974) 64–72.

ORNL-DWG 82-9320

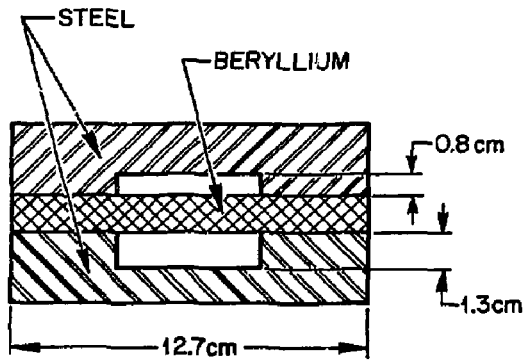

Fig. IV.C-1

Schematic of Compatibility Couple which is Submerged in Molten Lithium

IV.D CHOICE OF FERRITIC OR AUSTENITIC STEEL

In Table IV.D-1, six considerations useful for comparing magnetic, body-centered-cubic (ferritic) steels with non-magnetic, face-centered-cubic (austenitic stainless) steels as the main structural alloy in a mirror fusion machine are shown.

As shown in Figure IV.D-1, projected swelling rates for ferritic steels (eg., HT-9 or 2-1/4 Cr-1Mo) are expected to be substantially lower than swelling rates for austenitic stainless steels. Although the titanium modified 316 SS, or Prime Candidate Alloy (PCA) has potential to reduce stainless steel swelling dramatically, this effect may saturate beyond damage levels of 50 dpa and high swelling could result for higher damage levels. Since structural swelling is expected to be the life limiting mechanism in most blanket designs below 500°C, the expected low swelling characteristics of ferritics is an important consideration.

The second consideration shown in Table IV.D-1 asserts that ductile to brittle transition temperatures of ferritic steels are raised up to 350°C by irradiation and that austenitic steels will generate helium and become brittle by swelling above 450°C. The former assumption is quite dependent on impurity and strength levels of the steel. In particular, phosphorous and copper impurities are quite deleterious to ductile to brittle transition behavior in many ferritic steels. For thinner sections of ferritic steel (0.25 cm) it is possible that DBTT effects will be less critical. There is also a reasonable possibility that high temperature annealing can relieve the DBTT. Nevertheless, operation of ferritic steels above 350°C is expected to limit the DBTT to below the operating temperature (Figure IV.D-2).

The third consideration shown suggests a useful corrosion temperature limitation for ferritic steels above that of austenitic stainless steels. The fourth consideration means that proper heat treatment is required on all structural alloys in order to prevent sudden brittle failure. The fifth consideration is an important plus for certain ferritic steels. Nickel is deleterious to corrosion resistance and helium generation behavior. Some nickel may be required to suppress phosphorous concentration at grain boundaries, though adequate melt practice may eliminate both tramp impurities and the need for nickel to relieve impurity segregation. Low chromium is an advantage both in terms of liquid metal mass transfer and strategic metal availability. Finally, the greater strength of ferritic steels (tensile yield strength of 29 KSI for 2-1/4 Cr-1Mo vs. 18 KSI for 316 SS at 500°C and the higher thermal conductivity translates to mechanical and neutronic advantages.

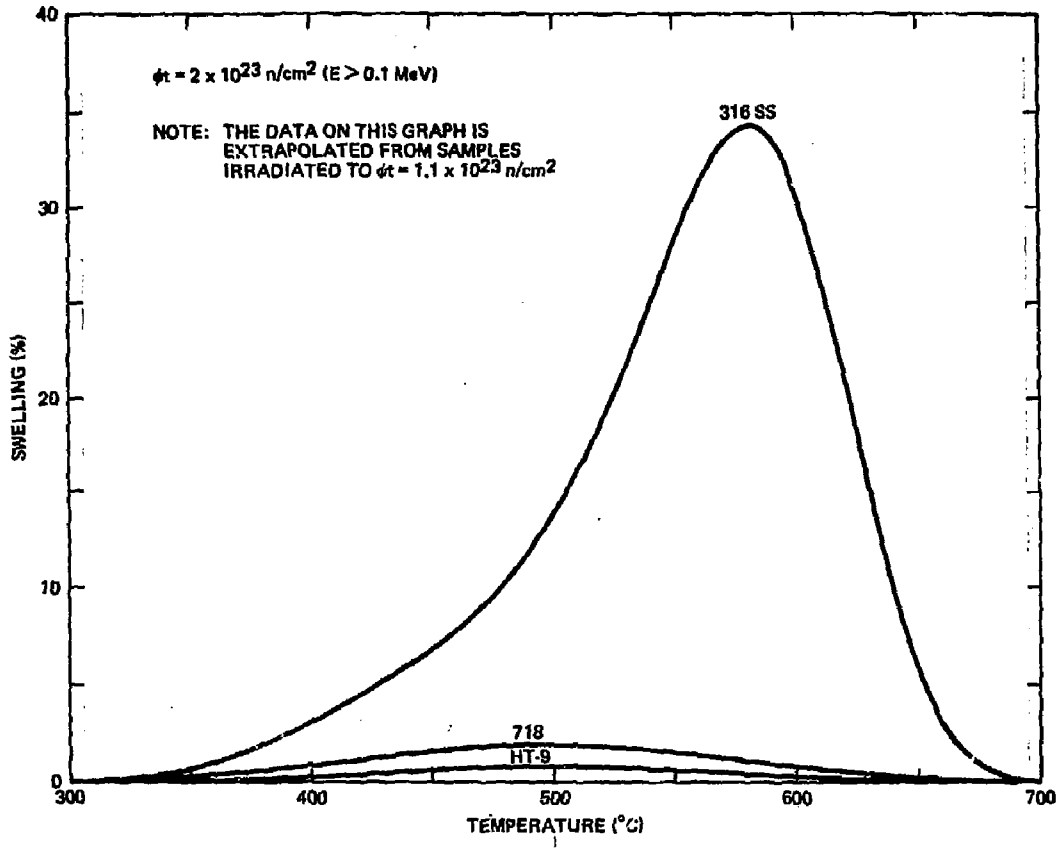

FIGURE IV.D-1. *Swelling of candidate CTR materials during neutron irradiation*

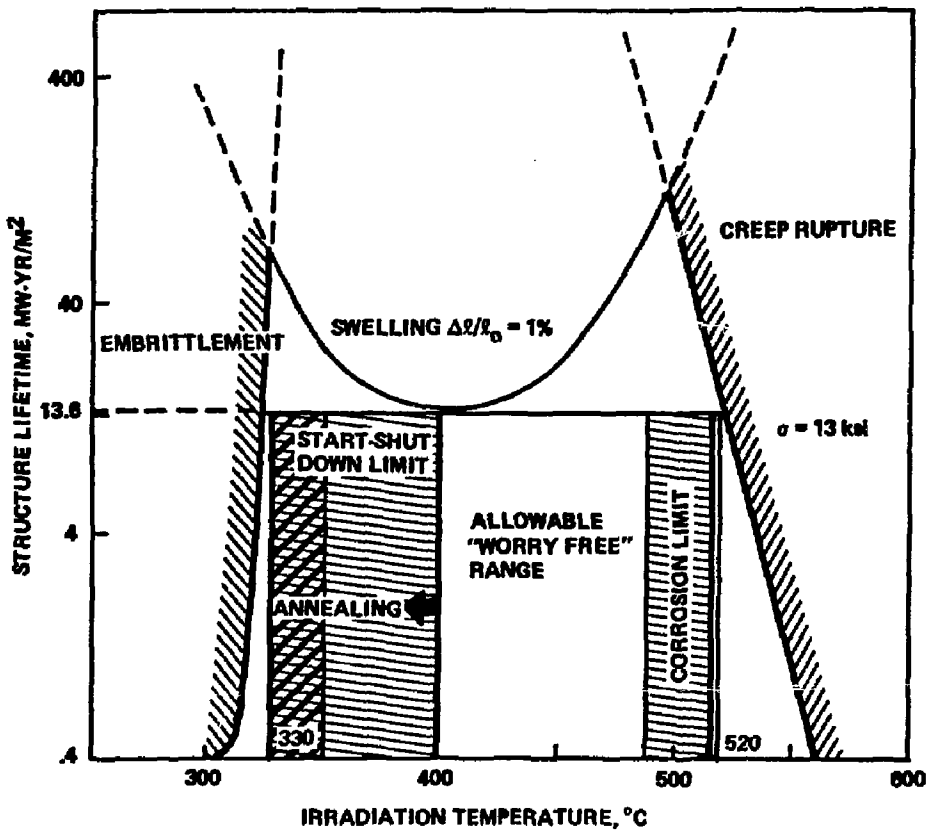

FIGURE IV.D-2. Typical expected life limiting mechanisms for ferritic steels

TABLE IV.D-1. Ferritic Steels vs. Austenitic Steels

- Ferritic steels are expected to provide 1-2 orders of magnitude lower swelling than stainless steels.
- Sections of ferritic steels thicker than 5 cm can have their ductile-to-brittle transition raised above 350°C by irradiation. Austenitic steels can become brittle by swelling above 450°C.
- Corrosion tests in lithium indicate a 500°C max for ferritic steels and some temperature between 400°C and 500°C max for austenitic steels.
- Various chemical embrittlement phenomena can occur on ferritic steels in lithium: embrittling phenomena can occur on austenitic steels in air or steam.
- Ferritic steels can be made with nickel less than 0.5% and chromium less than 3%; particularly useful for applications under 475°C.
- Ferritic steels are stronger than stainless steels in the 400-500°C range and have higher thermal conductivity (lower thermal stress).

Some initial conclusions with respect to ferritic steels versus austenitic stainless steels are shown in Table IV.D-2. If the system will operate under 350°C, austenitic stainless steel is recommended due to DBTT concerns. In the 350-475°C range, low chromium ferritic steels (eg., 2-1/4 Cr-1Mo) are recommended due to low swelling and other advantages. In the 475-500°C range, the penalty of chromium levels above 3 percent and more difficult fabrication may be compensated by the additional strength of such alloys (eg., HT-9). A new, stronger, low chromium alloy -- 3 chromium, 1.5 molybdenum, vanadium steel may eliminate any advantage of the very high chromium ferritic steels, such as HT-9.

TABLE IV.D-2. Initial conclusions: Ferritic steels vs. austenitic steels

- Sections less than 5 cm thick operating in the 350°C to 500°C range should be ferritic steels.
- Sections operating under 350°C should be austenitic steel.
- Avoid transitions between ferritic and austenitic occurring in liquid metal environments.
- Low chromium alloys, such as stabilized 2-1/4 Cr - 1Mo, have advantages in liquid metal systems in the 350°C to 475°C range.
- HT9 may become competitive with stabilized 2-1/4 Cr - 1Mo in the 475°C to 500°C range.

IV.E SWELLING TOLERANT DESIGN

Neutron irradiation is known to damage most materials in such a fashion that their volume is increased. The quantified effect of fusion neutrons is not known; however, high energy neutrons from other sources have demonstrated the effect. Structurally this is quite significant, and the components of the radiation-induced swelling problem are dealt with in this section.

It is important that the magnitude of this problem is appreciated. The following table of commonly encountered strains clearly identifies it as a major significance.

STRAINS

Typical Source	Value	Ratio
Structural	0.1%	1
Temperature differential ~300°C	0.05%	1/2
Low radiation-induced swelling (linear)	0.16%	1.6
High radiation-induced swelling (linear)	0.66%	6.6

IV.E.1 Creep and Swelling

There are various time and temperature dependent effects which interact with swelling. Simplistically, very slow strain rates at elevated temperature may be expected to allow high stresses to relax out. This is often true; however, this effect, which is similar to a lowering of modulus, is very detrimental when applied to a handling situation and most configurations can be shown to have nearly equal benefits and penalties when creep and swelling interact.

The following are practical examples of the swelling effect, which are likely to be of interest due to their recognizable role in the fusion breeder blanket.

The neutron flux profile in a fusion blanket decreases steeply with radial distance away from the plasma. The profile is exponential with distance, but is sometimes modeled as a linear function for structural analysis. Radial structure ties and flow dividers take the form of flat plates that are irradiated from one edge. The edge irradiated flat plate is shown in a linear and exponential flux profile in Figure IV.E-1. It will be seen that by supporting it very simply from the rear corners, the linearly irradiated plate can be relieved of stress, but this is not possible in the real exponential irradiation. It is unusual to discuss a component without regard to its function but a principle of swelling tolerant design is that the configuration must relieve swelling problems first, since they have no regard for function. The function can only be ascribed to the component after swelling concerns are addressed. Item 3 of the figure shows the most capable edge irradiated member we have yet identified. Its capabilities are that it can take short direction tension or compression and some comparatively light bending, again in the short direction, but is essentially free to move to accommodate swelling in the long direction. This is certainly a rather limited capability for a conventional plate, and is engendered by the requirement to reserve all stresses in one direction (the long direction) to serve swelling release functions.

Figure IV.E-2 shows the problem and some facets of its handling when a cylindrical module as might be used for a mirror reactor is irradiated from a plasma inside the cylinder. The first item in the figure shows that a disc which could be used to close the end of the module, will swell inward because of the large amount of nonswollen material restraining the most intensively irradiated material, which is thus only free to move inward. The second item shows the axial and diametrical growth of a cylinder irradiated internally. It will get both longer and larger in diameter, and the thickness will change but this will not be very important. These two components are shown together in the third item of the figure. As swelling

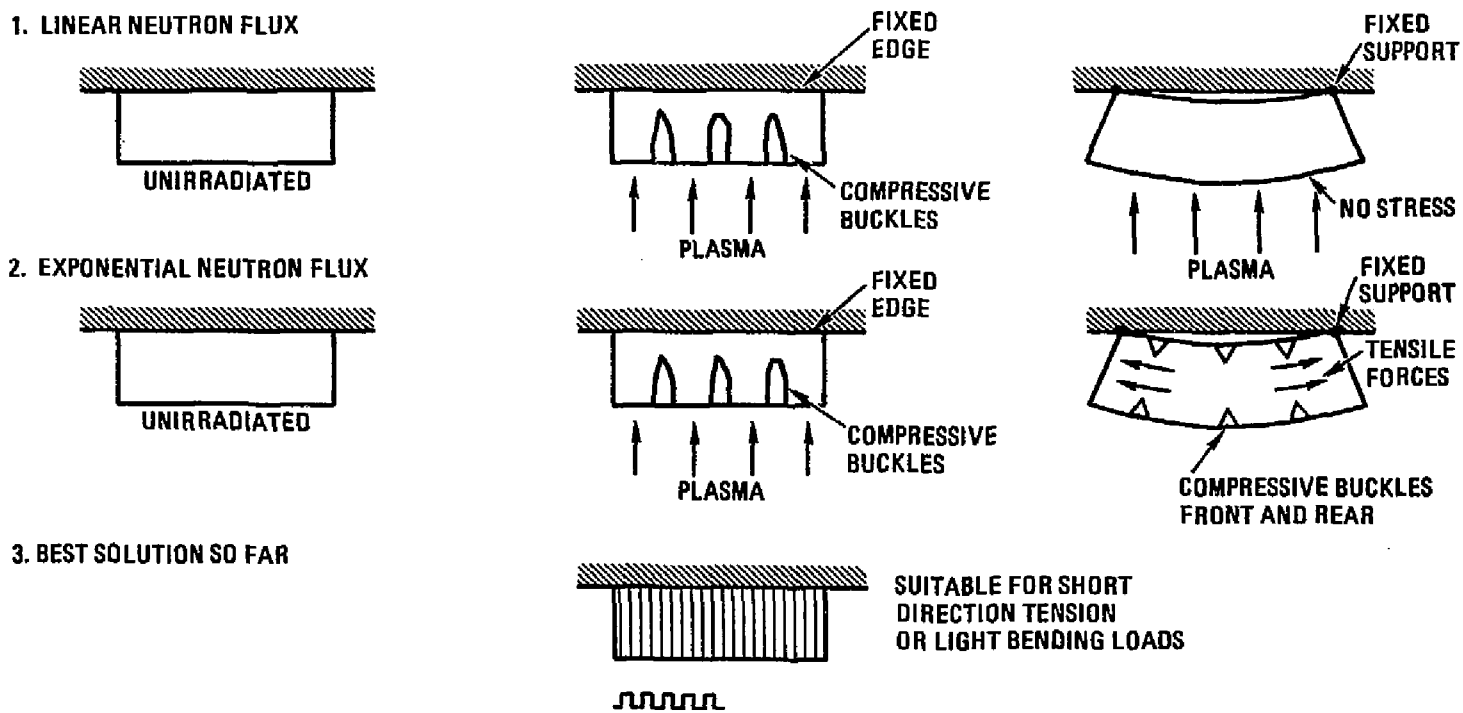

FIG. IV.E-1. Edge irradiated swelling effects on flat plate.

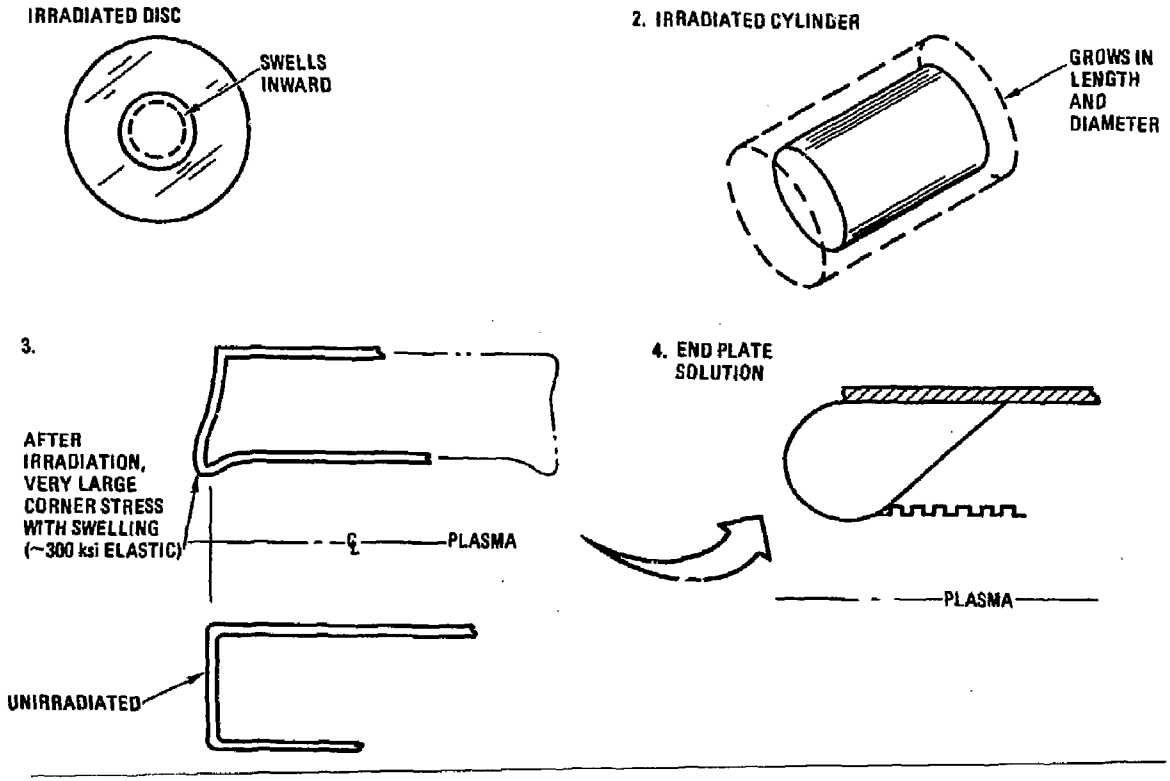

FIG. IV.E-2. Irradiated reactor vessel end.

occurs in the two parts, extremely large stresses can be elastically calculated, so large indeed that it is apparent that the calculation is unrealistic and that the mechanism of failure appropriate to the material will have operated.

The fourth item of this figure shows a present solution in which a "balloon" end is fitted to the module which is capable of internal diameter change and is tied against the axial force due to the internal pressure. The corrugated first wall can thus increase in diameter and absorb length increases within its corrugations without overstressing the ends.

It is significant that this wall must be free to grow in diameter by a few centimeters or it will be overstressed. If the blanket pressure is high, the stabilization of such a free-swelling wall against buckling collapse is a considerable problem. Figure IV.E-3 shows a possible answer to this problem.* The "A" frame attachments could allow both axial and radial movement to accommodate swelling, but prevent azimuthal motion, thus stabilizing the wall against buckling due to the external pressure load.

IV.E.3 Conclusions

The requirement to tolerate swelling puts a considerable burden on the blanket vessel design. There are indications that if appropriate measures are taken the effects can be minimized; however, a critical factor in the swelling tolerance scenario is the severity of the job the structure is doing. It is much more difficult to make a high pressure first wall swelling tolerant than one with minimum pressures. It often transpires in swelling tolerant design that adding material, which is usually undesirable from many non-structural considerations is also structurally undesirable. In short, the addition of material will raise rather than lower the stresses and thus present no solution whatsoever. The fusion breeder reactor blanket shares with other fusion blankets a requirement that the designers must be aware of swelling problems and that innovative solutions be sought and applied.

---

* "A" frame issues such as the number of frames, and the angle of attachment remain to be resolved.

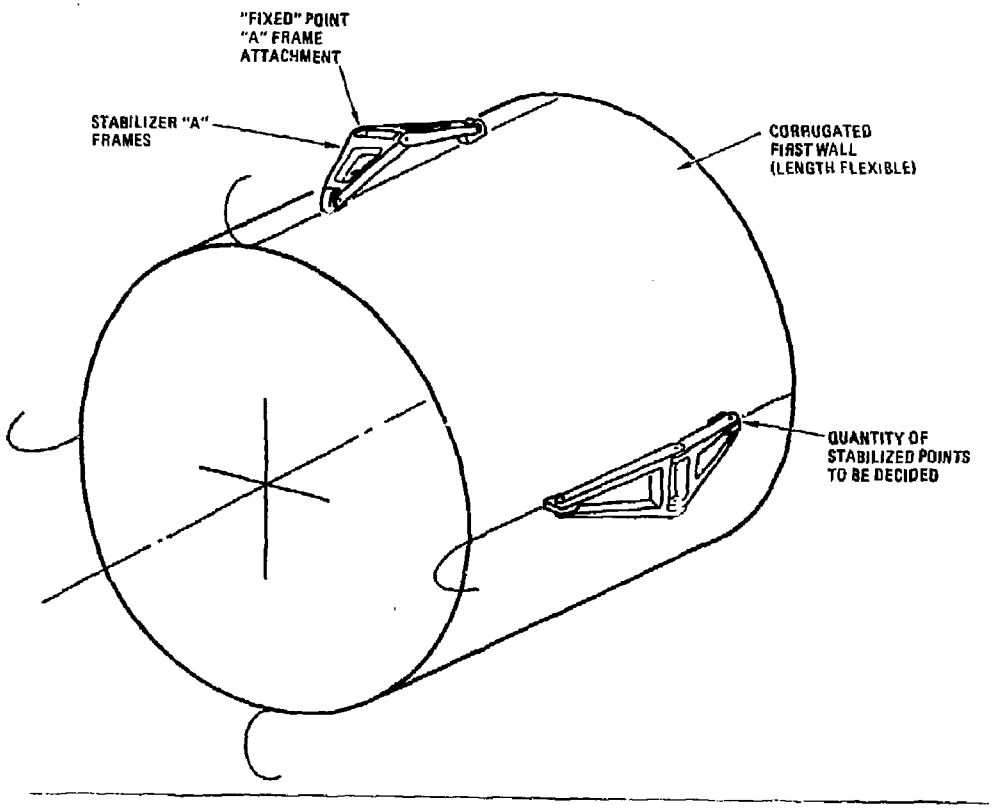

FIG. IV.E-3. Swelling tolerant cylindrical first wall.

IV.F SAFETY ASSESSMENT OF LITHIUM AND LEAD LITHIUM ($Li_{17}Pb_{83}$)

The superior heat transfer characteristics of liquid metals over alternative coolants have resulted in the proposed use of lithium or lead-lithium alloys in the fusion breeder reactor. As part of the overall evaluation of these materials, an assessment of the safety aspects of their use was carried out. The first part of the scoping assessment described below presents the basis for evaluating the relative safety merits of lithium and its lead eutectic, $Li_{17}Pb_{83}$. The second part, presented in the next section, consists of a preliminary survey and investigation of engineered safety systems that are routinely used or have been proposed for use in conjunction with liquid metals.

The alkali metals, most notably sodium and the eutectic NaK, have been successfully used in industrial cooling applications for several decades. At the present time, extensive experience is being accumulated with liquid metal cooling in conjunction with the fast breeder program. This experience indicates that lithium, the least reactive of the alkali metals, can be safely handled in the quantities required for the fusion breeder on the basis of present-day technology.

The characteristics of lithium and lead-lithium that necessitate the regard for safety can be summarized as follows:

1. Lithium reacts exothermically with a number of substances. The heat released must be dissipated to the surroundings faster than it is generated in order to prevent ignition.

2. The products of lithium reactions can potentially explode or initiate a pressure pulse.

3. Since lithium is the fusile breeder, it will be the source of tritium.

4. The corrosive nature of lithium and lead may present stringent cleanup requirements in the event of a spill or the deposition of aerosols. Lead is more difficult to clean up as the only known solvents are reactive metals (i.e., lithium and sodium).

5. Lead is toxic and will become activated during irradiation.

The corrosive properties of Li and $Li_{17}Pb_{83}$ are covered elsewhere in this report and thus not discussed in this section. Other characteristics are discussed in detail below.

A partial list of the potential chemical reactions involving lithium are shown in Table IV.F-1.[1] A review of the list shows that lithium releases heat in reacting with a number of common substances including water, oxygen, nitrogen, and the aggregate used to make concrete. The heat of reaction generally decreases with increasing temperature. The reaction products include hydrogen, LiH, LiOH, and Li_2O. The safety concerns associated with these reaction products include the potential for hydrogen explosion, the violent decomposition of LiH at temperatures near 1000°C and the corrosive nature of LiOH and Li_2O.

In comparisons of lithium with $Li_{17}Pb_{83}$ on a per gram of lithium basis, the heats of reaction of the eutectic with water and air are 20% and 25% lower than with the pure metal.[2] In reactions with both air and water, the enthalpy change of the alloy is one-seventh of that of the pure metal on a unit volume basis, due to the low lithium density in the alloy. Overall, $Li_{17}Pb_{83}$ is expected to be less reactive than lithium, having an expected activity of lithium of 10^{-4} to 10^{-3} in the temperature range of 500° to 700°C.[3,4,5]

At temperatures below its melting point (180°C), experiments show that solid lithium does not react with dry oxygen and reacts slowly with moist air. Lithium has been observed to react slowly with cold water, liberating hydrogen, but neither the hydrogen nor the lithium subsequently ignites. A brief synopsis of the experimentally observed reactions of lithium and $Li_{17}Pb_{83}$ at temperatures above their melting points with water, air, and concrete is presented in Tables IV.F-2 and -3, taken from References 6 through 9.

At liquid temperatures, Table IV.F-2 shows that lithium in excess water reacts vigorously, ignites, and releases heat, H_2, and aerosols. It has been postulated[9] that an occasional accompanying detonation can be attributed to the rapid decomposition of LiH at approximately 1000°C rather

TABLE IV.F-1. Heats of reaction of lithium chemical reactions (Mainly from Reference 1)

Reaction	Heat of Reaction (Kcal/Mole of Product)
$2Li + 2C \rightarrow Li_2C_2$	-55
$2Li + 3CO \rightarrow Li_2CO_3 + 2C$	-210
$4Li + 3CO_2 \rightarrow 2Li_2CO_3 + C$	-149
$2Li + H_2 \rightarrow 2LiH$	-22
$2Li + H_2 + O_2 \rightarrow 2LiOH$	-167
$2Li + 2H_2O \rightarrow 2LiOH + H_2$	-49
$4Li + H_2O \rightarrow 2LiH + Li_2O$	Not available
$2Li + 2LiOH \rightarrow 2Li_2O + H_2$	Not available
$6Li + N_2 \rightarrow 2Li_3N$	-48
$4Li + O_2 \rightarrow 2Li_2O$	-143
$2Li + O_2 \rightarrow Li_2O_2$	-152
$Li + Pb \rightarrow LiPb$	-15
$8Li + Fe_3O_4 \rightarrow 3Fe + 4Li_2O$	-151 (magnetite concrete)
$4Li + SiO_2 \rightarrow Si + 2Li_2O$	Not available (basalt concrete)

TABLE IV.F-2. Experimental results of lithium and $Li_{17}Pb_{83}$ reactions with water.

Experimental Conditions	Observations
Lithium	
• 500°C lithium in excess 95°C water[a]	• Lithium floats, reacts vigorously, ignites (2 s)
• 500°C lithium injected under excess 95°C water[b,c]	• Explosive pressurization in 0.25 to 0.5 s, in either air or argon environment
• 600°C lithium in excess 98°C water[d]	• Vigorous reaction forming white glowing mass, releasing H_2, heat, and white aerosol
• 98°C water on excess 600°C lithium[d]	• Bright glow where water remained; white aerosol
• 20°C water sprinkled on molten lithium[e]	• Water evaporates; white smoke; H_2 flares
• Small steam leak into hot Na, e.g., cracked Hx tube[e]	• Vaporized layer at interface: H_2 flares; lithium expected to behave similarly but with lower activity
$Li_{17}Pb_{83}$	
• 500°C Li17Pb83 in excess 95°C water[a]	• $Li_{17}Pb_{83}$ sinks; slow evolution of H_2; no pressurization
• 600°C $Li_{17}Pb_{83}$ in excess 98°C water[a]	• $Li_{17}Pb_{83}$ sinks; unexpectedly high H_2 evolution

[a]Reference 6.
[b]Reference 6.
[c]Reference 7.
[d]Reference 8.
[e]Reference 9.

TABLE IV.F-3. Experimental results of lithium and $Li_{17}Pb_{83}$ with air and concrete.

Experimental Conditions	Observations
Lithium	
• 230° and 510°C lithium in dry air[a]	• Immediate ignition; lithium pool temperature rises to 1000°C, remains for 1 hr; cools to 500°C in 5 hrs (air supply depletion)
• 230° and 510°C lithium in moist air[a]	• Few minutes to ignition; lithium pool temperature rises to 1000°C, remains for 1 hr; slower cooldown (800°C in 5 hrs)
• Blow torch to lithium in air[a]	• Ignition when pool reaches 800°C; temperature increases to ~1000°C; very short flame (1/8 in.)
• "Hot" lithium + concrete[a,b]	• Violent explosion; temperature rises to 1000°C
• 300°C lithium + concrete[a,b]	• No reaction for 7 hrs, then violent reaction
$Li_{17}Pb_{83}$	
• 300°C $Li_{17}Pb_{83}$ + air[c]	• Ignition with pool temperature rise to 1200°C; this is an undocumented personal communication for an LiPb alloy approximately $Li_{17}Pb_{83}$

[a]Reference 9.
[b]Reference 8.
[c]Reference 2.

than to ignition of the evolved H_2. In the case of small amounts of water contacting lithium, the water quickly evaporates, diminishing the chemical reactivity. In general, a vaporized layer appears at the reaction interface accompanied by white smoke. Hydrogen flares, invisible to the naked eye, have been detected with high speed photography.[9] With $Li_{17}Pb_{83}$, no evidence of a violent reaction or pressurization has been detected. An unexpectedly high measurement of H_2 evolution is still under investigation and additional tests are scheduled for the near future.[8]

With air, both lithium and $Li_{17}Pb_{83}$ have been reported to ignite. Lithium was observed to burn with a short (1/8 in.) flame.[9] The measured flame temperature was 900°C which is to be contrasted with the theoretical adiabatic flame temperature of 3600°C. The report of ignition in air of an Li-Pb alloy approximately $Li_{17}Pb_{83}$, indicated that ignition was reached at a pool temperature of 300°C with a flame temperature of 1200°C.[2] With concrete, only results of lithium reactions have been reported.[8,9] These results indicate that lithium has reacted violently with the two aggragates most commonly used in making concrete.

The third area of safety interest listed above entails the tritium permeation rates/solubilities associated with lithium and $Li_{17}Pb_{83}$. These parameters can be evaluated in terms of Sievert's constants for tritium in the materials. At 500°C, Sievert's constant for tritium in lithium has been quoted[4] as 7.1×10^4 appm/torr$^{1/2}$, which can also be expressed as 1.4×10^7 Ci/m^{3}Pa$^{1/2}$. Sievert's constant for tritium in $Li_{17}Pb_{83}$ in the temperature range of 400° to 600°C was recently reported[5] as 3.0 appm/ torr$^{1/2}$, which can be expressed as 410 Ci/m^{3}Pa$^{1/2}$. Thus, for a tritium control system that maintains a given tritium partial pressure, the tritium inventory in lithium will be 3×10^4 times that in $Li_{17}Pb_{83}$. Permeation of tritium is proportional to the difference of the square roots of the tritium partial pressure across a barrier. Therefore, the tritium permeation rates will be 1.8×10^2 times greater with $Li_{17}Pb_{83}$ than with lithium in a tritium system that maintains a given tritium inventory per unit volume. It is noted that these statements do not account for the relative ease with which the performance requirements imposed on the tritium control and recovery systems by

either lithium or $Li_{17}Pb_{83}$ can be met. In fact, <1 kg tritium inventories in lithium based upon molten salt extraction at 1 appm, appear to be possible. More definitive statements on tritium concerns require that tritium control and recovery systems be included in the analysis.

All forms of lead are potentially toxic. The risk of lead poisoning is greater through inhalation than through ingestion, the seriousness increasing with decreasing particle size. If exposure to lead is halted, the quantity of lead in circulation will decrease via excretion with body wastes. The slow return of lead stored in the bones will maintain a toxic level in the blood stream for some time after exposure. Recovery from lead poisoning is usually complete with no resultant disabilities.[10] The activation of lead was investigated in the STARFIRE report[11] in investigations of Zr_5Pb_3 as a neutron multiplier. At a neutron wall loading of 3.6 MW/m^2, an activation level on the order of 10^3 Ci/m^3 was calculated. This activity level is determined in the first 10 to 30 yr by ^{204}Tl (3.8 yr, beta or electron capture decay, no gamma rays observed between 0.1 and 2.5 MeV). Subsequently, an activity level of less than 10 Ci/m^3 is established by ^{205}Pb (1.4×10^7 yr, electron capture, no gammas). The relative importance of these activity levels in comparison with activity levels resulting from fission products, actinides, and activation products (including activated corrosion products) has not been evaluated in this study.

In summary, the experimental results of $Li_{17}Pb_{83}$ reactions with water are encouraging as they indicate fairly inert behavior. A recent report of its ignition in air is under investigation. Further work with $Li_{17}Pb_{83}$ is in progress. Air, water, and concrete must be prevented from contacting liquid lithium. In the event of its ignition, a lithium fire may not be as damaging as pessimistically predicted by adiabatic flame temperature calculations. Experimental observations have shown that the flame is shorter and cooler than predicted. Tritium solubility is greater in lithium than in $Li_{17}Pb_{83}$ and the converse is true for tritium permeation rates. Further comments on tritium require additional definition of tritium control and recovery systems.

In conclusion, both lithium and $Li_{17}Pb_{83}$ can be handled safely with present-day technology. From the point of view of safety, $Li_{17}Pb_{83}$ is preferred over lithium according to present data. Finally, it is pointed out that the presence of lithium and possibly of $Li_{17}Pb_{83}$, means that the potential for hazard cannot be eliminated, but can be reduced with safety systems. A discussion of fusion breeder safety system options is presented in the next section.

REFERENCES

[1]M. S. Tillack, and M. S. Kazimi, "Development and Verification of the LITFIRE Code for Predicting the Effects of Lithium Spills in Fusion Reactor Containments," MIT Plasma Fusion Center Report No. PFC/RR-80-11, July 1980.

[2]STARFIRE/DEMO Working Group, "STARFIRE/DEMO - A Demonstration Tokamak Power Plant Study," ANL Draft Interim Report, January 1982, pp. 4-184 to 4-186.

[3]N. J. Hoffman, et al., "Properties of Lead-Lithium Solutions," Proceedings of the Fourth Topical Meeting on the Technology of Controlled Nuclear Fusion, King of Prussia, Pa., October 1980, pp. 1754-1763.

[4]D. K. Sze, et al., "LiPb, A Novel Material for Fusion Applications," Proceedings of the Fourth Topical Meeting on the Technology of Controlled Nuclear Fusion, King of Prussia, Pa., October 1980, pp. 1786-1793.

[5]E. M. Larsen, et al., "Comments on the Hydrogen Solubility Data for Liquid Lead, Lithium and Lithium-Lead Alloys and Review of a Tritium Solubility Model for Lithium-Lead Alloys," University of Wisconsin Report UWFDM-415, May 1981.

[6]P. A. Finn, and V. A. Maroni, Personal Communication, February 11, 1982: also, P. A. Finn, et al., "The Reactions of Li-Pby Alloys with Water," ANS Transactions, v. 34, June 1980, p. 55.

[7]"Third Annual Progress Report on Special Purpose Materials for Magnetically Confined Fusion Reactors," DOE/ER-0113, November 1981.

[8]D. W. Jeppson, Personal Communication, February 9, 1982; also, L. D. Muhlestein and D. W. Jeppson, Handouts on HEDL Fusion Reactor Safety Support Studies, Fusion Reactor Safety Advisory Committee Meetings, November 8, 1981 and January 15, 1981; also, D. W. Jeppson and R. F. Kenough, "Fusion Reactor Blanket and Coolant Material Compatibility," Proceedings of the Second Topical Meeting on Fusion Materials, August 9-12, 1981, Seattle, Washington.

[9]J. A. Blink and N. J. Hoffman, Personal Communication, February 11, 1982; also, N. J. Hoffman, et al., "Lithium Safety Considerations," 1980 Laser Program Annual Report, v. 3, Lawrence Livermore National Laboratory Report, UCRL-50021-80, pp. 9-61 to 9-63; also, "1981 Laser Program Annual Report," to be published.

[10]R. N. Lyon, ed., Liquid-Metals Handbook, (for sale by the Superintendent of Documents, U.S. Government Printing Office), January 1954.

[11]C. C. Baker, et al., "STARFIRE - A Commercial Tokamak Fusion Power Plant Study," ANL/FPP-80-1, September 1980.

IV.G REACTOR SAFETY SYSTEMS

Major safety concerns in the fusion breeder and other hybrid reactors have been identified in numerous reports (e.g., References 1 through 5). In summary, the major concern is the release of radioactivity as a result of loss of cooling conditions to either the first wall/blanket region or the bred fuel handling equipment. In systems containing liquid metals, another conceivable mechanism for volatilization of radioactivity is presented by the potential for a liquid metal fire. To prevent or otherwise minimize the release of radioactivity, safety is incorporated by a number of techniques.

1. Eliminating hazards to the greatest extent possible.
2. Prioritizing redundancy to failure by proper design.
3. Incorporating mitigating barriers to the propagation of accident sequences.
4. Using dedicated engineered safety systems.

These techniques are discussed below.

The radioactive hazard in the fusion breeder has been minimized by adopting the fission-suppressed concept. The listed references have shown that a fertile-dilute fission-suppressed blanket offers one to two orders of magnitude reduction in the biological hazard potential (BHP) to be found in the reactor over fast-fissioning blankets. This safety advantage has been a major factor in selecting the fission-suppressed concept for the fusion breeder.

Advantageous use of a redundant design configuration can result in a safer reactor. An example of redundancy by design is as follows. Consider one of the blankets under consideration, the pipe cooling blanket. Two liquid metal systems in direct contact with the first wall provide redundancy in cooling in the event of a primary coolant system malfunction. Furthermore, if the first wall and alternate rows of tubes are independently cooled (as in STARFIRE/DEMO[6]), a tremendous improvement in safety may be possible. Additional examples can result from a concerted effort to include redundancy in the design in support of safety.

As the design of the fusion breeder blanket develops, specific hazards, failure modes, and hazard pathway will be identified and quantified. This will permit the erection of mitigating barriers to interrupt accident progressions. The safety analysis and design, performed integrally with the mechanical/thermal-hydraulic/materials systems design efforts will result in beneficial safety feedback.

The guiding philosophy in the design of dedicated safety systems for the fusion breeder is to employ passive safety systems to the greatest extent possible. Examples of passive and semipassive systems are those relying purely on natural properties and characteristics of materials for fail-safe operation, such as gravity, high heat capacity, natural convection currents, buoyancy, etc. A number of examples of these systems are listed in Table IV.G-1. With proper redundancy, semipassive and active safety systems are also acceptable, and examples of these are also listed in Table IV.G-1. Many of these techniques are presently being used in conjunction with the liquid-metal fast breeder program and can provide a sound data base for their adaptation to the fusion breeder.

TABLE IV.G-1. Some safety system options for the FBR

Passive

- Inert gas environment in reactor building
- Steel lined concrete chambers
- Sacrificial material between steel liner and concrete
- Deep, narrow sumps in reactor building floor
- Sloped surfaces to sumps
- Steel balls and hollow graphite microspheres in spillage areas

Semipassive

- Passively cooled dump tank (natural convection or heat pipes to heat dump)
- High heat capacity thermal exchange (i.e., pebbles or fluid)

Active

- Pump reactor building cover gas through plasma chamber
- Reduced primary loop coolant pressure
- Dump coolant system (e.g., STARFIRE/DEMO)
- Pool surface cooling
- Inert gas makeup or recirculation
- Chemical fire fighting methods
- Forced injection of hollow graphite microspheres

REFERENCES

[1]J. D. Lee, et al., "Feasibility Study of a Fission-Suppressed Tandem Mirror Hybrid Reactor," to be published, 1982; also, I. Maya, et al., "Safety Considerations in the Tandem Mirror Hybrid Reactor Study," ANS Transactions, v. 39, 1981.

[2]K. R. Schultz, et al., "Hybrid Reactor Safety Study, Second Annual Report," General Atomic Report GA-A16185, December 1980; also, I. Maya, et al., "Safety Evaluations of Hybrid Blanket Concepts," Fourth ANS Topical Meeting on the Technology of Controlled Nuclear Fusion, CONF-801011, 1980, and General Atomic Report GA-A16101, September 1980; also, K. R. Schultz, et al., "Hybrid Reactor Safety Study, Annual Report," General Atomic Report, GA-A15578, December 1979.

[3]W. E. Kastenbert, et al., "Some Safety Studies for Conceptual Fusion-Fission Hybrid Reactors," EPRI, ER-548, July 1978.

[4]D. J. Bender, et al., "Reference Design for the Standard Mirror Hybrid Reactor," joint Lawrence Livermore National Laboratory and General Atomic report UCRL-52478 and GA-A14796, May 1978, pp. 466-513.

[5]R. P. Rose, et al., "Fusion-Driven Breeder Reactor Design Study," Westinghouse Report, WFPS-TME-043, May 1977, Chapter 7.

[6]C. C. Baker, et al., "STARFIRE - A Commercial Tokamak Fusion Power Plant Study," Argonne National Laboratory Report ANL/FPP-80-1, September 1980, Chapter 10; also, "STARFIRE/DEMO -A Demonstration Tokamak Power Plant Study," Draft Interim Report, January 1982, Chapter 4.

IV.H PEBBLE FLOW AND PACKING

IV.H.1 Flow and Mixing of Spheres of Different Density

Both the directly cooled and internal coolant tube blanket concepts employ pebbles as breeding fuel and as neutron multiplier. The two types of pebbles would be homogeneously mixed and would be poured into or out of a blanket module in a batch or continuous process.

To extract thorium or uranium fuel pebbles after reasonable enrichment (about 5%) it would be necessary to dump the pebbles, separate the neutron multiplier pebbles for reuse, and send the fuel pebbles to a chemical processing plant for chemical separation and conversion to a fission reactor fuel form.

The necessity for having homogeneous distribution of fuel in the neutron multiplier stems from heat transfer considerations. Any tendency for fuel pebbles to "clump" can lead to hot spots and local welding of fuel pebbles or, conversely, a derating of the power density which would be allowed for totally uniform mixing. Complete disruption of the bred fuel extraction process might result from such local melting if it results in accidental welds.

We felt some tests of the mixing behavior of mixed spheres of the correct density ratio were necessary. Assuming thorium as the fuel and beryllium as the neutron multiplier the density ratio is:

$$\frac{\rho_{th}}{\rho_{be}} = \frac{11.7}{1.85} = 6.32$$

To model this we chose steel ball bearings and lucite spheres.

$$\frac{\rho_{st}}{\rho_{lu}} = \frac{7.85}{1.15} = 6.8$$

Mixture ratios in the range from 20:1 to 30:1 (number of light spheres:number of heavy spheres) were investigated. Although these tests were incomplete with respect to modeling of actual blanket geometries (e.g., the pipe grid in the internal coolant tube concept), variations in possible pebble size ratios, and variations in fueling mechanisms, valuable insights relating to pebble flow and mixing have resulted.

IV.H.2 Vibration Tests

A lucite cylinder, 4.5 inches in diameter and about 10 inches high, was closed at its lower end with a lucite plate. Mixing and settling of pebbles could be readily observed through the 1/4-inch-thick walls.

All pebbles used to date are 1/4-inch-diameter spheres. The steel ones are precision components, spherical to about 0.1%. The plastic spheres were commercial grade, spherical to about 5%.

One method of obtaining homogeneous mixing involves pouring the two different species simultaneously at the correct rate to fill the cylinder with the desired numerical ratio. This took some practice. It also never really achieved homogeneity. Clumps of 2 or 3 pebbles were always observed, their total, representing about 25% of the heavy pebble population, could be tolerable if factored into the design.

Hand vibration produced three notable results.

1) A partially filled container with vertical accelerations of about 1 g showed total segregation near the free surface. Spheres near the surface could displace slightly and this freedom allowed the heavy spheres in the upper region to all settle down to a level 3 to 5 sphere diameters from the surface--not a surprising result (and perhaps not representative of in situ blanket conditions) but nevertheless indicative of future problems (i.e., avoid free surfaces in high flux regions).

2) A filled container with a plastic diaphragm lid which exerted light compression on the bed showed no sphere movement under violent hand vibration.

3) With water present in case 1 above, all of the heavy pebbles migrated to a central region below the vertical center of the bed and tended to form one conglomerated mass. This clump never could be made to approach the wall of the cylinder with vertical hand vibration. The vessel geometry apparently exerted a centering influence radially and also prevented clump contact with the bottom. This test indicates that equal size pebbles of grossly different density will cause problems and similar tests for smaller sized steel spheres are indicated.

IV.H.3 Pouring Tests

From some surplus laboratory apparatus we fashioned a simulated slice of a blanket module. A cylindrical steel housing about 3-3/4 inches thick and 28-1/2 inches inside diameter was already equipped with three inlet ports at 90^{0} intervals. Two lucite sheets were bolted on as side plates with an inner lucite cylinder (simulating the plasma chamber first wall) attached between the side plates. Figure IV.H-1 shows this apparatus. So far our tests have been limited to pouring premixed spheres through a single port on the top centerline and observing the sphere distribution. No fluid occupied the apparatus prior to the pours.

Two identical tests were conducted. The sphere depth in the test fixture after pouring was limited to about 6 inches. Very similar results were achieved. Since the fueling port was at top dead center, all the spheres impacted on the top half of the inner diameter of the annulus. The pour was accomplished in three equal increments of spheres, each batch numbering about 9,000 spheres.

1) After batch #1 the mixing appeared good. It was similar to results achieved in the simultaneous pouring of the two species into the lucite cylinder.

2) After batch #2, the first batch appeared unchanged but this second layer showed a definite concentration of heavy spheres toward the vertical centerline, i.e., underneath the center cylinder.

3) After batch #3, the first two batches were unaltered, but this third layer showed a concentration of heavy spheres away from the centerline. The split was roughly symmetrical although the free surface was slanted. This resulted from our not attempting to pour exactly vertically. More spheres fell on one side of test rig. In our repeat test the same results occurred, but to a lesser degree. These tests indicate that multiple fueling ports could be required.

IV.H.4 Discussion of Results

Nothing quantitative can be deduced from these brief and unsophisticated

tests but one conclusion was inescapable. The probability of achieving a truly homogeneous mixture is very small. Many subtle geometric and gravitational influences produce different effects as the bed depth changes. The bounce pattern is altered and spheres with different physical properties react differently. Even if a perfectly homogeneous pre-mix were achieved, it would be segregated by dynamic effects which vary during the pouring time. These effects would be expected to be reduced in the presence of a heat transfer fluid. A partially segregated or clumped bulk mix will almost certainly not improve after being poured into a blanket annulus.

IV.H.5 Recommendations

We might conclude that the pebbles should all be the same mass. This can be achieved by fabricating hollow pebbles of the heavy material. This is a solution worthy of cost evaluation and testing. But it does not mean that their physical properties will be the same. Young's modulus and Poisson's ratio will be different for the two different materials. Their influence on dynamic trajectories of the falling pebbles will almost certainly cause some differences. Such differences might be masked by scattering interactions and the presence of a fluid background. Only tests will demonstrate those effects.

A better solution might be to distribute some fuel into or onto each beryllium pebble so every pebble in the entire blanket is identical to every other one. This might be accomplished by a mechanical design scheme or by coating fertile fuel onto the beryllium. For mechanical schemes, fuel separation and reloading of the beryllium would have to be accomplished during extraction. As the present scheme requires extraction of all the pebbles and separation of the two species, it may not be a great deal more difficult to process each pebble by extracting an old, and adding a new fuel element. Sketches of two possible pebble designs are shown in Fig. IV.H-2. The key issue is allowed cost to fabricate and handle a two-material pebble. This cost varies as the pebble size cubed with representative values being 25¢ for a 1-cm-diameter pebble and $6.75 for a 3-cm-diameter pebble.

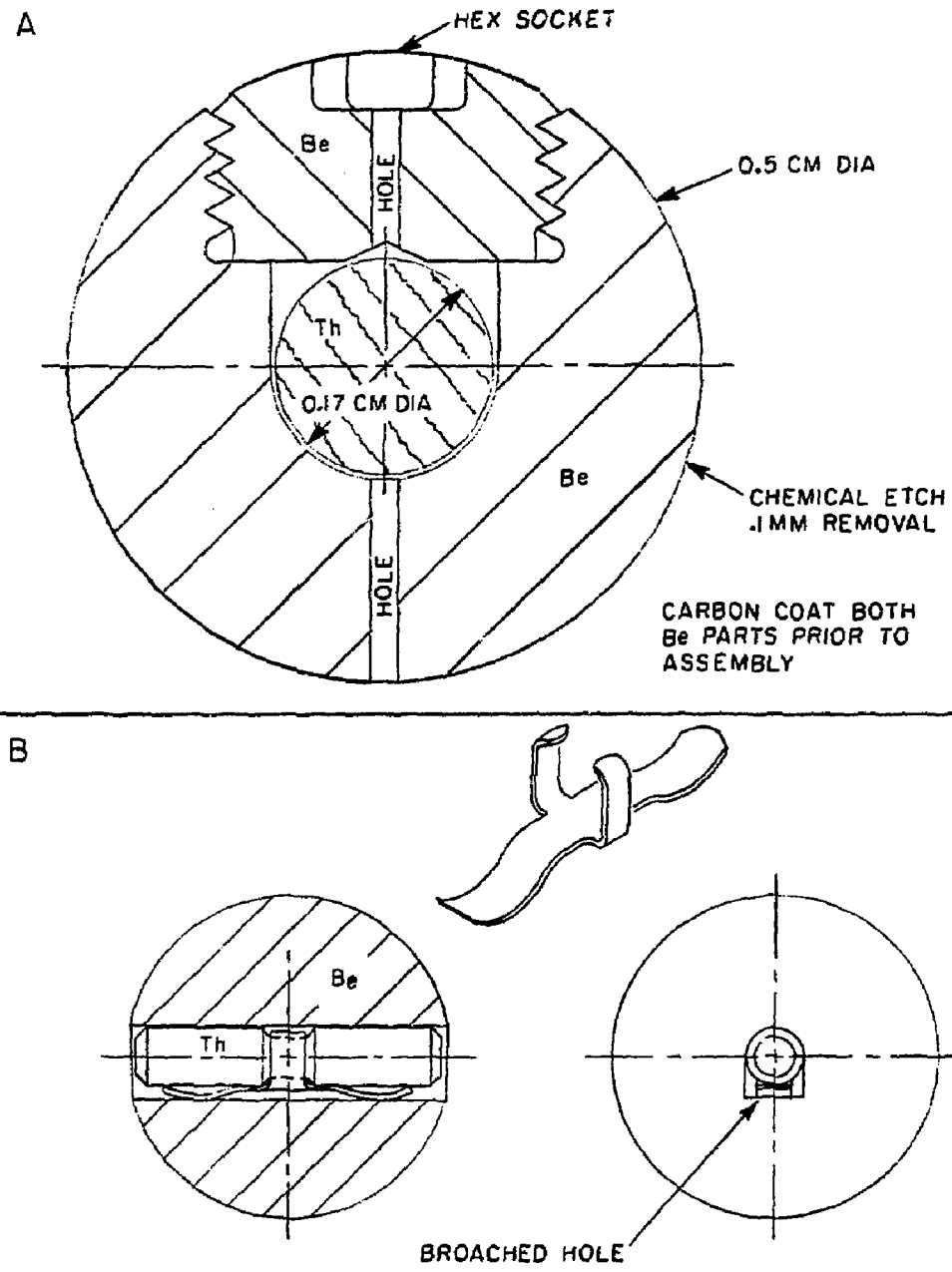
A
HEX SOCKET
Be
HOLE
0.5 CM DIA
Th
0.17 CM DIA
Be
CHEMICAL ETCH
.1MM REMOVAL
HOLE
CARBON COAT BOTH
Be PARTS PRIOR TO
ASSEMBLY
B
Be
Th
BROACHED HOLE

FIG. IV. H-2

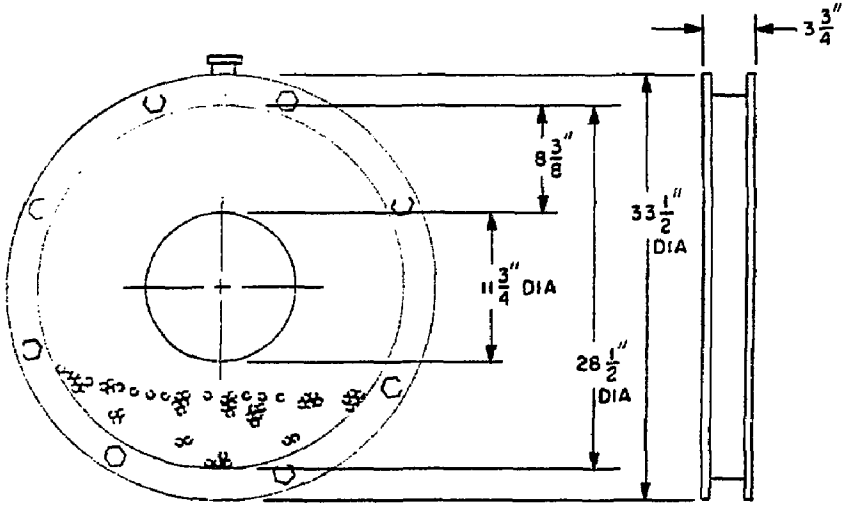

FIG. IV. H-1

IV.I TANDEM MIRROR PHYSICS BASELINE

The physics characteristics for both the FY81 and the current FY82 hybrid axicell fusion drivers are shown on Table 1. The wall loading, fusion power, central cell beta, central cell length, central cell field, barrier coil field, and mirror field have been kept the same. Changes have been made in the barrier length, and field at the barrier minimum. The physics model used to calculate the remaining parameters has been modified since FY81. One change has been to include plasma profiles in a more consistent manner than was done previously; this tends to improve the performance. Another change has been to include a thermalized alpha particle population; this tends to degrade the performance. For this baseline case, the two competing effects almost exactly cancel, as far as the Q value is concerned.

For the new baseline, there is assumed a thermalized alpha particle density, n_α, which is 10% of the D-T fuel ion density, n_c. To achieve this concentration, one must induce radial transport of alphas using either AC or DC VB pumping coils. These perturbations in $\underline{B}$ will also affect the D-T ions, so some allowance for enhanced radial transport of fuel must be accounted for. This has the detrimental effect of making the ignition condition more stringent. The lower values of $(n\tau)$ in the recent case is due to the improvements in treating profile effects, and is not related to the alpha particle questions.

To optimize plasma Q, the barrier length, L_B, barrier minimum field, B_b, barrier beta, β_b, and central cell ion temperature have been adjusted. The constraint in these optimizations is that the sloshing ions injected remain adiabatic. The optimum values are shown on Table 1. The reduced barrier length will make the machine more compact, but will reduce beam access. This reduction does not appear to be limiting. To maintain sloshing ion adiabaticity with a shorter barrier length, the barrier minimum field must be larger. This will increase the required ECRH frequencies at both the barrier midplane (pt. b) and at the potential peak (pt. a). For the new case, the increase over the FY81 case is by a factor of 1.7. The change in barrier geometry also changes the split between the ECRH powers at pts. "b" and "a". In FY81, the split was approximately 50-50. For FY82, the total is about the same, but now most of the power is required at pt. "b" where the required frequency is lower. The new split is 80-20.

In summary, the baseline case selected for the hybrid in the FY82 study incorporates the same basic physics except for the important introduction of thermal alpha particles. The performance (i.e., Q) is virtually the same because of improvements in treating profiles which cancel out the bad effects of a finite alpha concentration.

Since the above case was selected, Rosenbluth and Berk[1] have identified an electrostatic mode which can localize away from the yin-yang anchors, thereby nullifying its stabilizing properties. This mode has growth rates within a factor of 10 of an MHD instability, which would result in catastrophic loss of plasma. Stabilizing effects have been identified by Baldwin,[2] but invoking them requires that the passing ions (1) sample good curvature of the MHD anchor, and (2) they have their turning points after the passing electrons turn. These requirements can be met by moving the potential peak and barrier from the axicell to the anchor. The stability criterion sets a minimum passing ion density in the anchor, which competes with the desire to keep this density low to achieve good performance. Since we require a large passing density in the anchor, the transition region between the axicell and the anchor will have considerably more plasma flowing through it than previously. To keep the potential and β low there, the ions in this region must be pumped. Since this region is typically long, this may represent a large power. Reactors with high central cell magnetic field and small first wall radius satisfy the stability criterion with the lowest passing density. This will favor reactors like Mirror Advanced Reactor Study (MARS); the impact on the central cell parameters of the Tandem Mirror Hybrid Reactor (TMHR) with comparatively low B_c and large r_c is currently being assessed.

Another effect, which is presently not accounted for, is the reduced Q value resulting from the radial profile of confining potential. A revised Q calculation including this effect is underway.

IV. I References

1. Rosenbluth, M.N., and Berk, H.L. LLNL Trapped Particle Mode Workshop, March 1982.

2. Baldwin, D.E. Private communication. March 1982.

0715s:0050a

TABLE 1. Physics Parameters for the Baseline Axi-cell Case

Parameter	Value	
	FY81	FY82
Central Cell		
Fraction of thermalized alpha particles, $C_\alpha = n_\alpha/n_c$	0	0.1
Density, n_c (cm^{-3})	1.6×10^{14}	1.54×10^{14}
Ion Temperature, T_c (keV)	40	44
Electron Temperature, T_{ec} (keV)	32	27
Plasma Radius, r_{cc} (cm)	104	110
Vacuum Magnetic Field, $B_{c,vac}$ (T)	3	3
Beta, β_c	0.7	0.7
Floating Potential, ϕ_e (keV)	234	187
Cold Fueling Current, I_c (kamps)	1.6	2.3
Ion Confinement Parameter, $(n\tau)_i$ (sec cm^{-3})	1.3×10^{15}	3.85×10^{14}
Electron Confinement Parameter, $(n\tau)_e$ (sec cm^{-3})	1×10^{15}	4.79×10^{14}
First Wall Radius (cm)	> 130	> 130
Central Cell Length (m)	129	129
Axicell/Barrier		
Maximum Hybrid Coil Field B_{max} (T)	20	20
Sloshing Ion Injection Energy, $E_{inj,a}$ (keV)	250	250
Vacuum Magnetic Field at Barrier Minimum (point b) (T)	1.69	2.55
Total Barrier Beta ($\beta_\perp + \beta_\parallel$)	1.2	0.94
Perpendicular Barrier Beta, $\beta_\perp$	0.56	0.55
Passing Ion Density at Point "b", $n_{pass,b}$ (cm^{-3})	2.84×10^{12}	3.88×10^{12}
Hot Electron Energy at Point "b", E_{eh} (keV)	361	611
Warm Electron Energy at Point "a", T_{ew} (keV)	93	76
Barrier Length, L_B (m)	12	8.5
Cold Electron Density Fraction, F_{ec} (%)	2.54	1.0
Sloshing Beam Trapping Fraction (%)	23	23
Pump Beam Trapping Fraction (%)	70	72
Beta at Point "a", $\beta_{a\perp}$	0.35	0.34
Barrier Potential Dip, ϕ_b (keV)	192	171
Ion Confining Potential, ϕ_c (keV)	137	141
ECRH frequency applied at pt. "b" (GHz)	38	58
ECRH frequency applied at pt. "a" (GHz)	63	95

TABLE 1 (Continued)

Parameter	Value	
	FY81	FY82
Anchor		
Anchor Plasma Radius, r_{anch} (cm)	122	129
Anchor Effective Length, L_{eff} (cm)	168	378
Sloshing Beam Trapping Fraction (%)	33	35
Sloshing Ion Energy, $E_{slosh,anch}$ (keV)	150	150
Hot Ion Density, $n_{slosh,anch}$ (cm^{-3})	1.5×10^{13}	$1.53 \times$
Anchor Ion Confinement Parameter, $(n\tau)_{i,anch}$ (sec cm^{-3})	5.95×10^{12}	$5.78 \times$
Anchor Floating Potential, ϕ_{anch} (keV)	158	124

Power Balance	Trapped		Incident	
	FY81	FY82	FY81	FY82
Axicell Sloshing Beam Power (MW)	17	20	74	87
Anchor Sloshing Beam Power (MW)	6.4	17.4	19.4	50
Axicell Charge Exchange Pumping Power (MW)	120	106	170	150
ECRH Power Applied to Barrier Minimum (point b) (MW)	27	41	30	45
ECRH Power Applied to Potential Peak (point a) (MW)	25.7	10.6	28.5	11.8
Fusion Power (MW)	3000		3000	
Neutron Wall Loading (MW/m^2)	2		2	
Plasma Q (P_{fus}/P_{inj})	15.3	15.3	9.25	8.7
η^*Q	4.7		4.4	

*η is the efficiency of plasma heating by neutral beams and microwaves including trapping fractions and heating power generation efficiencies. The power generation efficiency is taken to be 50%.

IV.J ECONOMICS ASSESSMENT OF SUPPRESSED FISSION PLUTONIUM BREEDING vs. ^{233}U BREEDING

IV.J.1 Introduction

Many suppressed fission blankets can be adapted, with only minor modification, to breed either plutonium from ^{238}U or ^{233}U from thorium. Therefore, it is of interest to determine which fuel form provides the greatest economic benefit when considered in the context of a fusion breeder/LWR electricity generation system. In addition to economics, three other important considerations which bear upon the fuel cycle choice are listed below:

- Required technology development - are new fuel cycle technologies required? Could the development of these be avoided?
- Deployment - does the fuel cycle which provides the best economic performance enable the greatest impact upon fissile fuel and electricity generation requirements?
- Institutional factors - is either fuel cycle preferred with respect to proliferation safeguards, siting, waste disposal or other institutional factors?

In comparing suppressed fission ^{233}U versus plutonium breeding blankets, the former fuel cycle is more efficient in LWRs and provides a larger LWR support ratio* while the latter fuel cycle is more developed with respect to both fuel reprocessing and fuel fabrication.

One fuel cycle, the so-called "denatured uranium" fuel cycle (~3% ^{233}U, 97% ^{238}U feed to LWR) provides a conventional fuel form on the LWR side with a higher LWR support ratio than achievable using bred plutonium. This fuel cycle requires thorium reprocessing (THOREX) on the breeder side only. In this section the following three fuel cycles are compared with respect to the overall cost of electricity generation in a symbiotic system:

---

* Defined as the gross nuclear power of client LRWs divided by the gross nuclear power of the fusion breeder.

- Plutonium (Pu) - plutonium bred in the fusion breeder is mixed with depleted uranium and burned in LWRs.

- Denatured uranium (DU) - ^{233}U bred in the fusion breeder is mixed with depleted uranium and burned in LWRs. All fissile material is recovered and recycled. Plutonium produced by ^{238}U conversion in the LWRs can be co-mixed with ^{233}U or burned in separately safeguarded LWRs.

- Denatured thorium (DT) - Same as denatured uranium but ^{233}U bred in the fusion breeder is mixed with depleted uranium and also thorium ($\sim$ 3% ^{233}U, $\sim$ 18% ^{238}U, $\sim$ 79% ^{232}Th).

The denatured thorium fuel cycle results in the highest support ratio and is similar in cost and performance to a $^{233}U/^{232}Th$ fuel cycle, but could provide additional difficulties because of a requirement for thorium oxide reprocessing of LWR fuels.

IV.J.2 Basis for Comparison

To perform an economics comparison between these fuel cycles, several types of cost and fuel cycle data are required:

- Fusion breeder performance data including fissile and electricity production, fissile inventories, heavy metal throughputs.

- Fusion breeder cost data including the plant cost, costs of dedicated facilities (eg., a reprocessing plant), and other operating and materials costs.

- LWR performance data including electricity production, fissile requirements, fissile enrichment, fissile inventories, heavy metal throughputs.

- LWR plant and fuel cycle cost data.

- Financial data including inflation and escalation rates, taxes, depreciation, plant lifetime, etc.

The PERFEC code is used in this analysis to generate the cost of electricity and other figures of merit for the symbiotic electricity generation system consisting of the fusion breeder and its client LWRs. The PERFEC methodology has been used in past studies and is described in the references.[1,2,3]

In the case of a fusion breeder breeding either plutonium or ^{233}U, performance estimates are based upon the calculated performance of liquid metal cooled suppressed fission blankets, driven by the 20 tesla axicell tandem mirror reactor considered in FY81. Typical performance is reported in Appendix A of the final report of the FY81 study.[3] The cost of the fusion breeder (per unit of nuclear power) is taken to be 3.5 times that of an LWR - a typical value from previous Tandem Mirror Reactor Design Code (TMRDC) cost estimates.[3] Since the heavy metal throughput required for a single suppressed fission fusion breeder with a 3000 MW_{fusion} driver is large enough to justify dedicated fuel reprocessing/fabrication facilities, these facilities are considered to be integral to the breeder plant. Cost estimates for such fuel cycle facilities were developed in previous studies.[3,4]

Assumptions used for LWR fuel cycle performance and cost were developed from data provided by the NASAP study of alternative fuel cycles.[5] In some cases cost data was appropriately escalated to 1982 dollars. The 1982 estimated cost of an LWR was provided informally.[6]

Financial assumptions typical of a 7% general inflation rate (15.2% net cost of capital) and a 30 year plant life were repeated from previous studies.[3]

IV.J.3 LWR Performance and Cost Data

The LWR performance data used in this analysis is shown in Table IV.J.1. In this table the three fuel cycles discussed above are compared with a conventional fuel cycle burning natural uranium with full recycle of the unburned ^{235}U and the fissile plutonium bred in-situ in the LWR. As shown, the denatured thorium fuel cycle is most efficient and is followed by denatured uranium and plutonium. The denatured uranium fuel cycle results in the lowest equilibrium fissile inventory.

TABLE IV.J-1. LWR Performance Data (NASAP)

Makeup Fissile Fertile Fuel	LWR Fuel Cycle			
	$^{Pu}_{238U}$	^{233U} a $^{232Th}/_{238U}$	^{233U} b $^{238}_{U}$	$^{235U}_{238U}$
Net fissile requirement $g/kW_t\text{-}yr^c$	0.200	0.126	0.150	0.194
Equilibrium fissile enrichment, %	4.9	3.5	3.1	3.3
Equilibrium fissile inventory, g/kW_t	1.46	0.97	0.86	0.90
Net nuclear-to-electric efficiency, %	0.334	0.334	0.334	0.334

[a]denatured thorium fuel cycle (88% ^{233}U burners, 12% Pu burners)

[b]denatured uranium fuel cycle (73% ^{233}U burners, 27% Pu burners)

[c]at full power (no capacity factor included)

IV.J.4 Fusion Breeder Performance and Cost Data

Typical suppressed fission blanket fusion breeder performance and cost data is shown in Table IV.J-3. Differences for the thorium suppressed fission (TSF) and the uranium suppressed fission (USF) blankets are reflected in higher expected breeding per unit of nuclear power and lower blanket multiplication for the TSF blanket. Capital costs for fusion breeders include contributions due to both the fusion breeder plant and its dedicated reprocessing plant. The fusion breeder plant cost is taken to be 3.5 times the LWR cost ($3.5 \times 540\ \$/kw_{nuclear} = 1890\ \$/kw_{nuclear}$). This cost is typical of plant cost estimates generated using the Tandem Mirror Reactor Design Code (TMRDC) during the FY81 study.[3]

IV.J.5 Equivalent Cost of U_3O_8

The fusion breeder replaces natural uranium and uranium enrichment services as an alternative source of fissile fuel. Therefore, the fusion breeder will become economical when the price of mined U_3O_8 rises above a given price. In Figure IV.J-1, the levelized cost of electricity for conventional uranium fueled LWRs with full recycle of uranium and plutonium is shown as a function of the cost of U_3O_8 in the beginning of operation. The levelized electricity cost model used in this analysis assumes that the real cost of U_3O_8 would increase by 3%/yr over a 30 year plant life. For example, the figure indicates that when the cost of U_3O_8 reaches 230 \$/kg (~100 \$/lb) the expected cost of electricity over the 30 year plant life is 73 mil/kWeH. The figure provides a cross check of the breakeven U_3O_8 cost which is equivalent to a calculated levelized cost of electricity for the symbiotic electricity generation system.

TABLE IV.J-2. LWR Cost Data (1982 Dollars)

	LWR Fuel Cycle			
	Pu Makeup	Denatured Thorium	Denatured Uranium	^{233}U Makeup
Direct capital cost, $/kW$_t$ [a]	263	263	263	263
Total capital cost, $/kW$_t$	540	540	540	540
O & M cost, $/kW$_t$ yr.	9.6	9.6	9.6	9.6
Reprocessing cost, $/kg	558	600 (977)	558	558
Fabrication cost, $/kg	554	865	865	554
Transportation cost, $/kg	22	22	22	22
Waste disposal, $/kg	75	75	75	75

[a]Informal Ebasco data for 1200 MWe PWR

TABLE IV.J-3. Fusion Breeder Performance and Cost Data

	TSF	USF
Performance:		
Fissile production, g/kW$_{nuclear}$-yr [a]	1.9	1.8
Net electrical efficiency, % [b]	30	32
Fissile inventory, g/kW$_{nuclear}$-yr [a]	0.55	0.51
Cost:		
Total capital cost, $/kW$_{nuclear}$ [c]	2020	1976
O&M cost, $/kW$_{nuclear}$-yr	32.1	32.1
Fuel cycle cost:		
Fixed, $/kW$_{nuclear}$ [d]	131	87
Direct, $/kW$_{nuclear}$-yr	11.3	8.9

[a]Based upon packed bed blanket neutronics presented in Appendix A.3 of FY81 TMHR final report

[b]Blanket M values: TSF(1.5), USF(1.75)

[c]Basis: 3.5 x LWR total capital cost per kW$_t$

[d]Capital cost of dedicated fuel reprocessing plant

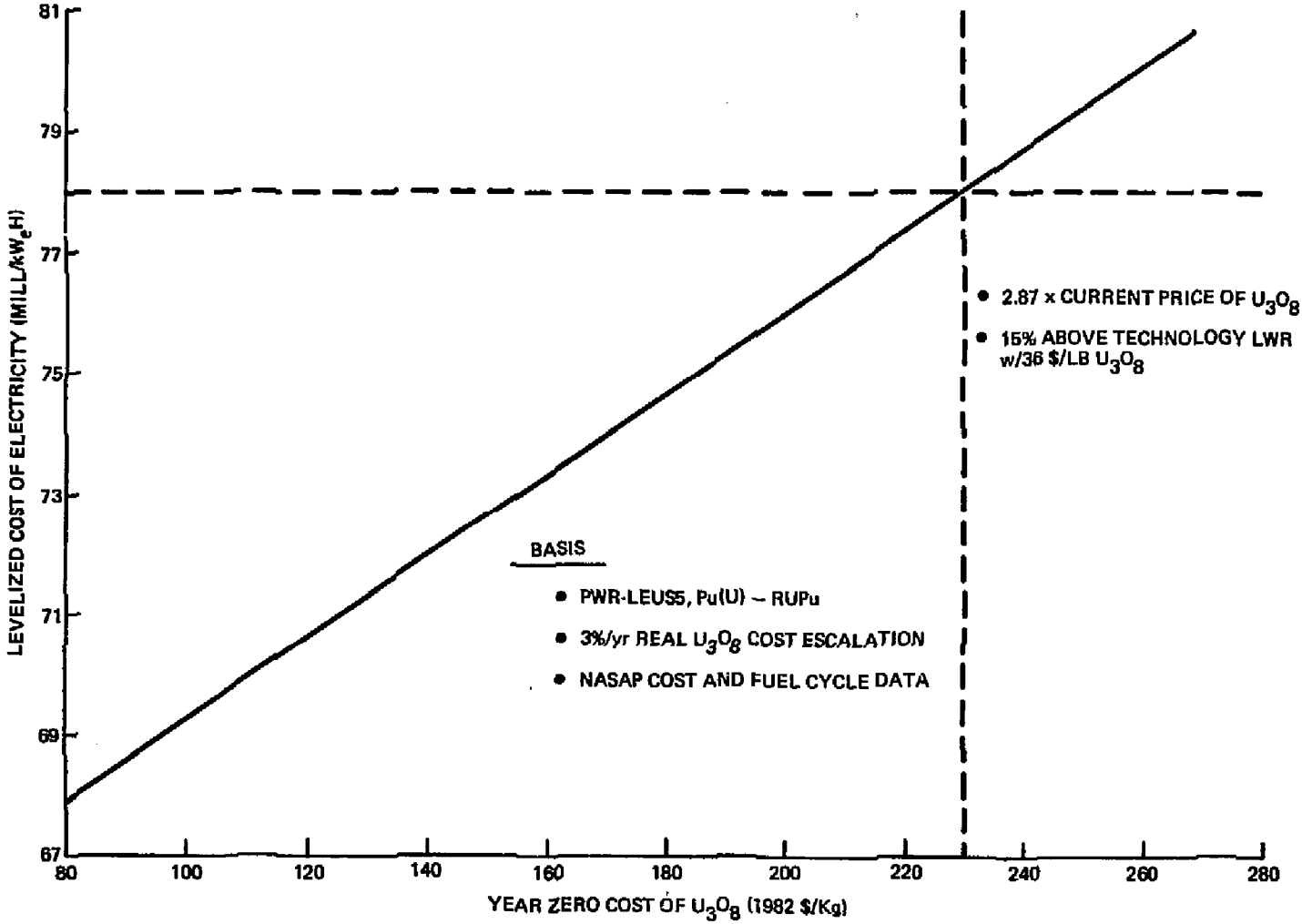

FIGURE IV.J-1. Cost of LWR Electricity vs. U_3O_8 Cost

IV.J.6 Results.

Results for the cost of electricity and the equivalent U_3O_8 cost for three suppressed fission blanket fuel cycles are shown in Table IV.J-4. These are designated by the blanket fertile fuel (TSF or USF) form on the top line and the LWR fuel cycle (Pu, DU, or DT) on the second line. DU and DT are denatured uranium and thorium, respectively.

As shown, the TSF/DU and DT fuel cycles result in similar electricity cost and similar equivalent U_3O_8 cost estimates. The USF/Pu fuel cycle is more expensive due to the lower support ratio and the higher fissile inventory associated with the plutonium burning LWR. Although, the electricity cost for this fuel cycle is only 7% higher than that of the TSF/DU fuel cycle, the equivalent U_3O_8 cost is 29% higher. This difference is a preliminary estimate but is considered to be large enough to indicate a real difference between the potential performance of plutonium and ^{233}U breeding.

The results of this analysis indicate three general conclusions:

- ^{233}U breeding TSF blankets have significantly, but not overwhelmingly, better economic performance than Pu breeding USF blankets.
- The choice between denatured uranium or thorium depends, to a large extent, upon the cost of THOREX reprocessing.
- Electricity costs less than 16% above those for current technology LWRs (with 36 \$/lb U_3O_8 and full recycle) appear to be reasonable based upon conservative cost and performance assumptions.

Based upon these results, and other considerations, the thorium suppressed fission blanket with a denatured uranium fuel cycle is recommended as the reference blanket/fuel cycle combination. This provides the following advantages:

- Competative economics
- Retains PUREX on the LWR side
- Significant diversion resistance due to ∿ 32 to 1 isotopic dilution.

The USF/Pu and TSF/DT (or thorium) fuel cycles should be retained as high and low technology options, respectively.

TABLE IV.J-4. Results of Economics Assessment

	USF	TSF	
	Pu	DU	DT
Nuclear support ratio	9.0	12.7	15.1
Cost of electricity, mill/kW_eH (levelized)	83.6	78.8	78.2 (80.8)[b]
Cost of electricity, % above current technology LWR[a]	23	16	15 (19)
Equivalent cost of U_3O_8, $/Kg	312	241	232 (271)

[a]Current technology LWR: LWR with full recycle, ^{233}U makeup from U_3O_8 at 36 $/lb ($1982) with 3%/year real escalation

[b]Cost for higher THOREX reprocessing cost

REFERENCES

1. D. H. Berwald and J. A. Maniscalco, "An Economics Method for Symbiotic Fusion-Fission Electricity Generation Systems," Nucl. Technol./Fusion, 1, 128, (1981).

2. J. A. Maniscalco, et.al., "Recent Progress in Fusion Fission Hybrid Reactor Design Studies," Nucl. Tech./Fusion, 1, 4 (1981)

3. R. W. Moir, et.al., "Feasibility Study of the Fission Suppressed Tandem Mirror Hybrid Reactor," UCID-19327, Lawrence Livermore National Laboratory (1982).

4. J. A. Maniscalco, et.al., "Laser Fusion Driver Breeder Design Study, Final Report, Contract DE-AC08-79DP40-11, TRW Inc. for the USDOE (1980).

5. "Nuclear Proliferation and Civilian Nuclear Power: Report of the Nonproliferation Alternative Systems Assessment Program," DOE/NE-001, U.S. Dept. Energy (1979).

6. Informal Ebasco data for 1200 MWe PWR in 1982.

IV.K Tokamak Hybrids: TORFA vs. STARFIRE

NOT AVAILABLE FOR FIRST DRAFT

CHAPTER V. REFERENCE CONCEPT SELECTION

In this chapter, a recommendation regarding the selection of a preferred blanket concept for the reference design phase of the fusion breeder program is provided. Our rationale for recommending selection of the radial flow direct cooling concept with thorium metal fuel is discussed in detail below. The chapter is separated into four sections:

- Basis for decision
- Strawman blanket design descriptions
- Comparison of key design areas
- Recommendation.

V.A BASIS FOR DECISION

Before discussing design specific issues, the logical approach which was used to select a design preference will be discussed. In developing a design preference, the first issue to consider is the overall attractiveness of a particular design concept including breeding, thermal conversion, reliability, fuel management complexity, fuel cycle cost, blanket lifetime, safety, and other characteristics. However, the choice of a particular blanket concept for the reference phase must also consider a lack of information relating to several design aspects of both the direct and pipe cooling configurations. In general these data needs will require resolution via experimental programs or, in a few cases, a level of design analysis which is not permitted in the current study. A listing of unresolved data needs which bear upon the selection process is in Table V.A-1.

Given that these data needs could not be resolved prior to the beginning of the reference phase of our study, our basis for decision was selection of the design which offered the greatest possibility of providing a feasible and attractive concept based upon presently available engineering data. It is important to note that both designs can be feasible and attractive depending upon the resolution of the above issues.

Also, depending upon the resolution of the above issues, other pipe cooled and direct cooled configurations could ultimately become more attractive. Table V.A-2 lists three promising alternative blankets featuring beryllium multiplication and liquid metal cooling which, due to design uncertainties may be less conservative than the two concepts described earlier. Two observations are apparent from our work during FY81 and the scoping phase of the FY82 program:

- The generic class of suppressed fission blanket utilizing beryllium and liquid metals appears to offer many design options which can be both feasible and attractive
- A modest experimental program is required to develop a more informed opinion regarding the best choice.

In summary, a selection strategy which was intended result in the reference design which is most defensible with respect to a review by others in the technical community was emphasized. In some cases (eg., fuel management mode) more difficult or higher cost options were chosen to obtain a higher confidence of overall feasibility. Implicit in this strategy is a bel ef that the demonstration of a viable fusion breeder blanket technology through a defensible reference design is a higher priority for our program than achieving the most attractive performance. As more favorable design information becomes available, the fusion breeder program can benefit from its introduction.

TABLE V.A-1. Unresolved data needs which bear upon the selection process

DATA NEEDED	DESIGN MOST AFFECTED	
	DIRECT	PIPES
• MHD effects for packed bed	X	
• Ability to obtain uniform pebble mixing in the blanket		X
• Ability to operate in continuous (vs. batch) fuel management	X	
• Allowable cost to fabricate equal density pebbles		X
• Onset of DBTT, operation below the DBTT, methods to cure DBTT (eg., annealing)		X
• Beneficial use of oxide coatings and related transport through the primary loop	X	
• Be/steel and Be/Be interactions		X
• Tritium breeding in fertile zone	X	

TABLE V.A-2: Selected alternative suppressed fission blankets utilizing beryllium and liquid metal coolants

BLANKET DESIGNATOR	COOLING MODE	COOLANT	HEAT TRANSFER FLUID	FERTILE FUEL FORM	COMMENTS
Li-Pb/ThO_2 Direct	Direct	Li-Pb	None	ThO_2 pebbles (1 mm dia)	Li-Pb provides low MHD pressure drop. ThO_2 about same density as Li-Pb forms suspension and circulates with coolant through the beryllium pebble bed. Simplified fuel management. Li-Pb compatibility and tritium release concerns. Li-Pb is non-reactive. Primary loop more difficult. Large static load on first wall.
Li-Pb/ThO_2 Pipes	Internal pipes	Lithium or Li-Pb	Li-Pb	ThO_2 particles (0.2 mm dia.)	Pipe cooling provides low MHD pressure drop. ThO_2 suspension in Li-Pb flows through beryllium pebble and is circulated slowly to remove tritium and mix fuel. Simplified conventional primary loop. Li-Pb compatability and tritium concerns. Large static load on first wall.
Pb/Th Pipes	Internal Pipes	Lithium or Li-Pb	Lead	Thorium Particles (0.2 mm dia.)	Same as Li-Pb/ThO_2, but Pb and Th are similar density and form suspension. Better tritium confinement. Thorium reprocessing less expensive. Particle agglomeration more of a concern.

V.B STRAWMAN BLANKET DESIGN DESCRIPTIONS

Before discussing the pipes vs. direct cooling issue, it is useful to construct "strawman" design descriptions which portray representative design points for these systems. Design specifications for internal pipe cooling and radial direct cooling are shown in Table V.B-1. Both designs have several features in common:

- lithium coolant
- thorium metal fuel pebbles
- beryllium multiplier pebbles
- ferritic steel structure
- general blanket module configuration

V.B.1 Internal Pipe Concept. Considering first the internal pipe cooling concept, initial thermal calculations indicate that fewer than 800 coolant pipes are required. This design most resembles the design of shell and tube heat exchangers being developed for the LMFBR program (which have several thousand tubes). Therefore, the requirements for many tubes is not considered to be a feasibility issue for this design. However, to limit the maximum ped temperature to an upper limit of 525° (more conservatively 500°C) we require a closest pipe spacing of ∿5 cm (with possibly only 2.5 cm clearance between the first row of tubes and the 2.85 cm deep radial corrugations at the intermediate wall. Based upon this constraint, a nominal 0.5cm diameter size was selected for both the beryllium and thorium pebbles. If we assume a 0.5% ^{233}U (in thorium) discharge concentration, the total value of ^{233}U in a 0.5 cm pebble (100% dense) is about 75¢. Therefore, any fabrication process (e.g., to equalize the beryllium and thorium densities etc.) will need to be quite inexpensive.

To achieve the 525°C temperature limit at a 1.6 MW/m^2 wall loading while maintaining the minimum structure temperature above 350°C (to minimize the DBTT issue), lithium inlet/outlet temperatures of about 305°C/365°C are required. In addition, it will be prudent to provide for periodic annealing of the ferritic steel by allowing for higher temperature operation (∿50°C) for limited periods. The details of such a process have yet to be determined, but are being addressed in this year's study. The proposed coolant temperature will enable a relatively efficient thermal conversion cycle. A selection between 2-1/4 Cr and HT-9 steel is not critical to concept feasibility, but 2-1/4 Cr

TABLE V.B-1: STRAWMAN BLANKET DESIGN SPECIFICATIONS

	Pipe Cooling	Comments	Radial Direct Cooling	Comments
Heat transfer fluid/Number of tubes	Sodium/ ∿1000		None/ None	
First wall loading, MW/m^2	1.6	max. for TH	2.0	
Coolant inlet/outlet, °C	305/365	305 → >350 min. str. temp. 365 → <525 max. bed temp.	340/490	335 → >350 min. str. temp, 485 → <510 max. bed temp.
Average first wall coolant plenum thickness, cm	3.35	corrugation depth + 0.5 cm	∿8	corrugation depth + ∿6 cm
Operating pressure @ fw, PSI	<100	calc. ∿64 PSI @ fw	< 250	calc. ∿ 200 PSI in bed flow
Structural material	2-1/4-Cr-1Mo	HT-9 alternate	HT-9	2-1/4 Cr-1Mo alternate
Min/Max structure temp, °C	350/525	400°C max in fw and tubes	350/500	
Max bed temp., °C	525	upper limit	510	
Min pebble flow clearance, cm	2.5	between first row of pipes and first wall corrugation	24-40	nominal 8 pebble diameters
Pebble size (dia), cm	∿0.5	based on 2.5 cm clearance to fw corrugation and 5 balls	2-4	
^{233}U value per pebble, $	0.75	value of ^{233}U in a 100% dense 0.5 cm dia. pebble at 0.5% discharge cone	120	value of ^{233}U in 16.4% dense 5 cm Th pebble with 0.5% discharge concentration (repro cost = $15)
Fuel management mode	Freq. Batch	continuous mode is attractive if possible	Freq. Batch	continuous mode is attractive if possible
Fissile fuel production, $T+F_{net}$	∿1.70	assumes TBR=1.3 in plenums	∿1.70	TBR = 1.3 in plenums, assumes ∿ 0 structure in packed bed, lithium replaces sodium in bed.

is recommended based upon a 400°C maximum temperature in the first wall and coolant tubes. The tube sheets will operate at 525°C, but these might be relatively thick without excessive neutronic penalty.

A preliminary calculation of the MHD pressure drop for the proposed coolant conditions indicates a pressure of 64 PSI at the first wall. We have conservatively assumed an operating pressure of less than 100 PSI at the first wall. The later pressure is clearly acceptable based upon the mechanical and neutronic analysis presented in Chapter II.

Concerning fuel management, a continuous process is preferred, but a batch process is recommended until such time that we are assured that all fuel pebbles will flow through the blanket in a predicted manner. It is important to note that a batch process will not require that the fusion reactor be shut down. Rather, a blanket module can be temporarily backfilled with sodium during and prior to receiving the next fuel charge. In any case, the actual process rate can be equal for the continuous and batch process with the only differences being provision for a holding tank and the out-of-blanket inventory. If the fuel management system is sized to process the contents of one blanket module per day, there are 20 modules, and a single process system for the entire reactor, then each blanket module can be cycled every 20 days (about 1/3 the mean time to discharge enrichment) with a working fuel inventory equivalent to the contents of only one blanket module. To accomplish this task, fuel must be transported to and from a central process location-possibly using electromagnetic pumps and a slurry mixture of liquid lithium, thorium and beryllium.

The possibility of radial zoning to improve the efficiency of fissile production (higher average discharge concentration) is attractive, but will be difficult with pipe cooling due to the many pipes and tube sheets. Most importantly, the number of fueling ports could scale as the product of the number of tube sheets and the number of radial zones. Since this concept will most likely require many ports per axial-radial zone, the complexity of radial zoning may be less desirable than penalties associated with increasing the batch rate and reducing the discharge enrichment. For this reason a one zone

design is proposed as the initial baseline for this concept. A net T+F of 1.70 is estimated based upon an effective TBR = 1.3 in the plenums and results presented in Chapter II.

V.B.2 Direct Cooling Concept. Considering the direct cooling concept, the first choice to be made concerns the flow orientation: radial or axial. The rationale for preferring the radial orientation is based upon three observations (see Chapter III).

- The radial flow orientation could result in lower pressure drops using conservative assumptions concerning flow through the bed.
- Because flow velocities, the flow path length, and the number of turns are less for radial flow, better confidence in the MHD calculation should result for this orientation.
- The exponentially peaked power density in the bed is better addressed by radial flow (ie., low coolant temperature matched to high power density and vice versa). Radial flow should aid in addressing possible problems posed by inhomogeneous fuel mixing (ie., two or more thorium pebbles in same location) and batch operation. Conversely, for axial flow, a larger flow requirement near the first wall will result in either an unnecessarily large coolant flow near the back of the blanket or a complex flow baffling scheme. In either case, the overall axial flow MHD pressure drop could increase several fold.

Several options exist regarding the first wall and plenum and three seem to be most interesting. The first two options were discussed in Chapter III and feature a coolant inlet from one and both sides, respectively. In the latter case, coolant flow concerns will be minimized, but designs which avoid trapping of the magnets will be difficult to achieve. A third option with both the inlet outlet pipes on the same side has distinct advantages and does not trap the magnets. These issues require closer examination in concert with consideration of module replacement and remote handling requirements.

For the direct cooling concept, pebble sizes can be larger - in the range of 3-5 cm dia. Although a final choice of a pebble size depends upon several considerations (e.g. thermal performance, pressure drop, fuel management, neutronics), no critical feasibility issue regarding thermal performance is obvious.

Most importantly, for the large thorium metal pebbles, there may be incentive to develop hollow pebbles that have the same bulk density as beryllium or composite pebbles which contain both beryllium and thorium (eg., coating or mechanical inserts). These types of fuel forms can eliminate many potential problems associated with species segregation and achievement of an adequate thorium distribution. For example, since the value of thorium in a pebble scales as the radius cubed, the calculated value of ^{233}U discharged in a 1/6 dense, 5 cm dia., hollow thorium pebble with 0.5% discharge concentration is about $120. The cost to reprocess the pebble is ~ $15, so we can easily affort $1-5 for fabrication. Similar results apply to the composite pebbles discussed in Section IV.H.

Coolant temperatures for the direct cooling design can be high (inlet/outlet: 335°C/485°C) and are limited by DBTT at the inlet temperature and chemical compatibility at the outlet temperature. Since the coolant ΔT is large (150°C) a possible requirement for a higher inlet temperature or a lower outlet temperature (eg., resulting from an improved understanding of materials issues) can be accommodated in this design. Design provision for periodic annealing is also recommended for this design, but may not be required.

Since the anticipated structural temperatures (350-500°C) are higher for direct cooling than pipe cooling (with the exception of tube sheets in the later case), the ferritic HT9 alloy is specified for the direct cooling design. The maximum bed temperature should be well matched to the coolant outlet temperature due to the coolant outlet near the back of the blanket (low power density). Therefore, a 510°C limit for the surface of a beryllium or thorium pebble should be attainable.

A typical MHD pressure drop calculation for radial direct flow indicates a 200PSI pressure drop through the bed. Adding 50 PSI for flow out of the back of the blanket yields a presumably conservative estimate of ~250 PSI at the first wall plenum. Lower pressure drops can be obtained in the current design by decreasing the wall loading and/or the bed thickness. The above calculations assumed a first wall loading of 2 MW/m^2 and a central cell B-field of 3 Tesla

An estimate of net T+F based upon Monte Carlo calculations and assuming an effective TBR = 1.3 in the coolant plenums is ∿ 1.70. Again, a frequent batch fuel management mode is recommended for the direct cooling option pending a determination that the flow of all pebbles through the blanket is assured. However, for the proposed blanket configuration, the experimental apparatus developed at LLNL seems well suited to provide an experimental determination using single density balls of radius approximately modeling the ratio of pebble radius to first wall radius in the design. Radial zoning is desirable (especially if the number of axial zones induced by "tube sheet" type supports can be reduced) and should be investigated with respect to structural design and fuel management. However, the penalties associated with a simple, one zone design require further study before a determination can be made.

V.C DESIGN COMPARISON OF KEY AREAS

In this section the internal pipes and radial direct cooling options are compared with respect to the following key areas:

- fluid mechanics and heat transfer
- mechanical design and maintenance
- fuel management and fuel cycle
- materials compatibility
- irradiation damage
- nuclear performance
- tritium containment and processing
- balance of plant and availability
- safety

V.C.1 Fluid Mechanics and Heat Transfer. The pipe cooling blanket operates at lower pressure and provides more confidence with respect to calculation of the pressure drop, but the coolant ΔT ($60^{\circ}C$) for pipe cooling is too small to easily accommodate an unfavorable resolution regarding one or more of the unresolved data needs shown in Table 1. In particular, constraints related to irradiation damage effects (DBTT), Be/steel or Be/Be compatibility, and/or pebble flow and mixing could introduce unreasonable requirements for the pipe cooling design if changes in coolant boundary conditions or the pipe spacing are required. For instance, a lowering of the maximum bed temperature to $500^{\circ}C$ ($25^{\circ}C$ decrease) would decrease the coolant ΔT to $35^{\circ}C$ and increase the first wall pressure drop and coolant pump power to $\sim$ 170 PSI and > 100 MW, respectively. For the direct cooling option, a large coolant ΔT ($150^{\circ}C$) allows for more flexibility in that a $\sim 50^{\circ}C$ decrease in ΔT could be accommodated if required, and on this basis the direct cooling option is preferred. The direct cooling option will also provide a higher thermal conversion efficiency with lower pumping power. Both options can be adversely affected by a significant increase in the central cell B-field since the MHD pressure drop scales as B^2. For higher B-fields the coolant of choice might be Li-Pb due to its lower electrical conductivity.

V.C.2 Mechanical Design and Maintenance. In this area a choice is more difficult, but the direct cooling concept is preferred because it is less complex (no pipes, fewer "tube sheets") and may be amendable to a more swelling tolerent design and/or radial zoning with less complication. However, the 200 PSI pressure for direct cooling will require a thicker first wall structure. Also, the more complex first wall coolant plenum

(∿ 8 vs. 3.35 cm) will be a more difficult design, but will provide more structural efficiency due to its increased thickness. A larger magnet bore is likely needed for direct cooling to accommodate the larger fuel outlet plenums needed to charge/discharge 2-4 cm pebbles.

V.C.3. Fuel Management and Fuel Cycle. The recommended fusion breeder cycle is ^{233}U/thorium metal based upon the comparative economics analysis presented at the meeting. The preferred LWR fuel cycle is denatured uranium, based upon economics and technology development considerations - most importantly, the avoidance of thorium oxide reprocessing on the LWR side. Breeding ^{239}Pu from UC (or UO_2) is also possible without major design alterations.

Regarding blanket fuel management, the pipe cooling option with sub-centimeter size pebbles can provide superior fuel handling characteristics with respect to ease of transport in and out of the blanket (and possibly dynamic separation), however, the achievement of adequate in-blanket fuel mixing is a key feasibility issue for both blanket design concepts. It has not been demonstrated that two density pebbles can achieve adequate mixing and flow in a batch refueling mode or that low density thorium pebbles for the pipe cooling concept can be manufactured at acceptable cost. Therefore, the ability to use a larger pebble in the direct cooling concept can provide increased confidence in the design concept because fabrication of a large composite (eg., beryllium/thorium) pebble appears to be reasonable based upon the value of ^{233}U discharged in the pebble (typically ∿ $100).

/

For this reason the direct cooling concept with large hollow thorium or composite beryllium/thorium pebbles is preferred. Continuous circulation of the pebbles is desirable with respect to limiting the size of fuel handling equipment and a method to ship fuel discharged from the blanket to a central processing facility (e.g. using EM pumps to transport a "slurry" mixture) is also recommended. The same manner of transport can be used to ship enriched fuel to be processed to a co-located fuel reprocessing plant. If continuous circulation is not possible, a batch process would be employed.

V.C.4. Materials Compatibility. In the materials compatibility area several data needs impact our ability to make a clear choice between candidate blanket configurations. If natural oxides in the sodium filled pipe cooled blanket act to prevent Be/steel reactions and Be/Be self-

welding, then pipe cooling will be preferred and the need to coat either the pebbles or structural members (e.g. with molyblenum) would be eliminated. If oxides do not act as described above, then the lithium cooled direct option could be favored due to a lower maximum structure temperature and design flexibility allowing a further decrease in the maximum structure temperature if needed. Also, the larger pebbles provide two orders of magnitude less available surface area for chemical interactions in the blanket. Their increased weight (three orders of magnitude) will provide larger breaking forces to act against self-weldings.

On the negative side, mass transport and plugging in the primary loop of the direct cooled concept (including Li_2O) is an issue. Similarly, tritium breeding in the fertile fuel zone (including possible diffusion into the beryllium and/or thorium) is an issue for direct cooling.

V.C.5. Irradiation Damage. Due to swelling concerns, a ferritic steel structure with possible, periodic annealing is recommended for both coolant concepts. Again, the direct cooling concept is preferred because of more flexibility regarding the possible need for a higher inlet temperature. This design might also be more tolerant of swelling.

V.C.6 Tritium Contamination and Processing. The pipe cooling option is a clear preference in this area since the tritium and fissile fuel breeding functions are separated. For the direct cooling blanket issues associated with tritium contamination of the beryllium and fertile fuel will require resolution.

V.C.7. Balance of Plant and Availablity. Three issues cause concern. First, heat exchanger tube plugging for the direct cooling option could occur due to unknown mass transfer of the beryllium, thorium, stainless steel, or Li_2O (formed due to degradation of natural BeO or ThO_2 coatings or other oxygen in the system). Second, if batch fuel management is required for direct cooling, it is possible that the reactor plasma would be shut down during each reload because effective heat transfer cannot occur when the blanket is "half full" of pebbles and the coolant avoids the higher pressure drop in the bed. It is not expected that all superconducting magnets would be deenergized in this event. The third issue concerns blanket coolant tube failure for the pipe cooling concept. The latter issue complicates tritium concerns, but operation with small lithium leaks into sodium appears reasonable, and on this basis the pipe cooling concept is preferred.

V.C.8 Safety. In this area the pipe cooling concept is marginally preferred because, with smaller pebbles, semi-passive freeze valve to dump tanks appear to be more viable. For direct cooling and an 8 pebble clearance 20-40 cm freeze valves could be required.

V.D RECOMMENDATION

The comparative evaluation of the pipe and direct cooling options is summarized in Table V.D-1, however, it is clear that all areas should not be equally weighted. Among all of the areas of consideration, three stand out:

- design flexibility
- overall confidence in the design
- projected performance.

In all probability the projected performance for both blankets will be adequate and similar. Therefore, no choice will be made on this basis.

Regarding overall confidence, materials compatibility issues, the MHD pressure drop for direct cooling, pebble flow and packing for pipe cooling represent the largest unknowns. These issues were not resolved prior to our choice of a reference concept, but there is considerable confidence that the materials and MHD issues can be favorable resolved. Since the direct coolant option provides more flexibility with respect to operating temperatures and is amendable to the development of a large, low density or composite pebble, the direct cooling option was recommended for further study during the reference blanket design phase.

Pending a resolution of the fuel management and compatibility issues for pipe cooling, this option should be deselected for the FY82 study. However, if future results indicate that Be/steel compatibility at temperatures greater than 525°C is predicted and if a viable fuel management option providing adequate thorium/beryllium mixing is identified, the pipe cooling option would be favored. A modest experimental program is required to resolve these issues.

TABLE V.D-1 Summary of Comparative Evaluations

Key Area	Preferences		
	Pipes	Indifferent	Direct
Fluid mechanics/heat transfer			X
Mechanical design and maintenance		X	
Fuel management/fuel cycle			X
Material compatibility		X	
Irradiation damage		X	
Nuclear performance		X	
Tritium control and processing	X		
BOP and availability	X		
Safety	X		

DISCLAIMER

Printed in the United States of America
Available from
National Technical Information Service
U.S. Department of Commerce
5285 Port Royal Road
Springfield, VA 22161
Price: Printed Copy $; Microfiche $3.50

Page Range	Domestic Price	Page Range	Domestic Price
001-025	$ 5.00	326-350	$ 18.00
026-050	6.00	351-375	19.00
051-075	7.00	376-400	20.00
076-100	8.00	401-425	21.00
101-125	9.00	426-450	22.00
126-150	10.00	451-475	23.00
151-175	11.00	476-500	24.00
176-200	12.00	501-525	25.00
201-225	13.00	526-550	26.00
226-250	14.00	551-525	27.00
251-275	15.00	526-550	28.00
276-300	16.00	601-up [1]	
301-325	17.00		

[1] Add 2.00 for each additional 25 page increment from 601 pages up.